



**LIBRARY**  
**Michigan State**  
**University**

This is to certify that the  
dissertation entitled

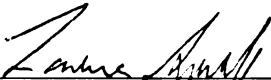
**ANATOMY AND FUNCTION OF OREXIN-CONTAINING  
NEURONS IN DAY- AND NIGHT-ACTIVE ANIMALS**

presented by

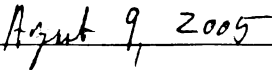
**JOSHUA PATRICK NIXON**

has been accepted towards fulfillment  
of the requirements for the

Ph.D.                      degree in                      Department of Zoology and  
Ecology, Evolutionary Biology  
and Behavior Program



Major Professor's Signature



Date

PLACE IN RETURN BOX to remove this checkout from your record.  
TO AVOID FINES return on or before date due.  
MAY BE RECALLED with earlier due date if requested.

DATE DUE	DATE DUE	DATE DUE

**ANATOMY AND FUNCTION OF OREXIN-CONTAINING NEURONS IN DAY-  
AND NIGHT-ACTIVE ANIMALS**

**By**

**Joshua Patrick Nixon**

**A DISSERTATION**

**Submitted to  
Michigan State University  
in partial fulfillment of the requirements  
for the degree of**

**DOCTOR OF PHILOSOPHY**

**Department of Zoology and Ecology, Evolutionary Biology, and Behavior  
Program**

**2005**



# **ABSTRACT**

## **ANATOMY AND FUNCTION OF OREXIN-CONTAINING NEURONS IN DAY- AND NIGHT-ACTIVE ANIMALS**

By

Joshua Patrick Nixon

The orexins are a family of hypothalamic peptides implicated in the modulation of feeding, arousal state, and somatomotor functions. The first part of this dissertation examines the distribution of cell bodies and fibers expressing immunoreactivity for orexin A (OXA) or orexin B (OXB) in two nocturnal rodents, the Long-Evans rat (*Rattus norvegicus*) and Syrian hamster (*Mesocricetus auratus*), and two diurnal rodents, the Nile grass rat (*Arvicanthis niloticus*) and the degu (*Octodon degus*). I show that although the overall distribution of orexin is very similar in these species, there are significant species differences in the distribution of orexin cell bodies as well as in the density of orexin-IR fibers in some regions. Specifically, I show species differences in the organization of the main body of orexin neurons in the lateral hypothalamus, and provide evidence for a previously undescribed population of OXA neurons in the magnocellular neurosecretory nuclei of the hypothalamus. With respect to orexin fiber density, the differences observed were few, but dramatic. The majority of the differences were observed in the degu, suggesting that this species is an outlier.

The second series of experiments investigated the functional and anatomical relationships between the orexins and patterns of activity in the grass rat. Some individuals of this species switch to a more nocturnal pattern of activity when given access to a running wheel, while others continue to be most active

during the day. In both day- and night-active grass rats, the percentages of orexin A (OXA) and orexin B (OXB) cells expressing Fos were highest when animals were actively running in wheels. In night-active animals, removal of the running wheel significantly decreased Fos expression in OXA and OXB cells. Additionally, in night-active animals, clear regional differences were apparent, such that the presence of a wheel induced Fos in a higher percentage of orexin cells in medial regions of the lateral hypothalamus (LH) than in lateral regions. No regional differences were observed in day-active animals.

I also characterize the relationship between the orexins and neuropeptide-Y cells in the intergeniculate leaflet (IGL). These cells are known to modulate effects of arousal on the mammalian circadian system. However, the route through which this information reaches the IGL has not been established. I present evidence that OXA and OXB cells have projections to the IGL that appear to make contact with NPY cells, and discuss the possibility that these fibers may be involved in relaying feedback regarding the activity state of the animal to the circadian system through these projections. Next, I demonstrate that many NPY cells in the grass rat IGL exhibiting OXA fiber appositions are significantly more likely to express Fos during nocturnal wheel running than are NPY cells without such contacts ( $p < 0.001$ ). Finally, using the retrograde tract-tracer cholera toxin B, I show that 20 percent of all OXA neurons project to the IGL, and that these OXA neurons projecting to the IGL do not form a topographically isolated cluster of cells within the lateral hypothalamus.

Copyright by

JOSHUA PATRICK NIXON

2005

For my mother, Jude, who encouraged me to dream; and my wife, Amy, for reminding me to work towards those dreams.

## **Acknowledgements**

I owe a debt of gratitude to a number of people who have helped me to complete this dissertation. First and foremost I would like to thank my advisor, Dr. Laura Smale, for taking me on as a graduate student. Despite my tendency to procrastinate, Laura has been incredibly patient and generous with her time, and I greatly appreciate her advice and friendship.

I would also like to thank the members of my committee, Drs. Kay Holekamp, Antonio Nuñez, and Lynwood Clemens for their input and feedback. I would like to specifically thank Kay for cutting me off when I got too wordy, Tony for correcting me the many times I was completely wrong, and Lyn for never losing his sense of humor every time I had to re-schedule a committee meeting.

I wish to extend thanks to past and present members of the Smale and Nuñez labs. I would like to thank Dr. Megan Mahoney, Michael Schwartz, Dr. Chidambaram Ramanathan, Dr. Gladys Martinez, Jessica St. John, and Alexandra Castillo-Ruiz for their friendship, feedback, and willingness to put up with my awful sense of humor. Special thanks to Megan and Mike for helping me to develop as a graduate student – their friendship, humor, and willingness to go for coffee at any time helped make this whole thing fun. I would like to thank Dr. Colleen Novak for getting me interested in orexin in the first place. I was also fortunate to have the assistance of a number of superb undergraduates and technicians working in the Smale Lab, including Heather Ross, Betty Gubik, Joel Breen, Janaina Gamez, Anna Baumgras, and Nicole Timm.

Thanks also to the many people in the Department who helped me develop as a student as well as an instructor, especially Dr. Susan Hill, Dr. Will Kopachik, and numerous fellow graduate students who have served as teaching assistants in the Biological Science, Developmental Biology and Comparative Anatomy courses over the last six years.

The work described in this thesis could not have been completed without the assistance of a number of additional people. I thank Drs. Theresa Lee, Cheryl Sisk, and Lyn Clemens for donating specimens used in Chapter 2. Dr. Sharleen Sakai provided invaluable advice on technical procedures for Chapters 4 and 5, and Dr. John I. Johnson graciously offered his assistance in the organization and analysis of data for Chapter 2. I also thank David McFarlane for the many hours he spent helping to set up and troubleshoot the data recording systems and computers used in our lab.

Financial support for this research came from NIMH RO1-MH53433 awarded to Laura Smale, a grant from the Sigma Xi Foundation, and funding from the Graduate School, the Department of Zoology, and the Ecology, Evolutionary Biology and Behavior Program at Michigan State University.

Finally, I would like to thank my friends and family for their support and encouragement. Thanks to my fellow Spartan alumni from 8 South Hubbard for your friendship from our undergrad days to the present. Special thanks to the Pavelka family for your amazing generosity and friendship over the years. Last but not least, to my wife, my parents, my siblings, and my extended family, thank you all for believing in me.

## TABLE OF CONTENTS

<b>LIST OF TABLES.....</b>	<b>x</b>
<b>LIST OF FIGURES .....</b>	<b>xi</b>
<b>KEY TO ABBREVIATIONS.....</b>	<b>xv</b>
<b>CHAPTER 1</b>	
<b>Introduction .....</b>	<b>1</b>
General Introduction .....	1
Overview of orexin .....	1
Orexin discovery .....	1
Orexin and feeding .....	4
Orexin and arousal .....	8
Other actions of orexin .....	9
Introduction to the grass rat .....	11
Overview of chapters .....	13
<b>CHAPTER 2</b>	
<b>A comparative analysis of the distribution of orexin in the brains of nocturnal and diurnal rodents.....</b>	<b>17</b>
Introduction.....	17
Methods and materials .....	23
Animal handling .....	23
Tissue collection and processing .....	23
Cell and fiber counts and analysis .....	25
Results .....	26
Orexin cell bodies .....	26
Orexin fiber distribution .....	49
Discussion .....	74
General observations .....	74
Species differences in OXA and OXB cell distribution .....	77
Species differences in OXA and OXB fiber distribution.....	82
Summary.....	85
<b>CHAPTER 3</b>	
<b>Individual differences in wheel-running rhythms are related to temporal and spatial patterns of activation of orexin A and B cells in a diurnal rodent (<i>Arvicanthis niloticus</i>).....</b>	<b>88</b>
Introduction.....	88
Methods.....	91
Animal housing and determination of activity patterns .....	91
Tissue processing and analysis .....	92

Patterns of Fos Expression in Orexin Cells.....	97
IGL Anatomy .....	100
Results .....	101
Patterns of Fos Expression in Orexin Cells.....	101
IGL Anatomy .....	105
Discussion .....	108
IGL Anatomy .....	108
Fos expression in orexin cells: general patterns .....	110
Fos expression in orexin cells: heterogeneity of orexin cell function.....	111
General conclusions .....	113
 <b>CHAPTER 4</b>	
<b>Orexin fibers form appositions with Fos expressing</b>	
<b>neuropeptide-Y cells in the grass rat intergeniculate leaflet....</b>	<b>117</b>
Introduction.....	117
Materials and Methods .....	120
Results .....	123
Discussion .....	125
 <b>CHAPTER 5</b>	
<b>Retrograde labeling of orexin neurons projecting to the grass rat</b>	
<b>intergeniculate leaflet .....</b>	<b>130</b>
Introduction.....	130
Methods.....	133
Animal handling .....	133
Surgical procedures .....	134
Tissue collection and processing .....	135
Cell counts and analysis .....	136
Results .....	137
Discussion .....	139
 <b>References.....</b>	<b>150</b>



## LIST OF TABLES

Table 2.1. Distribution of orexin A and B cell bodies in the Long-Evans rat, grass rat, Syrian hamster, and degu. The relative densities of OXA- or OXB-containing cells are indicated in each column as very dense (++++), dense (+++), moderately dense (++) , sparse (+), or absent (-). .....33

Table 2.2. Pairwise correlation matrix of orexin A (top) and orexin B (bottom) fiber distribution in the Long-Evans rat, grass rat, Syrian hamster, and degu. Correlation values were obtained from a principal component factor analysis of orexin A and orexin B fiber density patterns in all four species. Values listed at intersections between rows and columns represent the correlation in fiber density between species indicated by the corresponding row and column labels. All values represent significant correlations ( $p < 0.001$ ). .....51

Table 2.3. Distribution of orexin A and B fibers in the Long-Evans rat, grass rat, Syrian hamster, and degu. The relative densities of OXA- or OXB-containing fibers are indicated in each column as very dense (indicated by ++++), dense (+++), moderately dense (++) , sparse (+), or absent (-). Unmarked rows indicate areas for which no data are available.....52

# LIST OF FIGURES

Images in this dissertation are presented in color.

Figure 1.1. Actogram, double-plotted, depicting wheel running patterns typical of day-active (top) and night-active (bottom) grass rats maintained in a 12:12 light-dark cycle. Each horizontal line in the actogram represents 48 hours; vertical marks indicate wheel running activity. Lighting conditions are indicated by the bar at the bottom. Note that both day- and night-active animals exhibit a bout of activity just prior to lights-on.....14

Figure 2.1. Photomicrographs of orexin A and orexin B cell bodies in the Long-Evans rat, grass rat, Syrian hamster, and degu. Scale bar = 100  $\mu\text{m}$ . .....27

Figure 2.2. Photomicrographs of orexin A cell bodies in the paraventricular nucleus (Pa) of the Long-Evans rat (A), grass rat (B), and Syrian hamster (C). Note lack of similar cell bodies in the degu (D). 3V: third ventricle. Scale bar = 200  $\mu\text{m}$ . .....30

Figure 2.3. Photomicrographs of orexin A cell bodies in the supraoptic nucleus (SO) of the Long-Evans rat (A), grass rat (B), and Syrian hamster (C). Note lack of similar cell bodies in the degu (D). OC: optic chiasm. Scale bar = 200  $\mu\text{m}$ . ....31

Figure 2.4. Photomicrographs of paraventricular nucleus (Pa; column 1) and supraoptic nucleus (SO; column 2) of the Long-Evans rat, grass rat, and Syrian hamster after preabsorption with orexin A blocking peptide. Note that preabsorption with blocking peptide eliminates cell bodies seen in Figures 2.6 and 2.7. 3V: third ventricle; OC: optic chiasm. Scale bar = 200  $\mu\text{m}$ . .....32

Figure 2.5. Line drawing of every 6th section through the region of the Long-Evans rat hypothalamus that contains orexin cells. Sections are ordered from rostral (A) to caudal (N). Filled circles indicate locations where both orexin A and orexin B neurons are found, while open circles indicate orexin A neurons only. 3V: third ventricle; SCN: suprachiasmatic nucleus; OC: optic chiasm; f: fornix; mt: mammillothalamic tract. Scale bar = 500  $\mu\text{m}$ . .....34

Figure 2.6. Line drawing of every 6th section through the region of the grass rat hypothalamus that contains orexin cells. Sections are ordered from rostral (A) to caudal (L). Filled circles indicate locations where both orexin A and orexin B neurons are found, while open circles indicate orexin A neurons only. 3V: third ventricle; SCN: suprachiasmatic nucleus; OC: optic chiasm; f: fornix; mt: mammillothalamic tract. Scale bar = 500  $\mu\text{m}$ . .....38

Figure 2.7. Line drawing of every 6th section through the region of the Syrian hamster hypothalamus that contains orexin cells. Sections are ordered from rostral (A) to caudal (J). Filled circles indicate locations where both orexin A and

orexin B neurons are found, while open circles indicate orexin A neurons only. 3V: third ventricle; SCN: suprachiasmatic nucleus; OC: optic chiasm; f: fornix; mt: mammillothalamic tract. Scale bar = 500  $\mu\text{m}$ . .....41

Figure 2.8. Line drawing of every 6th section through the region of the degu hypothalamus that contains orexin cells. Sections are ordered from rostral (A) to caudal (N). Filled circles indicate locations where both orexin A and orexin B neurons are found. 3V: third ventricle; OC: optic chiasm; f: fornix; mt: mammillothalamic tract; aq: cerebral aqueduct. Scale bar = 500  $\mu\text{m}$ . .....44

Figure 2.9. Photomicrographs of orexin A fibers around the suprachiasmatic nucleus (SCN) of the Long-Evans rat (A), grass rat (B), Syrian hamster (C), and degu (D). 3V: third ventricle; OC: optic chiasm. Scale bar = 200  $\mu\text{m}$ . .....64

Figure 2.10. Photomicrographs of orexin A fibers in the ventromedial hypothalamic nucleus (VMH) of the Long-Evans rat (A), grass rat (B), Syrian hamster (C), and degu (D). Note markedly higher density of orexin fibers in the degu VMH than in the other three species. 3V: third ventricle; Arc: arcuate nucleus. Scale bar = 300  $\mu\text{m}$ . .....65

Figure 2.11. Photomicrographs of orexin A fibers in the lateral mammillary nucleus (LM) of the Long-Evans rat (A), grass rat (B), Syrian hamster (C), and degu (D). Note higher density of orexin fibers in the hamster LM than in the other three species. MM: medial mammillary nucleus. Scale bar = 200  $\mu\text{m}$ . .....66

Figure 2.12. Photomicrographs of orexin A fibers in the intergeniculate leaflet (IGL) of the Long-Evans rat (A), grass rat (B), Syrian hamster (C), and degu (D). DLG: dorsolateral geniculate nucleus; VLG: ventrolateral geniculate nucleus. Scale bar = 200  $\mu\text{m}$ . .....68

Figure 2.13. Photomicrographs of orexin A fibers in the centrolateral nucleus (CL) of the Long-Evans rat (A), grass rat (B), Syrian hamster (C), and degu (D). Note higher density of orexin fibers in the degu CL than in the other three species. LV: lateral ventricle; PVT: paraventricular thalamic nucleus, MHb: medial habenular nucleus; LHb: lateral habenular nucleus. Scale bar = 300  $\mu\text{m}$ . .....69

Figure 2.14. Photomicrographs of orexin A fibers in the xiphoid nucleus (Xi) of the Long-Evans rat (A), grass rat (B), Syrian hamster (C), and degu (D). Note relative lack of orexin fibers in the degu Xi in comparison with the other three species. 3V: third ventricle. Scale bar = 200  $\mu\text{m}$ . .....70

Figure 2.15. Photomicrographs of orexin A fibers in the dorsal raphe nucleus (DR) of the Long-Evans rat (A), grass rat (B), Syrian hamster (C), and degu (D). 4: trochlear nucleus; Aq: cerebral aqueduct. Scale bar = 300  $\mu\text{m}$ . .....72

Figure 2.16. Photomicrographs of orexin A fibers in the locus coeruleus (LC) of the Long-Evans rat (A), grass rat (B), Syrian hamster (C), and degu (D). 4V: fourth ventricle. Scale bar = 200  $\mu\text{m}$ . .....73

Figure 2.17. Photomicrographs of orexin A fibers in the flocculus (FI) of the Long-Evans rat (A), grass rat (B), Syrian hamster (C), and degu (D). Note higher density of orexin fibers in the degu FI than in the other three species. PFI: paraflocculus; VC: ventral cochlear nucleus. Scale bar = 200  $\mu$ m. ....75

Figure 3.1. (A) Actogram illustrating wheel running activity of an individual grass rat. Although initially day-active, this individual exhibited a spontaneous switch to a night-active pattern, illustrating both the two basic patterns and the lack of transients during a switch. This spontaneous switch is atypical; most animals in our colony establish stable day- or night-active rhythms shortly after introduction of a wheel. (B) Line graph illustrating average hourly wheel revolutions over a 5 day monitoring period of all day-active (n = 18, open circles) and night-active (n = 18, closed circles) grass rats used in this study. Arrows at ZT 4 and ZT 16 indicate sampling times for animals used in this study. Bar at bottom indicates light cycle. ....93

Figure 3.2. Drawing of representative sections through (A) rostral, (B) middle and (C) caudal sections of the grass rat LH. Boxes representing sampling area are 1200 x 700  $\mu$ m, divided from left to right into medial, central, and lateral divisions. Dots represent cells stained for OXA. Distribution of OXB cells were similar (not shown). 3V = 3<sup>rd</sup> ventricle; f = fornix. ....99

Figure 3.3. Photomicrograph (40x) of orexin A and B cells in the grass rat LH. Cells marked \* are expressing Fos-IR only; Open arrows indicate cells expressing only OXA (Panel A) or OXB (Panel B); Solid arrows point to double-labeled cells. Scale bar = 50  $\mu$ m. ....102

Figure 3.4. Temporal patterns of mean ( $\pm$  SEM) levels of Fos expression in OXA (top) and OXB (bottom) cells in day- and night-active animals sacrificed at ZT 4 and ZT 16. Light bars represent day-active animals; dark bars represent night-active grass rats. Significant differences ( $p < 0.05$ ) noted by different letters. ...103

Figure 3.5. Fos-IR in orexin cells in grass rats housed with (+) and without (-) running wheels. Day-active grass rats (top) were sacrificed at ZT 4, night-active animals (bottom) at ZT 16. Dark bars = OXA; light bars = OXB. Significant differences ( $p < 0.05$ ) noted by different letters. Removal of running wheel caused significant reductions in Fos-IR only in night-active animals. Effects of wheels were not significant in day-active animals, although trends were similar ( $p = 0.06$  and  $p = 0.08$  for OXA and OXB, respectively). ....104

Figure 3.6. Regional patterns of orexin Fos-IR in night-active grass rats housed with (top) or without (bottom) running wheels at ZT 16 demonstrating both the medial to lateral gradient in orexin cell activity, and the differences and similarities between OXA- and OXB-labeled cells. Significant differences ( $p < 0.05$ ) noted by different letters. Dark bars = OXA; light bars = OXB. ....106

Figure 3.7. Photomicrographs of OXA (Panels A and B) and OXB (Panels C and D) fibers and NPY cells in the grass rat IGL. Arrows indicate where contacts between NPY cells and orexin fibers appear to be present. Panels (A) and (C) are 40x; scale bar is 50  $\mu\text{m}$ . Panels (B) and (D) are 100x close-ups of regions marked with \* in panels (A) and (C), respectively; scale bar is 20  $\mu\text{m}$ . .....107

Figure 4.1. Photomicrographs (100x) of orexin A (OXA) fiber appositions with neuropeptide-Y (NPY) cells (Panels A, B, C) or NPY cells expressing Fos (Panels D, E, F) in the grass rat IGL. Arrows indicate appositions between OXA fibers and NPY cells; Scale bar is 50  $\mu\text{m}$ . .....124

Figure 4.2. Percentages ( $\pm$ SEM) of Fos expression in neuropeptide-Y (NPY) cells that do (NPY-OXA) or do not (NPY-Only) exhibit appositions with orexin A (OXA) fibers in the IGL of day- and night-active grass rats. Asterisk indicates significant difference between columns ( $p < 0.0001$ ). Dark bars = NPY+OXA cells; light bars = NPY-Only cells. ....126

Figure 5.1. Line drawing of the lateral hypothalamic area at low magnification (5x) depicting the 1600  $\mu\text{m}$  x 700  $\mu\text{m}$  sampling area used in this study. The sampling box is aligned to the third ventricle and ventral border of the fornix, and divided from left to right into 40  $\mu\text{m}$  divisions labeled Medial (M), Central (C), Lateral 1 (L1), and Lateral 2 (L2), respectively. Circles represent cells containing orexin A. Scale bar = 500  $\mu\text{m}$ ; f = fornix, mt = mammalothalamic tract, 3V = third ventricle. ....138

Figure 5.2. Line drawings depicting injection sites for animals described in this study. Darkly shaded area indicates placement of needle tip; lighter shaded area indicates spread of cholera toxin tracer from injection site. All drawings were traced under low magnification (10x). Drawings are arranged rostrally to caudally through the intergeniculate leaflet. Scale bar = 300  $\mu\text{m}$ . APT: anterior pretectal nucleus; ar: acoustic radiation; DLG: dorsolateral geniculate nucleus; IGL: intergeniculate leaflet; LP: lateral posterior thalamic nucleus; ml: medial lemniscus; opt: optic tract; Po: posterior thalamic nuclear group; SubG: subgeniculate nucleus; VLG: ventrolateral geniculate nucleus; VPM: ventral posteromedial thalamic nucleus; ZID: zona inserta, dorsal; ZIV: zona incerta, ventral. ....140

Figure 5.3. Photomicrographs depicting cells in the lateral hypothalamus after staining with Texas Red labeled orexin (red fluorescence, panels A, D, and G) and injection of FITC-conjugated cholera toxin B (green fluorescence, panels C, F, and I). Panels B, E, and H are composite images showing both labels. Neurons exhibiting immunoreactivity for both orexin and cholera toxin B are marked with an asterisk (\*). Arrows indicate cells labeled with cholera toxin B only. Scale bar = 25  $\mu\text{m}$ . ....142

## KEY TO ABBREVIATIONS

Abbreviation	Definition
AB complex .....	avidin-biotin complex
ANOVA .....	analysis of variance
Arc.....	arcuate nucleus
AVP.....	arginine vasopressin
BNST .....	bed nucleus of the stria terminalis
CL .....	centrolateral thalamic nucleus
CRF.....	corticotrophin releasing factor
CSF.....	cerebrospinal fluid
CTB.....	cholera toxin subunit B
CTB-FITC.....	CTB conjugated with AlexaFluor 488
DAB.....	diaminobenzidine
DH.....	dorsal hypothalamic area
DMH.....	dorsomedial hypothalamic nucleus
GFAP .....	glial fibrillary acidic protein
GHT .....	geniculohypothalamic tract
GnRH.....	gonadotropin releasing hormone
HPA.....	hypothalamic-pituitary-adrenal axis
HPG .....	hypothalamic-pituitary-gonadal axis
IGL .....	intergeniculate leaflet
IR .....	immunoreactive, immunoreactivity
LC .....	locus coeruleus
LD .....	light-dark
LE.....	Long-Evans
LH .....	lateral hypothalamus
LHA.....	lateral hypothalamic area
LM.....	lateral mammillary nucleus
MCH.....	melanin concentrating hormone
NDS .....	normal donkey serum
NHS .....	normal horse serum
NPY.....	neuropeptide-Y
OT .....	oxytocin
OX <sub>1</sub> R.....	orexin receptor 1
OX <sub>2</sub> R.....	orexin receptor 2
OXA .....	orexin A
OXB .....	orexin B
Pa.....	paraventricular hypothalamic nucleus
PBS.....	phosphate buffered saline
PBS-TX .....	PBS with 0.3% Triton-X 100
PC .....	paracentral thalamic nucleus
PCA.....	principal components factor analysis
PeF .....	perifornical region
PH .....	posterior hypothalamic area

Abbreviation	Definition
PPO .....	preproorexin
PV .....	paraventricular thalamic nucleus
RCh.....	retrochiasmatic area
REM .....	rapid eye movement
RHT.....	retinohypothalamic tract
SCN .....	suprachiasmatic nucleus
SD .....	Sprague-Dawley
SO .....	supraoptic nucleus
Sol.....	nucleus of the solitary tract
SOR .....	supraoptic retrochiasmatic nucleus
Subl.....	subincertal thalamic nucleus
SuM.....	supramammillary nucleus
TC .....	tuberum cinerum
VMH .....	ventromedial hypothalamic nucleus
Xi.....	xiphoid nucleus
ZT .....	Zeitgeber time

# **CHAPTER 1**

## **Introduction**

### **General Introduction**

The research in this dissertation focuses upon two major goals. One is to describe species differences in the distribution of the orexins, peptides implicated in the regulation of ingestive behavior, sleep-wake and general arousal, and the modulation of somatomotor functions. The second is to examine the functional and anatomical relationships between the orexins and activity state in the diurnal grass rat, *Arvicanthis niloticus*. In this introductory chapter I will provide (1) an overview of the orexins and their function, (2) a short description of the grass rat, the primary animal model used in these studies, and (3) a summary of the questions addressed in each chapter of this thesis.

### **Overview of orexin**

#### **Orexin discovery**

When the discovery of a novel peptide apparently limited to cell bodies in the hypothalamus was announced in 1998 (de Lecea et al. 1998; Sakurai et al. 1998), interest was high due to the possibility of its involvement with feeding. The peptide, dubbed orexin by Sakurai et. al. (1998) and hypocretin by de Lecea et. al. (1998), was independently discovered in two laboratories using very different methods. One group isolated the long form of orexin, orexin A (OXA), by searching for ligands for “orphaned” G-protein coupled receptors (Sakurai et al. 1998). The second group first isolated the precursor protein, preproorexin, in



1996 using a subtractive PCR technique to recover hypothalamus-specific proteins (Gautvik et al. 1996) but did not publish a detailed investigation of the precursor or its derivatives until early in 1998 (de Lecea et al. 1998).

The initial reports of these discoveries showed that the orexins are a family containing two peptides, the 33 amino acid OXA (hypocretin-1) and the shorter 28 amino acid orexin B (OXB, hypocretin-2), both derived from the precursor protein, preproorexin (PPO), through proteolytic processing (de Lecea et al. 1998; Sakurai et al. 1998). The PPO gene, which is highly conserved across species, has some similarities with the secretin/incretin family of peptides (de Lecea et al. 1998), and appears to have arisen early during chordate evolution through a circular mutation of an incretin gene (Alvarez and Sutcliffe 2002). Orexin has been identified in all major vertebrate taxa, including fish (Kaslin et al. 2004; Huesa et al. 2005), amphibians (Shibahara et al. 1999; Yamamoto et al. 2004; Singletary et al. 2005), reptiles (Farrell et al. 2003), birds (Ohkubo et al. 2002), and mammals (Sakurai et al. 1999). Preproorexin mRNA was initially reported to be limited to cell bodies in the lateral hypothalamus (LH) (Gautvik et al. 1996), although more recent reports have provided evidence for orexin neurons in other brain regions, including the amygdala, median eminence, and ependyma (Chen et al. 1999; Kummer et al. 2001; Ciriello et al. 2003c). Because the orexin cells outside of the lateral hypothalamus have not been extensively studied, references to orexin neurons in this dissertation will refer only to neurons in the main population of orexin cells located near the fornix, unless otherwise specified. To avoid confusion when discussing the distribution

of orexin-containing neurons, references to the lateral hypothalamus as a whole in this dissertation will be designated using the abbreviation LH, while the lateral hypothalamic area, a specifically defined subregion of the LH, will be referred to as LHA.

The orexins bind to two G-protein coupled receptors; OXA binds equally to either orexin receptor 1 (OX<sub>1</sub>R) or orexin receptor 2 (OX<sub>2</sub>R); OXB binds to both receptors but displays moderate selectivity for OX<sub>2</sub>R (Sakurai et al. 1998; Smart et al. 1999). Orexin A and B have been shown to act directly upon axon terminals to increase the release of both GABA and glutamate (van den Pol et al. 1998). The orexins may also affect the presynaptic effect of Ca<sup>2+</sup>-dependent transmitters by increasing calcium levels, both through mobilization of internal Ca<sup>2+</sup> stores and through secondary influx of external calcium (Smart et al. 1999).

Although the total number of orexin neurons is fairly small, axonal projections from these cells extend from the LH to many regions of the rat brain and spinal cord (Peyron et al. 1998; Chen et al. 1999; Cutler et al. 1999; Date et al. 1999; Nambu et al. 1999). The overall distribution of orexin fibers in the rat brain and spinal cord suggested that, in addition to feeding actions, the orexins might be involved in the sleep-wake cycle, emotional responses, thermoregulation and nociception (Peyron et al. 1998; Cutler et al. 1999; Nambu et al. 1999).

There is also strong evidence for an important role for orexin outside of the central nervous system. Both orexin and orexin receptors are present in peripheral tissues. Both PPO and orexin receptor mRNA are present in the gut in

several species, including rats, guinea pigs, sheep, and humans (Kirchgessner and Liu 1999; Ehrstrom et al. 2005). Additionally, PPO mRNA has been identified in the heart and testicular tissue of rats (Johren et al. 2001), and orexin receptors have been found in rat lung, as well as the adrenal glands and gonads of both rats and sheep (Johren et al. 2001; Zhang et al. 2005a).

### **Orexin and feeding**

The hypothalamic distribution of cell bodies containing the precursor protein suggested that orexins are involved in feeding behavior. Prior to the discovery of orexin, the only other peptide known to be found in cell bodies limited to the LH was melanin concentrating hormone (MCH), a peptide known to be involved the regulation of feeding (Qu et al. 1996). Early experiments showed that 48 hours of fasting resulted in a 2.4-fold increase in rat preproorexin mRNA (Sakurai et al. 1998), and that injections of OXA and OXB could elicit ingestion in rats, although the effects of OXA appeared to be stronger than those of OXB, perhaps due to its more stable structure (Sakurai et al. 1998). This difference in the orexigenic effects of OXB in comparison to OXA has been replicated several times, with most studies suggesting that OXB is less effective than OXA in eliciting feeding or drinking behavior (Sakurai et al. 1998; Edwards et al. 1999; Kunii et al. 1999). In some cases OXB has been ineffective in eliciting any ingestive behavior whatsoever (Lubkin and Stricker-Krongrad 1998; Sweet et al. 1999).

Orexin effects on ingestive behavior appear to depend upon interactions with other food-related signaling systems, such as neuropeptide-Y (NPY), leptin,

MCH, grehlin, galanin, and agouti-related protein (Broberger et al. 1998; Horvath et al. 1999a; Rauch et al. 2000; Schwartz et al. 2000; Sakurai 2003; Ehrstrom et al. 2005; Takenoya et al. 2005). For example, the ingestive behavior stimulated by orexin is attenuated or blocked by leptin, a potent inhibitor of food intake (reviewed in Schwartz et al. 2000). In one study, pretreatment with leptin blocked orexin-induced activity in nearly half of the orexin responsive neurons identified in the arcuate nucleus (Rauch et al. 2000). In addition, leptin injections in the rat are capable of blocking both OXA-induced feeding behavior and NPY-induced Fos immunoreactivity in OXA cells (Niimi et al. 2001). Leptin may block the effects of orexins directly or indirectly, as some OXB cells have been shown to express leptin receptors, and NPY cells in the rat and monkey Arc receiving orexin fiber contacts also expressed leptin receptors (Horvath et al. 1999a). Orexin appears to have a reciprocal blocking effect on leptin, as OXA administered intravenously reduces plasma leptin concentrations in humans (Ehrstrom et al. 2005).

There are several lines of evidence that suggest interactions between orexin and blood glucose levels. Insulin-induced hypoglycemia results in a rapid rise in nuclear c-Fos expression in OXA cells of the rat (Moriguchi et al. 1999). Orexin-containing pancreatic islet cells also contain insulin in humans, and some of these cells express orexin receptors (Ehrstrom et al. 2005). Intravenous orexin administration raises insulin levels in the blood, presumably by stimulating pancreatic cells expressing orexin receptors (Ehrstrom et al. 2005). In addition, there are some indications that defects in the orexin system may affect the regulation of glucose in humans. For example, in humans with narcolepsy, a

condition associated with low or nonexistent levels of orexins (Nishino et al. 2000; Nishino et al. 2001), there appears to be a higher risk of non-insulin dependent diabetes (Honda et al. 1986).

Despite the documented relationship between the orexins and feeding and satiety systems, there is some controversy over the actual effect orexins have on feeding behavior. The administration of orexins into the central nervous system has not always reliably increased feeding behavior (reviewed in Sutcliffe and de Lecea 2000). While it is generally agreed that the orexins do not represent as potent a stimulator of feeding as NPY, for example, the relative strength or weakness of the orexins as compared to other peptides such as MCH has not been clearly established (Lubkin and Stricker-Krongrad 1998; Edwards et al. 1999). Indeed, in studies performed in various laboratories, the orexins elicited an ingestive response ranging between very robust (Sakurai et al. 1998; Yamanaka et al. 2000), moderate (Edwards et al. 1999; Sweet et al. 1999), and weak (Lubkin and Stricker-Krongrad 1998).

The variation in feeding behavior elicited in individual studies may be explained by several factors. First, orexins have been shown to increase both GABA and glutamate release in the rat *in vitro* (van den Pol et al. 1998). These peptides thus appear to have the ability to affect the fast synaptic excitatory or inhibitory activity of many parts of the hypothalamus. Therefore, the reported effects of centrally administered orexins may not be physiologically relevant, as spillover into other brain regions might activate or inhibit systems not normally involved in the feeding effects of orexin. The actual discrete local effects of

naturally released peptides are presumably much more finely controlled by the nervous system than even the most carefully placed injection. Indirect actions or spillover effects of injected orexins have been proposed as explanations for differences seen among several studies (Lubkin and Stricker-Krongrad 1998; Edwards et al. 1999). Secondly, the relative degree of feeding behavior observed after introduction of orexin may be related to stress, as at least some orexin-induced ingestive responses rely upon interactions between orexin, NPY, and corticosterone levels (Horvath et al. 1999a; Ida et al. 2000a; Jászberényi et al. 2000; Yamanaka et al. 2000). Finally, orexin-induced feeding might be time-dependent. Circadian responsiveness of the feeding effect of OXA in the rat has been observed in at least one study, with an increase in food intake following OXA injection only occurring during the light phase of the daily light-dark cycle (Kotz et al. 2002).

Although the exact role of the orexins in feeding has yet to be established, it is possible that the orexins are involved in the coordination of locomotor activity and arousal in response to stress and variation in food availability. During short-term food deprivation, orexin receptor mRNA is up-regulated (Lu et al. 2000). Orexins promote wakefulness, occasionally leading to increased searching and exploratory behavior (Ida et al. 1999; Jones et al. 2001). A decrease in food availability may thus increase arousal at times when the animal is normally quiescent, leading to increased locomotion and searching behaviors. By modifying the timing of arousal, the orexin system might increase the probability of the animal encountering a food source that is not available at other times of

the day. The orexin system is clearly uniquely situated for involvement in the coordination of an interrelated suite of behaviors related to food intake and arousal.

### **Orexin and arousal**

The overall distribution of orexin fibers in the brain has suggested that the orexins play a role in a number of behaviors, including the maintenance of arousal (Hagan et al. 1999; Horvath et al. 1999b). Orexin fibers have been shown to project to various brain nuclei implicated in the control of sleep state (Peyron et al. 1998; Date et al. 1999; Nambu et al. 1999; Mintz et al. 2001; Moore et al. 2001). Application of OXA in the locus coeruleus (Hagan et al. 1999; Bourgin et al. 2000) and lateral preoptic area (Methippara et al. 2000) of the rat have been shown to increase wakefulness, primarily through a decrease in rapid eye movement (REM) sleep (Bourgin et al. 2000). Activity in locus coeruleus neurons increases following application of OXA (Hagan et al. 1999; Horvath et al. 1999b; Bourgin et al. 2000). In contrast to OXA, OXB does not seem to affect wakefulness (Bourgin et al. 2000).

The orexin cells also receive input from brain circuits involved in regulation of sleep-wakefulness. In mammals, circadian organization of activity including sleep-wake behavior is regulated by an endogenous clock located in the suprachiasmatic nucleus (SCN) (reviewed in Weaver 1998). Orexin cell bodies in the lateral hypothalamus receive both limited direct contact from the SCN (Abrahamson et al. 2001), as well as substantial indirect contact from the SCN via the medial preoptic area (Deurveilher and Semba 2005). Introduction of

chemicals known to increase arousal in rats, such as methamphetamines or the anti-narcoleptic drug Modafanil, increase nuclear Fos expression in orexin cell bodies (Weaver 1998; Chemelli et al. 1999; Estabrooke et al. 2001). Furthermore, increasing the behavioral arousal of rats by sleep deprivation induced by handling also increases the expression of nuclear Fos in OXA cells (Estabrooke et al. 2001). Orexin cells thus appear to be capable of both receiving information relating to the arousal state of the animal, and relaying arousal information to other nuclei known to promote wakefulness. The recent finding that a defect in the orexin system is associated with the sleep disorder narcolepsy (Chemelli et al. 1999; Lin et al. 1999; Hara et al. 2001; Hungs et al. 2001) has strengthened the association between the orexins and arousal.

### **Other actions of orexin**

In addition to the feeding and arousal-related actions of the orexins, there is evidence for the involvement of orexins in the modulation of general activity. For example, in rats, injections of OXA and, to a lesser extent OXB have been shown to increase locomotor activity (Ida et al. 2000b; Nakamura et al. 2000; Jones et al. 2001; Yoshimichi et al. 2001; Kotz et al. 2002) and burrowing behavior (Ida et al. 1999). Orexin B does not appear to have as strong an effect on general locomotor activity in lab rats as does OXA, but has been shown to be more effective than OXA in eliciting searching behavior (Ida et al. 1999; Jones et al. 2001) or exploration of novel environments (Jones et al. 2001). The increase in locomotor activity observed in rats after application of OXA does not appear to be related to the concurrent increase in feeding often observed following orexin



injections (Kotz et al. 2002). Face washing and grooming behavior also increase in frequency following injections of OXA but not OXB (Ida et al. 1999; Ida et al. 2000b; Nakamura et al. 2000; Duxon et al. 2001; Jones et al. 2001). The increase in grooming following injection of OXA in the rat is blocked by prior application of a CRF antagonist, suggesting that the behavior may be linked to stress (Ida et al. 2000b). Both the grooming and locomotor effects of orexins may also involve interactions with dopaminergic (Nakamura et al. 2000) and serotonergic (Nakamura et al. 2000; Duxon et al. 2001) systems.

Orexin may also be involved in the regulation of autonomic functions. There are extensive projections from orexin neurons to hindbrain nuclei that regulate cardiovascular and sympathetic processes (Date et al. 1999; Zheng et al. 2005). Several studies have shown that application of OXA increases heart rate, blood pressure, and respiration rate in rats and mice (Shirasaka et al. 2002; Ciriello et al. 2003a; de Oliveira and Ciriello 2003; Zhang et al. 2005b; Zheng et al. 2005). Body temperature, which generally rises during active periods and decreases when animals are quiescent, increases following injection of OXA (Yoshimichi et al. 2001), but not after injection of OXB (Jones et al. 2001). The increase in body temperature following application of OXA does not appear to be a result of increased locomotor activity (Yoshimichi et al. 2001).

Finally, orexins have been implicated in modulation of the hypothalamic-pituitary-gonadal (HPG) axis at several levels. First, within the hypothalamus, orexin has been shown to stimulate the release of gonadotropin releasing hormone (GnRH) (Russell et al. 2001). Cells containing GnRH receive direct

contact from orexin fibers in rats and sheep (Iqbal et al. 2001; Campbell et al. 2003), and in rats GnRH neurons have also been shown to express orexin receptors (Campbell et al. 2003). In addition, orexin projections to the hypothalamic magnocellular nuclei that in turn project to the pituitary also appear to be important in HPG regulation. Magnocellular neurons in the Pa express orexin receptors, and these receptors are selectively upregulated during the estrous cycle and early lactation in rats (Wang et al. 2003).

At the level of the pituitary, more evidence for orexin involvement in HPG regulation has been found. Specifically, both rat and human pituitary express orexin receptors (Blanco et al. 2001; Johren et al. 2001), and OXA acting on these receptors appears to directly block GnRH-mediated release of luteinizing hormone in proestrous female rats (Russell et al. 2001). With respect to the gonads, testicular tissue in rats expresses orexin, and testicular tissue in both rats and sheep expresses orexin receptor mRNA (Johren et al. 2001; Zhang et al. 2005a). Although orexin mRNA appears to be absent in rat ovary, orexin receptors are present (Johren et al. 2001). Although the specific actions of orexin on gonadal tissue are currently unknown, the presence of orexin and orexin receptors in the gonads suggests the possibility that orexins may affect the HPG axis at this level as well as at the hypothalamic and pituitary levels.

### **Introduction to the grass rat**

The unstriped Nile grass rat (*Arvicanthis niloticus*, hereafter referred to as the grass rat) is a diurnal murid rodent indigenous to large portions of sub-Saharan Africa. Our laboratory maintains a breeding colony of grass rats, derived

from wild animals captured in 1993 in the Masai Mara National Reserve in Kenya (Katona and Smale 1997). Although there has been some confusion over the taxonomic grouping of the genus *Arvicanthis* (reviewed in McElhinny 1996), a recent karyological analysis performed at the Museum National d'Histoire Naturelle (Paris) confirms that the grass rats in our colony are *Arvicanthis niloticus* Desmarest 1822 (Challet et al. 2002). The grass rat exhibits strong diurnal rhythms of daily activity in the wild (Blanchong and Smale 2000). In the laboratory, the grass rat is diurnal with respect to body temperature, general activity, and reproductive behavior (McElhinny et al. 1997). The grass rat is a murid rodent, and as such is closely related to the standard laboratory rat (*Rattus norvegicus*). The grass rat has proven to be a useful diurnal animal model for studies of sleep (Novak et al. 1999, 2000b), reproduction (McElhinny et al. 1997; Mahoney et al. 2004; Mahoney and Smale 2005b, 2005a), and the circadian regulation of activity (Katona et al. 1998; Nuñez et al. 1999; Mahoney et al. 2000; Novak et al. 2000a; Smale et al. 2001a; Schwartz et al. 2004).

Although the grass rat appears to be a strictly diurnal animal, there is some degree of plasticity in their behavior. Specifically, when given continuous access to a running wheel, some individual grass rats exhibit what appears to be an unusual form of masking, switching from a day-active to a night-active pattern of activity (Blanchong et al. 1999). In our colony, this shift from day- to night-active patterns occurs in approximately 30% of animals given free access to a wheel (Mahoney et al. 2001). Unlike circadian phase-shifting, which involves a gradual transition to a new activity pattern due to re-entrainment of the circadian

clock, this switch to a night-active pattern appears to happen quickly, and is not associated with the transients typical of a phase shift (Nixon and Smale 2004; Redlin and Mrosovsky 2004), and appears to reflect a masking effect of the wheel rather than a shift in the internal clock (Nixon and Smale 2004). Day-active grass rats in a 12:12 light-dark (LD) cycle begin to run in the wheel about one hour prior to lights-on, exhibit moderate to high levels of wheel running throughout the day, and cease running in the wheel within 1 to 2 hours after lights-out (Katona and Smale 1997) (Figure 1.1). The night-active grass rats are like the day-active ones in that they show a rise in activity just prior to lights-on. However, in the night-active grass rats, this bout ends when the lights come on, and there is virtually no activity during the 12 hours of light. They begin to run in the wheel just before lights-out, and this activity continues for five or more hours into the dark period (Blanchong et al. 1999).

## **Overview of chapters**

I present here a series of investigations intended to (1) evaluate species differences and similarities in the distribution of orexin cell bodies and fibers; and (2) shed light on the functional relationship between orexin cells and activity in the grass rat. Two of the four chapters that are a part of this dissertation (Chapter 3 and Chapter 4) have been published with a co-author; for the sake of consistency I have therefore elected to use the term “we” in all chapters that present data. I address the first issue in Chapter 2, where I examine the distribution of OXA and OXB-containing cell bodies and fibers in the brains of two nocturnal and two diurnal species. This study has two primary goals: first, to

**Figure 1.1.** Actogram, double-plotted, depicting wheel running patterns typical of day-active (top) and night-active (bottom) grass rats maintained in a 12:12 light-dark cycle. Each horizontal line in the actogram represents 48 hours; vertical marks indicate wheel running activity. Lighting conditions are indicated by the bar at the bottom. Note that both day- and night-active animals exhibit a bout of activity just prior to lights-on.

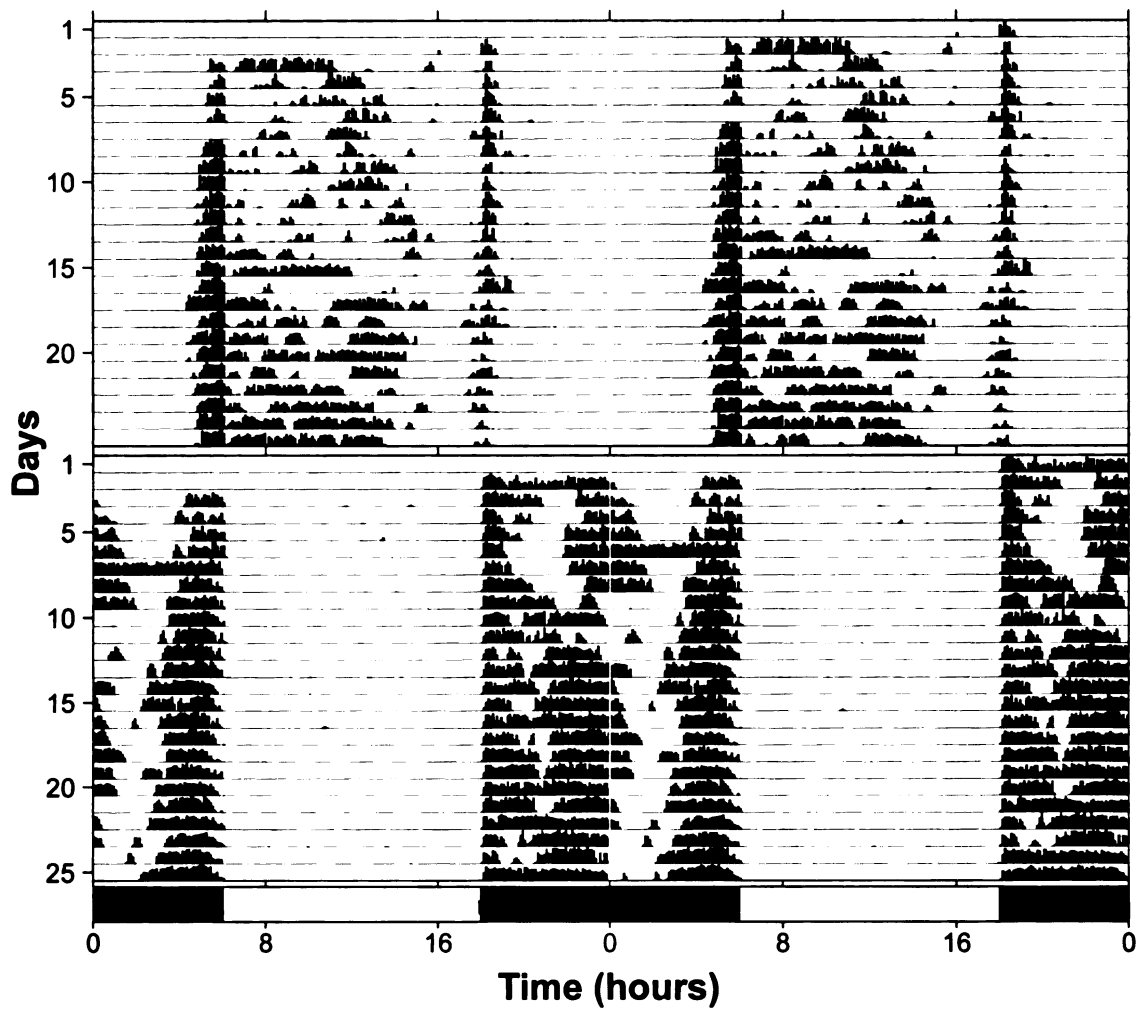


**Figure 1.1.** Actogram, double-plotted, depicting wheel running patterns typical of day-active (top) and night-active (bottom) grass rats. Each horizontal line in the actogram represents 48 hours; vertical marks indicate wheel running activity. Lighting conditions are indicated by the bar at the bottom. Note that both day- and night-active animals exhibit a bout of activity just prior to lights-on.

identify potential species differences in the overall distribution of orexin in these animals, and second, to determine whether differences in orexin distribution might be related to behavioral or anatomical differences in the species examined.

In the remaining chapters, I address the second theme of this dissertation, related to the relationship between orexin and activity patterns in the grass rat. We have previously shown that a difference in Fos activation in NPY cells of the intergeniculate leaflet (IGL) is associated with the differences in wheel running patterns expressed by the individual grass rats (Smale et al. 2001b). The existence of a projection from orexin cells to the IGL led us to hypothesize that orexin plays a role in the modulation of these NPY cells by activity. In Chapter 3, I examine orexin neurons in wheel running grass rats to determine whether patterns of Fos activation in these cells are consistent with a role for orexin in the activation of NPY neurons in the IGL. I then determine whether orexin cells are in a position to modulate NPY cells within the IGL through direct projections to them. In Chapter 4, I continue my investigation of orexin-NPY interactions by determining whether NPY cells that receive input from orexin cells express Fos, and whether this varies as a function of the activity state of the animal. Finally, in Chapter 5, I use a retrograde tract-tracer to determine the distribution of orexin cells that project to the grass rat IGL.

## **CHAPTER 2**

### **A comparative analysis of the distribution of orexin in the brains of nocturnal and diurnal rodents**

#### **Introduction**

The orexins (hypocretins) are a recently described family of peptides originating in cells of the lateral hypothalamus (Sakurai et al. 1998; de Lecea and Sutcliffe 1999). Orexins are thought to be primarily involved in the regulation of arousal and sleep-wake behavior, general activity, body temperature, drinking, and feeding (Lubkin and Stricker-Krongrad 1998; Edwards et al. 1999; Hagan et al. 1999; Kunii et al. 1999; Mondal et al. 1999b; Piper et al. 2000; Estabrooke et al. 2001; Hungs et al. 2001; Yoshimichi et al. 2001; Kotz et al. 2002; Diano et al. 2003; Yamanaka et al. 2003; Kiwaki et al. 2004; Berthoud et al. 2005; Kodama et al. 2005; Thorpe and Kotz 2005). Anatomical studies of orexin fiber distribution in the rat brain show that the densest projections extend to the locus coeruleus, raphé nuclei, periaqueductal central gray, paraventricular hypothalamic nucleus, arcuate nucleus, and the lining of the third ventricle (Peyron et al. 1998; Chen et al. 1999; Cutler et al. 1999; Date et al. 1999; Mondal et al. 1999a; Nambu et al. 1999). Orexin cell bodies in the rat are primarily limited to the perifornical nucleus and lateral hypothalamic area, with more sparse distributions in the dorsal hypothalamic area, posterior hypothalamic area and the dorsomedial hypothalamic nuclei (Peyron et al. 1998; Chen et al. 1999; Cutler et al. 1999; Nambu et al. 1999). Published descriptions of orexin cell and fiber distributions are similar to those in the rat for the Syrian and Djungarian hamster



(McGranaghan and Piggins 2001; Mintz et al. 2001; Khorooshi and Klingenspor 2005) as well as for humans (Moore et al. 1998; Arihara et al. 2000; Moore et al. 2001).

The orexins consist of two peptides, orexin A (OXA, hypocretin-1) and orexin B (OXB, hypocretin-2), derived from the same precursor protein, preproorexin (de Lecea et al. 1998; Sakurai et al. 1998). The orexins bind to two G-coupled protein receptors, orexin receptors 1 (OX<sub>1</sub>R, HCRTR-1) and 2 (OX<sub>2</sub>R, HCRTR-2) (Sakurai et al. 1998). Although OXA and OXB appear to be equally effective in activation of OX<sub>1</sub>R, OXA is 30- to 100-fold more effective than OXB in activating OX<sub>1</sub>R (Sakurai et al. 1998; Smart et al. 1999). The two orexin receptors exhibit distinctly different distribution patterns in the rat brain (reviewed in Kilduff and de Lecea 2001). For example, while the raphé nuclei, thalamus, and layer 6 of the cortex express OX<sub>1</sub>R and OX<sub>2</sub>R equally, only OX<sub>1</sub>R is present in cortical layer 5, hippocampal field CA1, and locus coeruleus (LC), whereas cortical layer 2, hippocampal field CA3, septal nuclei, and tuberomammillary nuclei express only OX<sub>2</sub>R (Lu et al. 2000; Hervieu et al. 2001; Marcus et al. 2001). The differential distribution and potential selectivity of the two orexin receptors raises the possibility that there may be some differences in the functional roles played by OXA and OXB within the central nervous system.

Several other lines of evidence have also suggested that that OXA and OXB may be differentially involved in particular functional systems. First, repeated studies have shown that OXA is more effective than OXB in promoting ingestive behavior (Sakurai et al. 1998; Edwards et al. 1999; Kunii et al. 1999).

This conclusion is supported by data from orexin receptor studies. Orexin-induced ingestive behavior is attenuated by OX<sub>1</sub>R antagonists (Rodgers et al. 2000; Thorpe and Kotz 2005), and food deprivation selectively up-regulates OX<sub>1</sub>R mRNA in the amygdala without affecting OX<sub>2</sub>R mRNA in this structure (Lu et al. 2000). Second, although OXB is generally ineffective in eliciting feeding or drinking behavior, there is evidence that OXB may be important in the promotion of arousal. Several studies have shown that the effects of orexins on arousal in thalamic midline and raphé nuclei depend primarily upon OX<sub>2</sub>R (Bayer et al. 2002; Brown et al. 2002), and disruption of OX<sub>2</sub>R has been linked to the sleep disorder narcolepsy in dogs (Lin et al. 1999). In at least one study, OXB has been shown to be more effective than OXA in activation of wakefulness-promoting thalamic nuclei in the rat (Bayer et al. 2002), although this is not likely to be the case for all structures involved in the regulation of sleep and wakefulness, (Marcus et al. 2001). While both orexins are clearly involved in a multitude of homeostatic and regulatory processes, most published reports on their functions have not fully addressed potential differences between OXA and OXB.

Most published data on the distribution of orexin cells has focused on OXA, and relatively little is known about OXB. The distribution of OXB is generally described as being identical to that of OXA but is often presented incompletely (Cutler et al. 1999; Date et al. 1999; Nambu et al. 1999) or not at all (Peyron et al. 1998; Chen et al. 1999). Because the two orexins are produced by the same precursor protein, there may have been a tendency in the early

literature on the orexins to assume that the peptides are produced equally in each orexin cell, and at least one study has provided some support for this assumption (Zhang et al. 2002). However, there is evidence that the up-regulation of one orexin peptide over the other is very possible, and may serve some physiologically relevant function (Mondal et al. 1999a; Cai et al. 2001).

A second issue that has received little attention involves the tendency to assume that distributions of orexin-containing cells and fibers seen in one strain or species of research animal are representative of all strains and species. Although partial descriptions of orexin distribution in within the central nervous system have been published for many species, including mice (Broberger et al. 1998; van den Pol 1999; Tritos et al. 2001), cats (Zhang et al. 2002, 2004), and humans (Moore et al. 1998), the majority of studies examining orexin distribution in detail throughout the brain have been in rats (*Rattus norvegicus*). In addition, most descriptions of the orexins in the rat were performed using the highly inbred Wistar strain (Peyron et al. 1998; Cutler et al. 1999; Nambu et al. 1999). The occasional difference found in orexin distribution between rat strains tends to be largely ignored or overlooked, even for differences as fundamental as the distribution of orexin-immunoreactive (IR) cell bodies. For example, OXA-IR cells have been described in the median eminence (Chen et al. 1999) in the Sprague-Dawley (SD) rat, a less inbred strain, but not in the Wistar rat. Although previous studies of the Wistar rat showed orexin-IR cell bodies only in the lateral hypothalamus, at least one study has shown OXB-IR, but not OXA-IR cells in the amygdala of both Wistar and SD rats (Ciriello et al. 2003c). These studies

highlight both the importance of examining orexin distribution in more than one specific animal type, and the previously mentioned importance of examining both forms of orexin.

While the orexins have been studied in some depth in nocturnal laboratory rodents, little attention has been paid to them in diurnal animal models. Detailed descriptions of orexin cell or fiber distributions in diurnal animals are limited, and currently there are no descriptions of the distribution of both peptides in any diurnal species that are as complete as those available for the Wistar rat. Studies in humans (Moore et al. 1998) and sheep (Archer et al. 2002) describe OXA in limited portions of the brain, and the distribution of OXA-IR cell bodies has also been described in the Korean chipmunk (*Tamias sibiricus barberi*) (Kodama et al. 2005) and the African green (vervet) monkey (*Cercopithecus aethiops*) (Diano et al. 2003). The most complete study to date in a diurnal animal describes OXB, but not OXA in the Nile grass rat (*Arvicanthis niloticus*) (Novak and Albers 2002). Given the reported relationship between the orexins and regulation of sleep and arousal (reviewed in Hungs and Mignot 2001), it is especially important to investigate potential differences in orexin distribution in animals with completely different sleep patterns, such as those seen in nocturnal and diurnal animals. This is especially important because the loss of orexin or the dysfunction of its receptors have been linked to several disorders in humans (Nishino et al. 2000; Thannickal et al. 2000; Nevsimalova et al. 2005; Petersén et al. 2005), a diurnal species.

One potential diurnal animal model with which to investigate this issue is the Nile grass rat, a rodent native to sub-Saharan Africa. The grass rat exhibits strong diurnal patterns of activity both in the laboratory and in the field (McElhinny et al. 1997; Blanchong and Smale 2000). The grass rat is a murid rodent, and as such is closely related to the standard laboratory rat (hereafter referred to as the lab rat). The grass rat is an excellent model for investigation of various physiological differences between nocturnal and diurnal animals, including those associated with sleep (Novak et al. 1999, 2000b), reproduction (McElhinny et al. 1997; Mahoney et al. 2004; Mahoney and Smale 2005b, 2005a), and the circadian regulation of activity (Katona et al. 1998; Nuñez et al. 1999; Mahoney et al. 2000; Novak et al. 2000a; Smale et al. 2001a; Schwartz et al. 2004). We have recently demonstrated that the grass rat exhibits a diurnal rhythm in Fos-immunoreactivity in OXB cells (Martinez et al. 2002).

A second diurnal animal model being used in laboratory study of circadian biology is the degu (*Octodon degus*), a highly social South American hystricomorph rodent (Nowak 1999). The degu is relatively long-lived and matures slowly, unlike the precocial rats and mice commonly used in laboratory research (Reviewed in Lee 2004). Like hamsters, rhythms in degus are strongly influenced by social and olfactory cues (Governale and Lee 2001; Jechura and Lee 2004), and there is some evidence for seasonal (photoperiodic) changes in reproductive structures (Reviewed in Lee 2004). The degu is a suitable model for research on sleep and the circadian regulation of behavior (Krajnak et al. 1997;

Goel et al. 1999; Jiao et al. 1999; Kas and Edgar 1999; Jechura et al. 2000; Mohawk et al. 2005; Mohawk and Lee 2005).

In this study we characterized the distribution of OXA and OXB cell bodies and fibers and systematically compared them in two diurnal species (the grass rat and the degu) and two nocturnal species, the lab rat and golden hamster (*Mesocricetus auratus*). As previous studies have already described orexin distributions in the highly inbred Wistar rat, we chose to use a less inbred strain, the Long-Evans (LE) rat, in the current study.

## **Methods and materials**

### **Animal handling**

Adult male grass rats (n = 4) and degus (n = 4) were obtained from captive breeding colonies at Michigan State University and the University of Michigan, respectively. Long Evans rats (n = 3) and hamsters (n = 4) were obtained from a commercial breeder (Charles River Laboratories, Raleigh, North Carolina). All animals were housed under standard light-dark (LD) cycles (LE rat, grass rat, and degu, 12:12 LD; hamster, 14:10 LD) with food and water provided *ad libitum* prior to perfusion. All animal handling procedures in this study followed National Institutes for Health guidelines and were approved by the Michigan State University All-University Committee for Animal Use and Care.

### **Tissue collection and processing**

At the time of sacrifice, all animals were anesthetized with sodium pentobarbital (Nembutal; Abbot Laboratories, North Chicago, IN) and perfused

transcardially with 0.01 M phosphate-buffered saline (PBS; pH 7.4, 150-300 ml/animal), followed by 150 to 300 ml of fixative (4% paraformaldehyde in 0.1 M phosphate buffer, pH 7.4). Brains were post-fixed for 4 to 8 hours in 4% paraformaldehyde before being transferred to 20% sucrose in 0.1 M phosphate buffer. After 24 h in sucrose, brains were sectioned in three series at either 30  $\mu$ m (grass rat and hamster) or 40  $\mu$ m (LE rat and degu) using a freezing microtome. Coronal sections from the olfactory bulb through the brain stem of four grass rats, three LE rats, four hamsters and three degus were used to determine orexin A and B fiber distribution. A third series of sections from one grass rat and one degu was stained with Cresyl violet, mounted on gelatin-coated slides and coverslipped to aid in delineation and identification of different structures. Additional sections through the preoptic area and lateral hypothalamus from two LE rats, three grass rats and one hamster were used in OXA blocking experiments.

Tissue was processed for OXA or OXB immunoreactivity in the following manner. Unless otherwise specified, all steps were carried out at room temperature. Free-floating tissue was incubated in 5% normal donkey serum (NDS; Jackson Laboratories), in PBS with 0.3% Triton-X 100 (Research Products International, Mount Prospect, IL; PBS-TX) for 1 h. Tissue was then incubated in primary antibody for 42 h at 4°C (goat anti-orexin A 1:10,000, or goat anti-orexin B 1:10,000, Santa Cruz Biotechnology; in PBS-TX and 3% NDS), and then in biotinylated secondary antibody for 1 h (donkey anti-goat 1:500, Santa Cruz; in PBS-TX and 3% NDS), followed by 1 h in avidin-biotin complex (0.9% each

avidin and biotin solutions, Vector Laboratories, Burlingame, CA; in PBS-TX). Tissue was rinsed and reacted in diaminobenzidine (DAB, 0.5 mg/ml, Sigma) in a tris-hydrochloride buffer (Trizma, Sigma; pH 7.2) with hydrogen peroxide (0.35  $\mu$ l 30% hydrogen peroxide/ml buffer). Control sections were incubated in the PBS-TX/NDS solution, with the primary antibody omitted. Tissue used in blocking experiments was processed as described above, but prior to adding tissue to the primary antibody solution, the primary antibody was preabsorbed with one or both orexin blocking peptides for 48 h at 4°C (1:50 OXA, 1:50 OXB, or 1:50 each OXA and OXB blocking peptide, Santa Cruz; in PBS with 0.3% Triton-X 100 and 3% NDS). All tissue was mounted on gelatin-coated slides, dehydrated, and coverslipped.

### **Cell and fiber counts and analysis**

For analysis of orexin A or B fiber distribution, all sections were examined under a light microscope (Leitz, Laborlux S, Wetzlar, Germany), and the presence or absence of labeled fibers, as well as their density, was recorded for brain regions from the olfactory bulbs through the brainstem. The distribution of all OXA or OXB-IR cell bodies was also mapped for each species. High-resolution digital photographs of representative sections were taken using a digital camera (Carl Zeiss, AxioCam MRc; Göttingen, Germany) attached to a Zeiss light microscope (Axioskop 2 Plus). Image contrast and color balance were optimized using Zeiss AxioVision software (Carl Zeiss Vision). Final figures were prepared using Adobe Illustrator and Adobe Photoshop (Adobe Systems, San Jose, CA).



To systematically record the distribution and relative density of OXA and OXB fibers within each species, fiber densities were divided into the following five categories: very dense (++++), dense (+++), moderately dense (++), low density (+), and absent (-). Terminology and abbreviations for neural structures in this study follow Paxinos and Watson (1998), except for divisions of the hamster bed nucleus of the stria terminalis (BNST) which follows Morin and Wood (2001). Comparisons of BNST divisions between species follow the comparison of terminologies between rat and hamster outlined in Alheid et al. (1995). Stereotaxic atlases for the rat (Paxinos and Watson 1998) and Syrian hamster (Morin and Wood 2001) were used to aid in identification of specific structures in these species. In the degu and grass rat, Nissl-stained tissue was used in concert with the rat atlas (Paxinos and Watson 1998) for identification of nuclei. Functional and anatomical grouping of brain structures for analysis followed Paxinos (1995), as modified by John I. Johnson (personal communication). Because of the resulting size and complexity of the orexin fiber data set, fiber densities in the regions examined in this study were subjected to a principal components factor analysis (PCA; Statistica, StatSoft, Tulsa, OK) to identify patterns in the data.

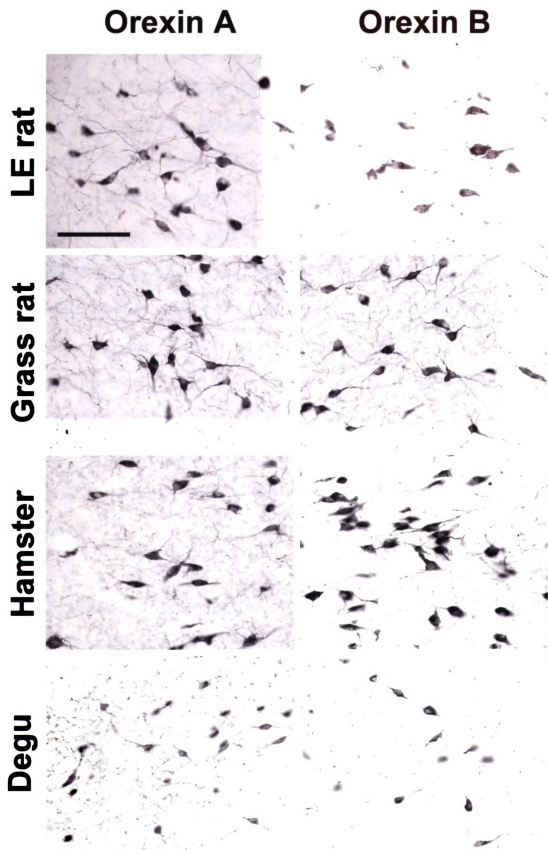
## **Results**

### **Orexin cell bodies**

#### General

In all animals examined, OXA- and OXB-IR cell bodies were present in the lateral hypothalamus (Figure 2.1). Although the distribution of orexin neurons

**Figure 2.1.** Photomicrographs of orexin A and orexin B cell bodies in the Long-Evans rat, grass rat, Syrian hamster, and degu. Scale bar = 100  $\mu$ m.



differed among species, the majority of the orexin cells in all species were observed in the perifornical region (PeF) and lateral hypothalamic area (LHA). In the LE rat, grass rat and hamster, cell bodies immunoreactive for OXA were also found in the paraventricular hypothalamic nucleus (Pa), supraoptic nucleus (SO), and the supraoptic retrochiasmatic nucleus (SOR) (Figure 2.2, Figure 2.3). Orexin A-IR neurons in the Pa and SO were generally smaller and less intensely stained for OXA than were cells in the PeF. For all three species exhibiting orexin-IR neurons in the Pa and SO, the OXA-IR nuclei did not appear to represent nonspecific binding of the primary antibody, as preabsorption of the primary antibody with OXA blocking peptide supplied by the manufacturer reduced or eliminated OXA immunoreactivity in these nuclei (Figure 2.4). No OXB-IR neurons were observed in Pa, SO, or SOR of any species. Orexin A and OXB cell body distribution in the LE rat, grass rat, degu and hamster are summarized in Table 2.1 and are depicted in Figures 2.5, 2.6, 2.7, and 2.8, respectively.

#### Orexin cell bodies in the LE Rat

In the LE rat, OXA- and OXB-IR cells were observed at high density in the PeF, LHA, and dorsomedial hypothalamic nucleus (DMH) (Figure 2.5). Moderate densities of labeled cells were present in the posterior hypothalamic area (PH) and tuberum cinereum (TC). Sparsely scattered cells were also observed in the dorsal hypothalamic area (DH), retrochiasmatic area (RCh), and the subincertal thalamic nucleus (SubI). Orexin A-IR cell bodies in SO and magnocellular Pa

## Paraventricular Nucleus

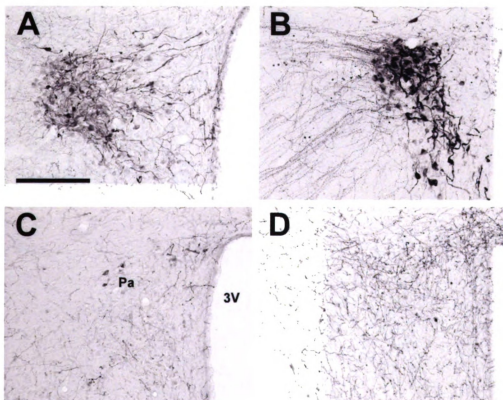


**Figure 2.2.** Photomicrographs of orexin A cell bodies in the paraventricular nucleus (Pa) of the Long-Evans rat (A), grass rat (B), and Syrian hamster (C). Note lack of similar cell bodies in the degu (D). 3V: third ventricle. Scale bar = 200  $\mu$ m.

## Supraoptic Nucleus

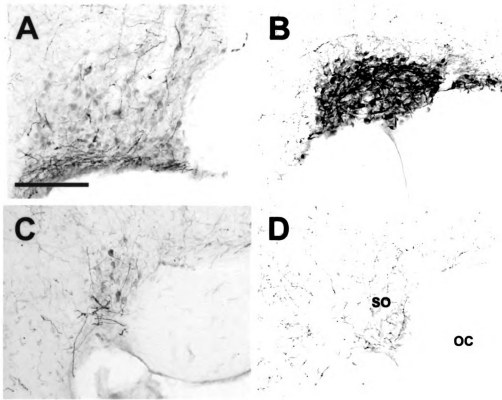


**Figure 2.3.** Photomicrographs of orexin A cell bodies in the supraoptic nucleus (SO) of the Long-Evans rat (A), grass rat (B), and Syrian hamster (C). Note lack of similar cell bodies in the degu (D). OC: optic chiasm. Scale bar = 200  $\mu\text{m}$ .

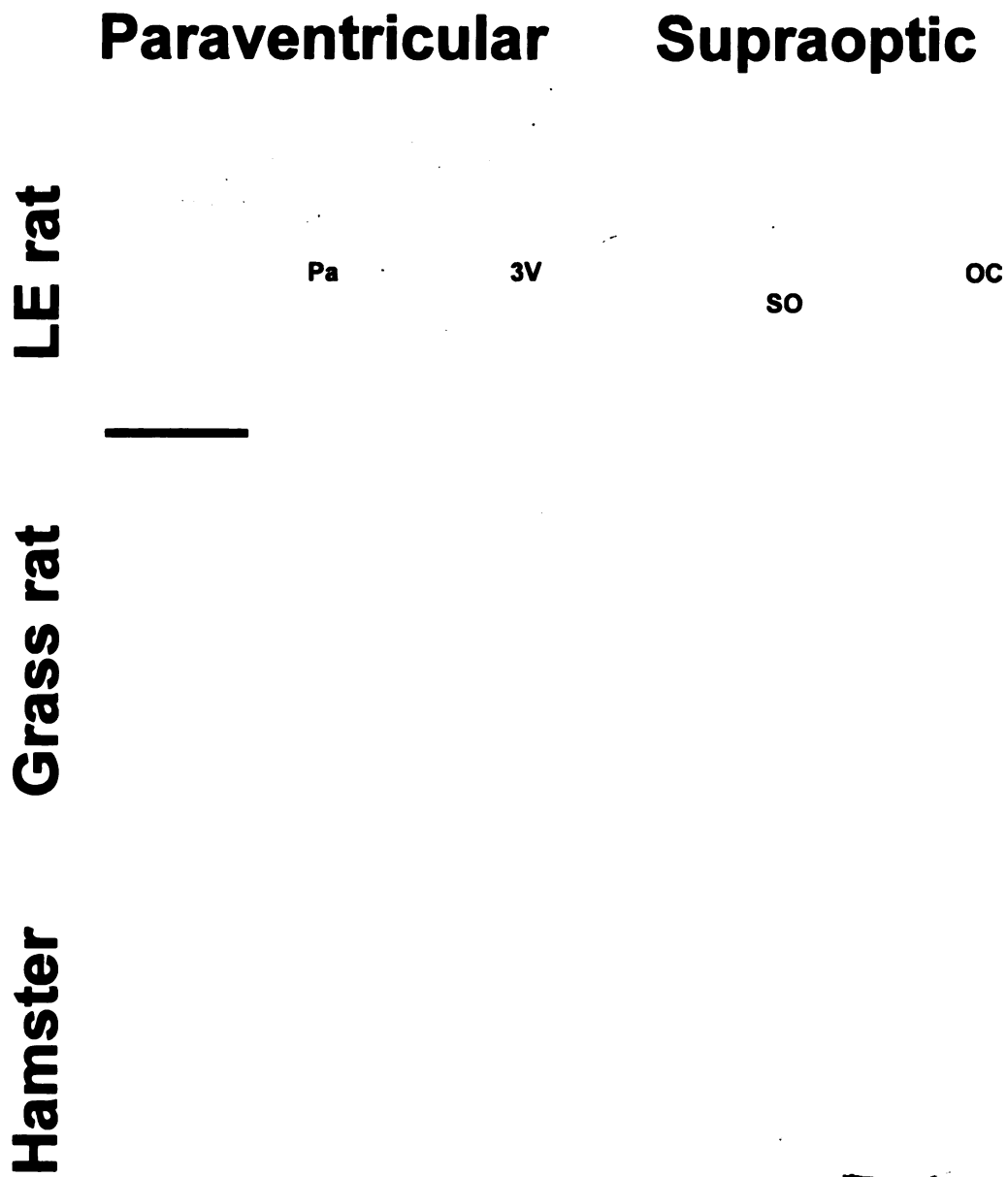


**Figure 2.4.** Photomicrographs of paraventricular nucleus (Pa; column 1) and supraoptic nucleus (SO; column 2) of the Long-Evans rat, grass rat, and Syrian hamster after preabsorption with orexin A blocking peptide. Note that preabsorption with blocking peptide eliminates cell bodies seen in Figures 2.2 and 2.3. 3V: third ventricle; OC: optic chiasm. Scale bar = 200  $\mu$ m.

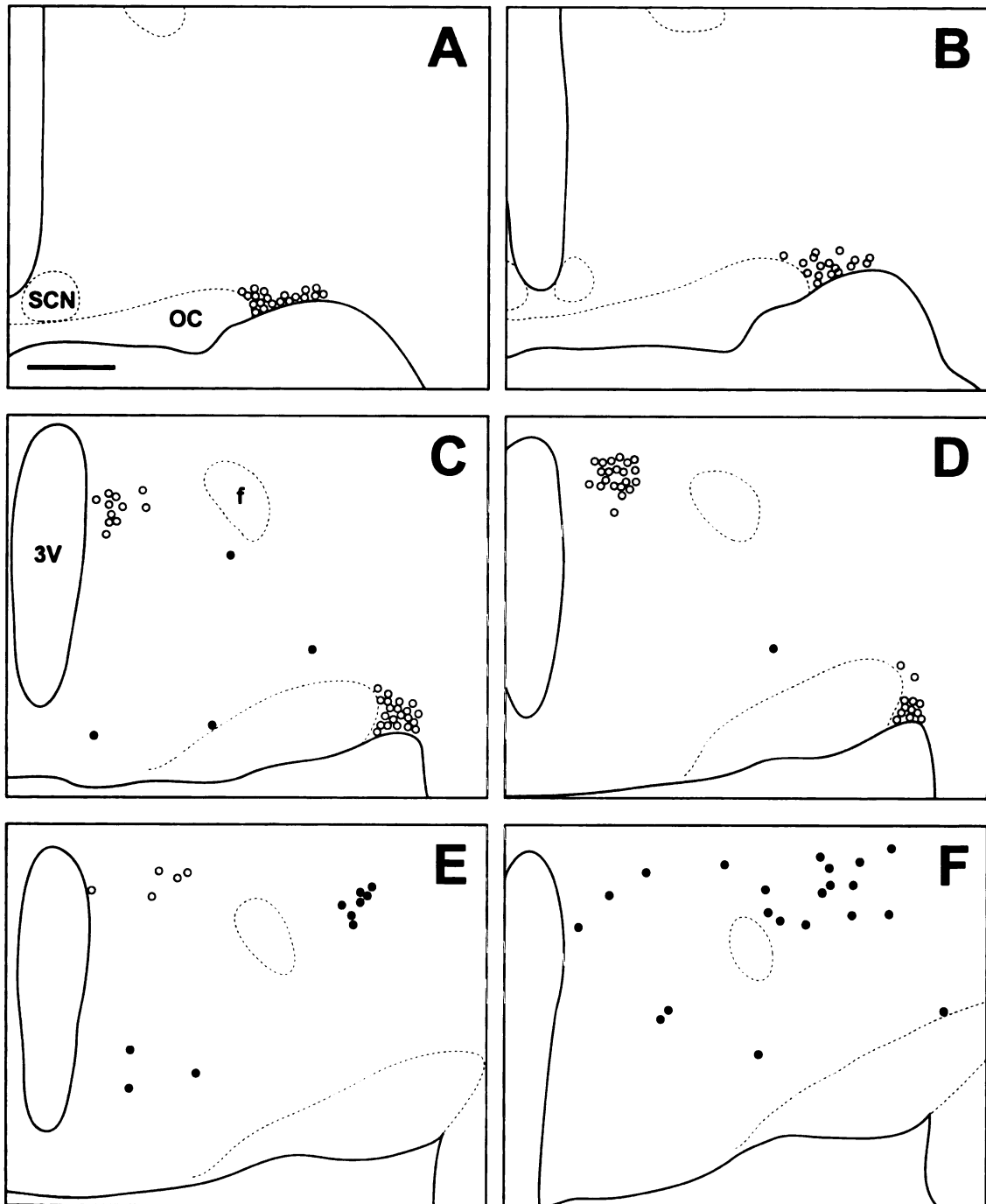
Brain region	LE rat		Grass rat		Hamster		Degu	
	A	B	A	B	A	B	A	B
Dorsal hypothalamic area	+	+	+	+			++	++
Dorsomedial hypothalamic nucleus	+++	++	++	++	++	++	++++	++++
Lateral hypothalamic area	+++	+++	+++	+++	++++	+++	++++	++++
Paraventricular hypothalamic nucleus, magnocellular	+++	-	++++	-	-	-	-	-
Perifornical nucleus	++++	++++	++++	++++	+	+	++	++
Posterior hypothalamic area	++	++	+++	+++	-	-	++	++
Retrochiasmatic area	+	+	+	+	-	-	+	+
Subincertal thalamic nucleus	+	+	++	+	+	+	+	+
Supramammillary nucleus		-		-	-	-	+	+
Supraoptic nucleus	++++	-	++++	-	++	-	-	-
Supraoptic nucleus, retrochiasmatic	++	-	+++	-	+	-	-	-
Tuberum cinereum	++	++	+++	+++	+	+	++	++

**Table 2.1.** Distribution of orexin A and B cell bodies in the Long-Evans rat, grass rat, Syrian hamster, and degu. The relative densities of OXA- or OXB-containing cells are indicated in each column as very dense (++++), dense (+++), moderately dense (++), sparse (+), or absent (-).



**Figure 2.5.** Line drawing of every 6th section through the region of the Long-Evans rat hypothalamus that contains orexin cells. Sections are ordered from rostral (A) to caudal (N). Filled circles indicate locations where both orexin A and orexin B neurons are found, while open circles indicate orexin A neurons only. 3V: third ventricle; SCN: suprachiasmatic nucleus; OC: optic chiasm; f: fornix; mt: mammillothalamic tract. Scale bar = 500  $\mu$ m.

# Long-Evans rat



## Long-Evans rat (continued)

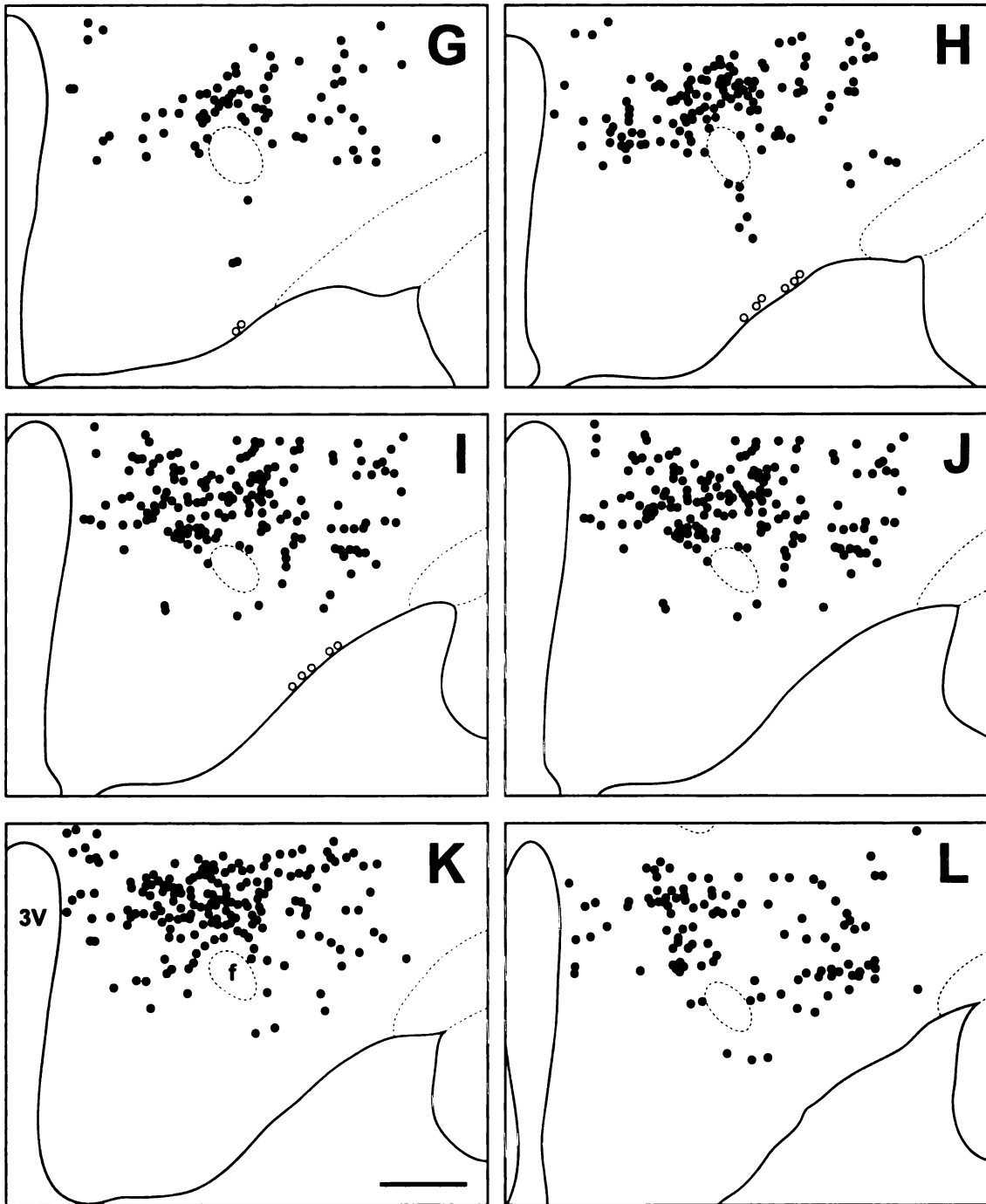


Figure 2.5 (continued)

## Long-Evans rat (continued)

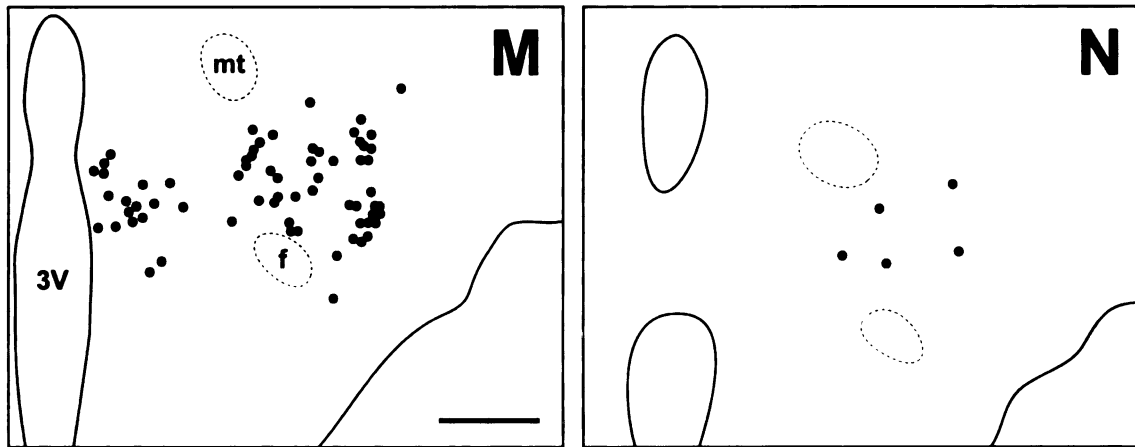
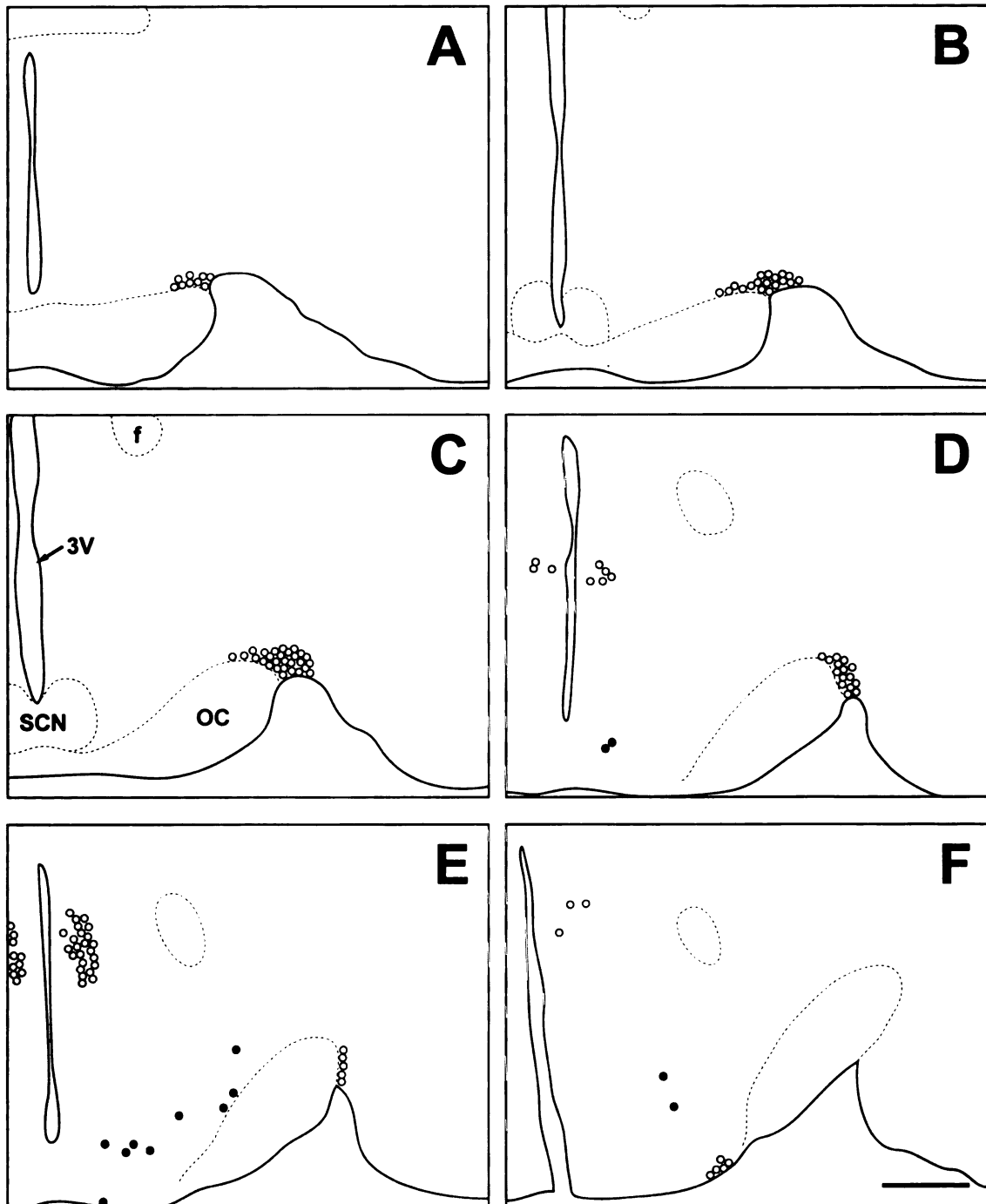


Figure 2.5 (continued)

**Figure 2.6.** Line drawing of every 6th section through the region of the grass rat hypothalamus that contains orexin cells. Sections are ordered from rostral (A) to caudal (L). Filled circles indicate locations where both orexin A and orexin B neurons are found, while open circles indicate orexin A neurons only. 3V: third ventricle; SCN: suprachiasmatic nucleus; OC: optic chiasm; f: fornix; mt: mammillothalamic tract. Scale bar = 500  $\mu$ m.

# Grass rat



## Grass rat (continued)

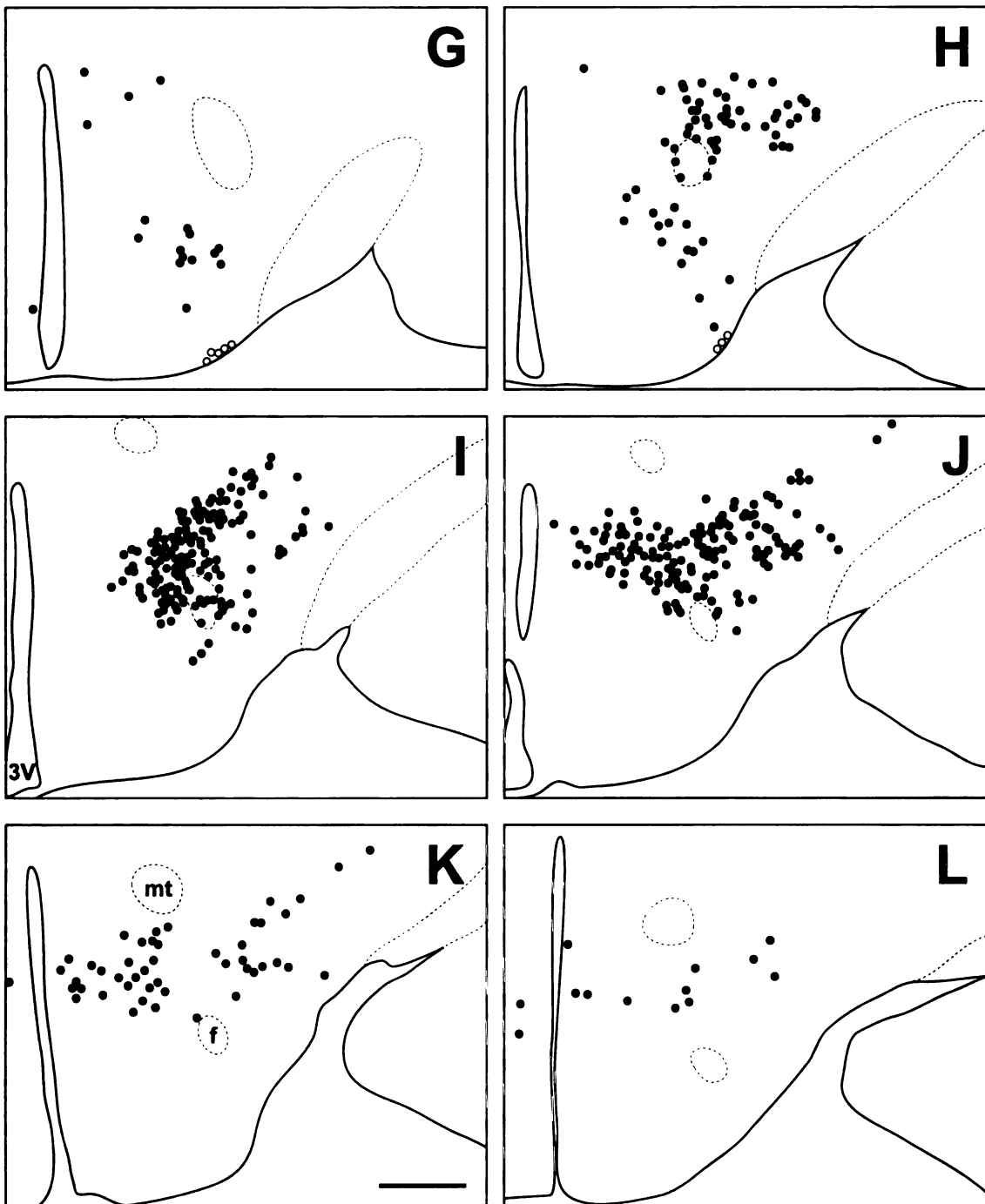
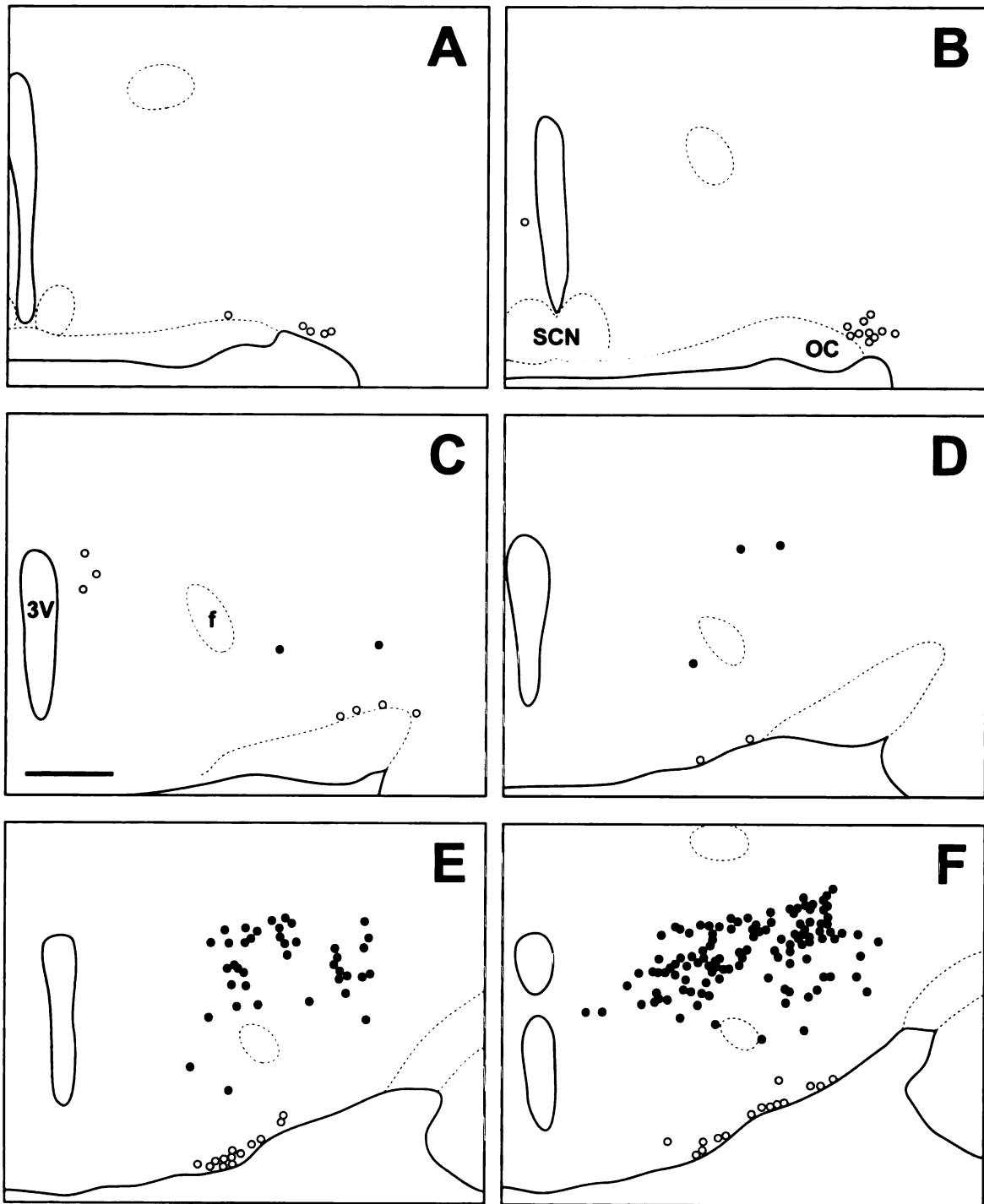


Figure 2.6 (continued)

**Figure 2.7.** Line drawing of every 6th section through the region of the Syrian hamster hypothalamus that contains orexin cells. Sections are ordered from rostral (A) to caudal (J). Filled circles indicate locations where both orexin A and orexin B neurons are found, while open circles indicate orexin A neurons only. 3V: third ventricle; SCN: suprachiasmatic nucleus; OC: optic chiasm; f: fornix; mt: mammillothalamic tract. Scale bar = 500  $\mu\text{m}$ .



# Syrian hamster



## Syrian hamster (continued)

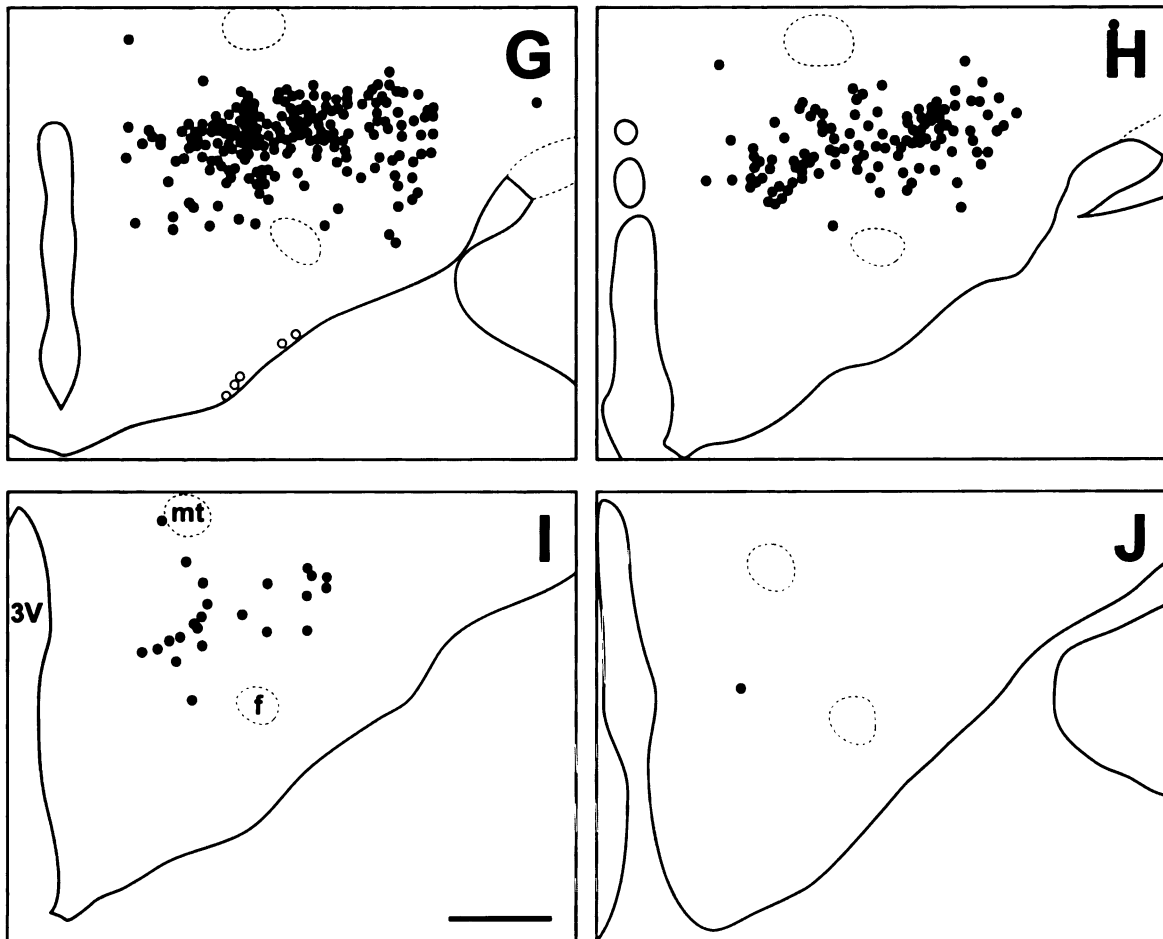
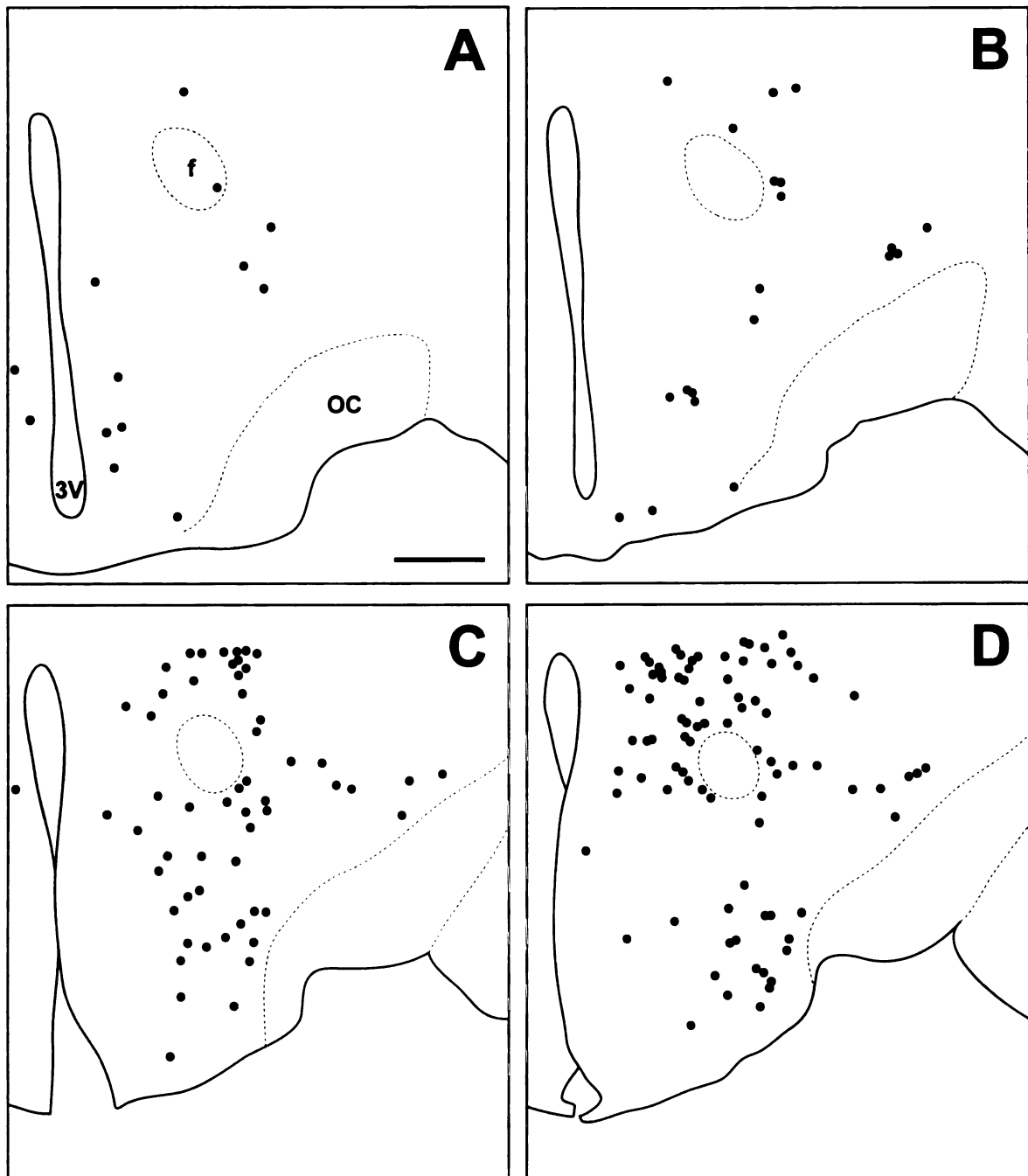


Figure 2.7 (continued)

# Degu



**Figure 2.8.** Line drawing of every 6th section through the region of the degu hypothalamus that contains orexin cells. Sections are ordered from rostral (**A**) to caudal (**N**). Filled circles indicate locations where both orexin A and orexin B neurons are found. 3V: third ventricle; OC: optic chiasm; f: fornix; mt: mammillothalamic tract; aq: cerebral aqueduct. Scale bar = 500  $\mu$ m.

## Degu (continued)

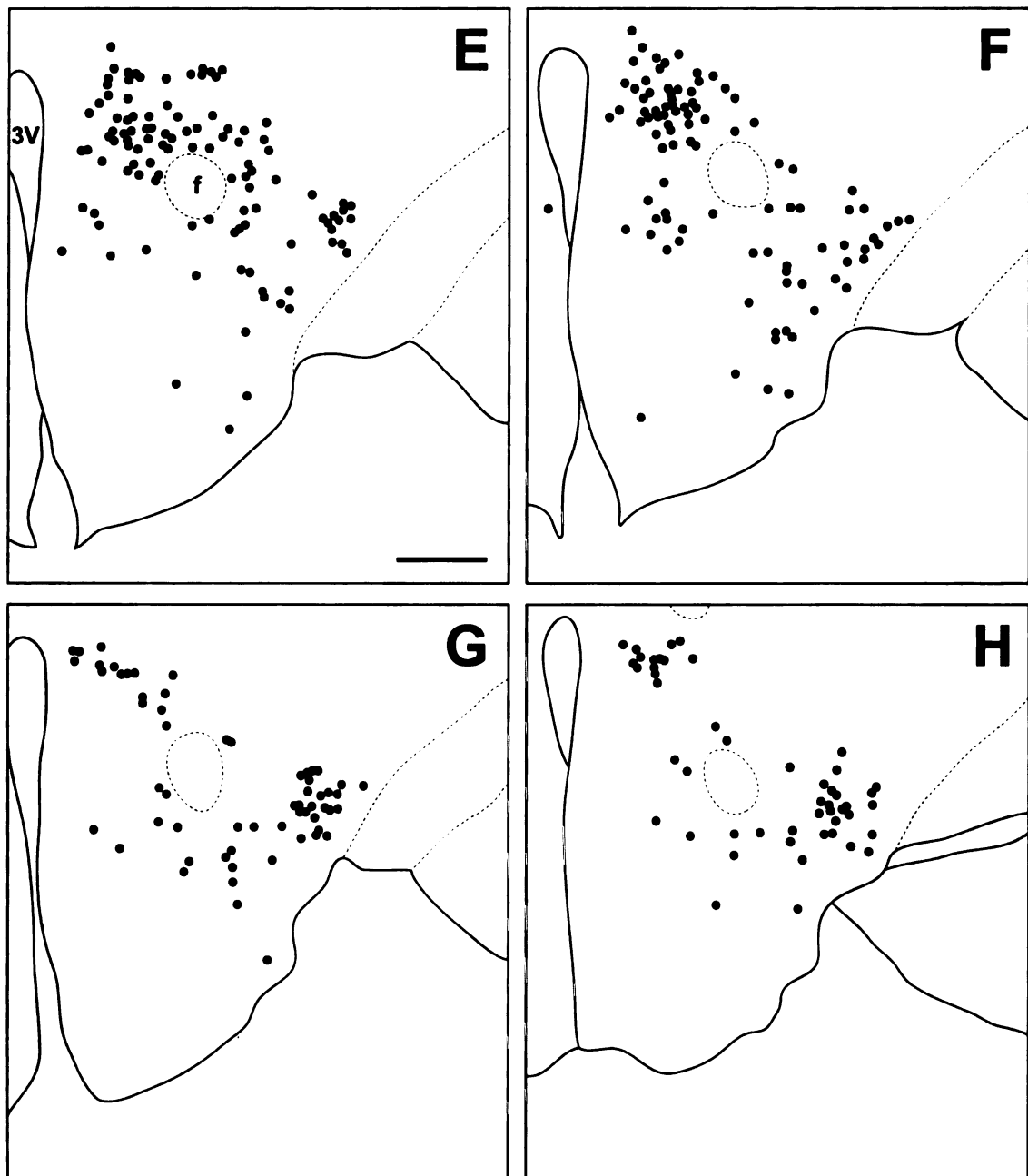


Figure 2.8 (continued)

Degu (continued)

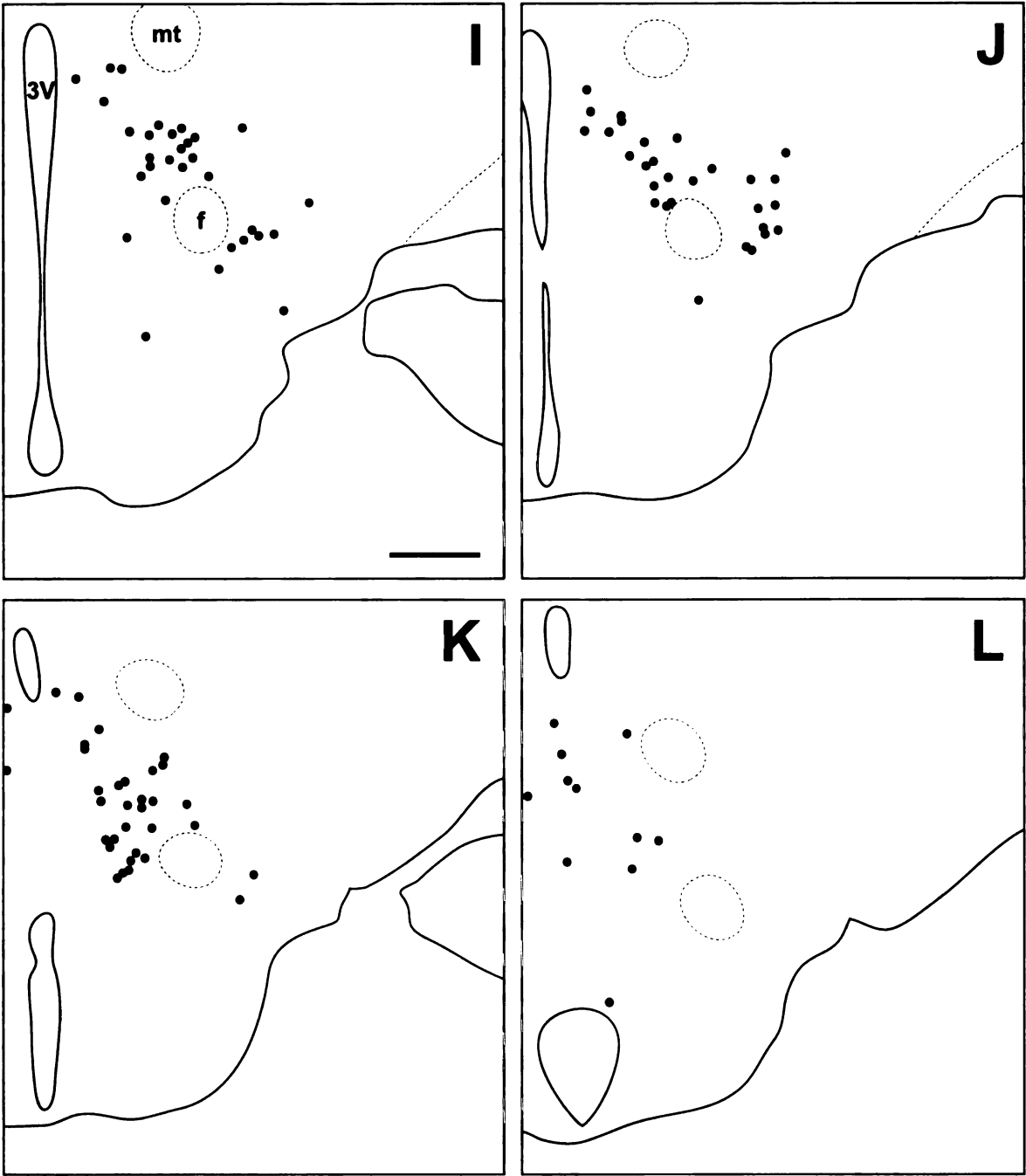


Figure 2.8 (continued)

## Degu (continued)

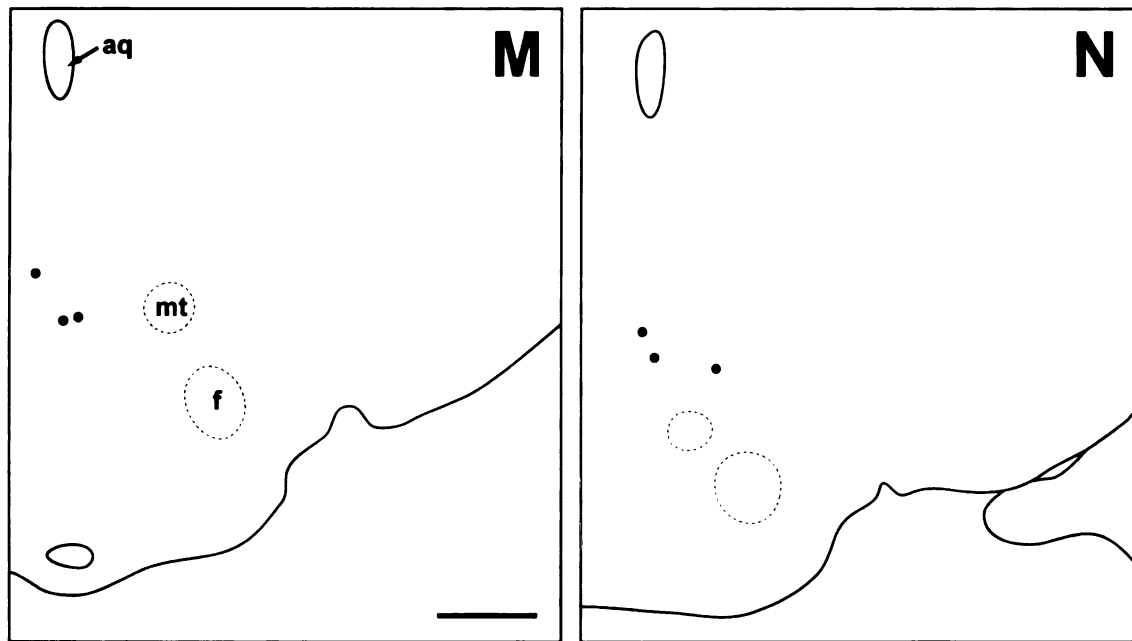


Figure 2.8 (continued)

were very dense (Figure 2.2), while cell bodies in SOR were only moderately dense (Figure 2.3). No OXB-IR neurons were seen in the Pa or SO.

#### Orexin cell bodies in the grass rat

The distribution of OXA- and OXB-IR neurons in the grass rat was similar to the pattern seen in the LE rat. Cell bodies expressing OXA and OXB were observed at very high density in PeF, TC, LHA, and PH (Figure 2.6). Unlike the LE rat, OXA- and OXB-IR neurons in the PeF were often observed inside the grass rat fornix. Moderate densities of OXA- and OXB-IR cell bodies were visible in DMH and Subl, with sparsely scattered cells also present in RCh and DA. As in the LE rat, cell bodies expressing strong OXA immunoreactivity were present in PA, SO, and SOR (Figure 2.2, Figure 2.3). No OXB-IR neurons were present in these nuclei. Orexin A-IR cell bodies were very densely distributed in the magnocellular Pa and SO. Moderately dense OXA-IR cell bodies were present in SOR.

#### Orexin cell bodies in the hamster

Unlike the LE rat and grass rat, OXA- and OXB-IR neurons in the hamster were conspicuously absent in PeF; the majority of orexin cells were observed in LHA and DMH, dorsal or dorsomedial to PeF, with sparsely scattered cells also present in TC and Subl (Figure 2.7). Although OXA-IR neurons were present in the hamster magnocellular PA, SO, and SOR (Figure 2.2, Figure 2.3), the overall density of OXA-IR cell bodies in these structures was far lower than that in the

LE rat or grass rat. As in the LE rat and grass rat, no OXB-IR neurons were present in these nuclei.

#### Orexin cell bodies in the degu

The distribution of OXA- and OXB-IR cell bodies was very different in the degu than in the LE rat, grass rat and hamster. The regions of highest density of OXA and OXB cells formed two distinct clusters, in the DMH and in the LHA ventrolateral to the fornix (Figure 2.8). Orexin A and OXB neurons were less densely distributed in the PeF, DA, and PH. In the PeF, orexin-IR neurons were clustered tightly against the boundaries of the fornix, but did not intrude into this structure as observed in the grass rat. Cells labeled for OXA and OXB were sparsely distributed throughout the RCh and Subl. Unlike the hamster, grass rat and LE rat, no orexin-IR neurons were visible in the Pa, SO, or SOR. Orexin A- and B-IR cells in the degu were also different from those seen in the other three species in that orexin neurons were scattered through the TC caudal to the ventromedial hypothalamic nucleus (VMH), with small numbers of cells observed near the midline in sections through the supramammillary nucleus (SuM).

#### **Orexin fiber distribution**

##### General

Orexin A- and OXB-IR fibers were visible in many regions throughout the forebrain, midbrain, and hindbrain in all species examined. Numerous varicosities were noted on these fibers, especially in the most dense projections extending



rostrally from the lateral hypothalamus to the preoptic area and amygdala, and posteriorly through the periaqueductal gray to the raphé nuclei and brainstem. The average density of OXA and OXB fiber innervation in over two hundred individual brain regions was examined for each species. A PCA analysis of these fiber densities revealed only one significant eigenvector (eigenvalue = 5.740, cumulative variance explained = 71.748%); no other factors with eigenvalues greater than 1 were revealed. Factor coordinates for all species along this eigenvector were similar (LE Rat OXA = -0.8753, OXB = -0.8669; Grass rat OXA = -0.8275, OXB = -0.8178; Hamster OXA = -0.8657, OXB = -0.8446; Degu OXA = -0.8270, OXB = -0.8498), suggesting a strong overall similarity between OXA and OXB fiber densities across species. Overall, the PCA analysis revealed that correlations in OXA measurements between pairs of species ranged from 59.2% to 72.2% similarity, while these measurements for OXB ranged from 57.1% to 68.6%. Within species, correlations between OXA and OXB fiber densities were quite high (LE rat: 85.8%; grass rat: 85.2%; hamster: 92.4%; degu: 98.5%). Significance levels for all correlations were  $< 0.001$ . The PCA correlation matrix summarizing between-species correlations for OXA and OXB is presented in Table 2.2. The overall details of the distribution and relative density of OXA and OXB fibers for each species are summarized in Table 2.3. Below we provide a general description of the patterns of fiber distribution and highlight the differences between species.

## Orexin A

	LE rat	Grass rat	Hamster	Degu
LE rat	1.0000			
Grass rat	0.7220	1.0000		
Hamster	0.6982	0.6086	1.0000	
Degu	0.6412	0.5706	0.6458	1.0000

## Orexin B

	LE rat	Grass rat	Hamster	Degu
LE rat	1.0000			
Grass rat	0.6989	1.0000		
Hamster	0.6862	0.6054	1.0000	
Degu	0.6321	0.5709	0.6401	1.0000

**Table 2.2.** Pairwise correlation matrix of orexin A (top) and orexin B (bottom) fiber distribution in the Long-Evans rat, grass rat, Syrian hamster, and degu. Correlation values were obtained from a principal component factor analysis of orexin A and orexin B fiber density patterns in all four species. Values listed at intersections between rows and columns represent the correlation in fiber density between species indicated by the corresponding row and column labels. All values represent significant correlations ( $p < 0.001$ ).



**Table 2.3.** Distribution of orexin A and B fibers in the Long-Evans rat, grass rat, Syrian hamster, and degu. The relative densities of OXA- or OXB-containing fibers are indicated in each column as very dense (indicated by ++++), dense (+++), moderately dense (++), sparse (+), or absent (-). Unmarked rows indicate areas for which no data are available.

Brain region	LE rat		Grass rat		Hamster		Degu	
	A	B	A	B	A	B	A	B
<b>Hypothalamus</b>								
Anterior hypothalamic area	++	++	+	+	+++	++	+++	+++
Anterodorsal preoptic nucleus	+	+	+	+	+++	+	++	++
Anteroventral periventricular nucleus	++	+	+	-	++	++	++	++
Arcuate nucleus	+++	+++	+++	+	++	++	++	++
Circular nucleus	++	+	++	+	+++	+++	+++	+++
Dorsal hypothalamic area	++	++	++	++	++	++	++	++
Dorsomedial nucleus	+++	++	++	+	+++	++	+++	+++
Lateral hypothalamic area	+++	+++	+++	+++	+++	+++	++	++
Lateral mammillary nucleus	+	+	+	+	+++	+++	+	+
Lateral preoptic area	+++	+	+	+	++	+	++	++
Lateroanterior nucleus	++	+	++	++	+++	+++	+++	+++
Magnocellular preoptic nucleus	+	+	+	+	++	++	++	++
Medial mammillary nucleus, lateral part	-	-	-	-	-	-	+	+
Medial mammillary nucleus, medial part	-	-	-	-	-	-	-	-
Medial mammillary nucleus, median part	+	+	+	+	-	-	+	+
Medial preoptic area	++	+	+	+	++	++	++	++
Medial preoptic nucleus	++	+	++	++	++	+	++	++
Median preoptic nucleus	+++	+++	+++	+++	+++	+++	+++	+++
Parastrial nucleus	+++	++	+++	++	+	+	+	+
Paraventricular nucleus, magnocellular	++++	++	+++	+	++	++	++	++
Paraventricular nucleus, parvocellular	+++	++	+++	++	++	++	++	++
Perifornical nucleus	++++	+++	+++	++	+	+	+++	+++
Periventricular nucleus	+++	++	++	+	++	++	+++	+++
Posterior hypothalamic area	+++	+++	++	++	++	++	++	++
Posterodorsal preoptic nucleus	++	+	++	++	++	+	++	++
Preoptic nucleus, ventromedial	+++	+++	+++	++	++	++	+++	+++
Retrochiasmatic area	+++	++	++	++	+++	++	+++	+++
Subincertal nucleus	+++	+++	++	++	+	+	+	+
Submammillothalamic nucleus	++	+	++	++	+	+	++	++
Suprachiasmatic nucleus, anterior	-	-	-	-	+	+	-	-

Table 2.3 (continued) Brain region		LE rat		Grass rat		Hamster		Degu	
		A	B	A	B	A	B	A	B
<b>Hypothalamus (continued)</b>									
Suprachiasmatic nucleus, posterior		+	+	-	-	+	+	+	+
Supramammillary nucleus		+++	++	++	+	++	++	+++	+++
Supraoptic nucleus		++++	+	++++	++	++	+	+	+
Supraoptic nucleus, retrochiasmatic		++++	++	+++	+	++	+	+++	+++
Tuberomammillary nucleus		++++	++++	+++	+++	++++	++++	++++	++++
Tuberum cinereum		++	++	+++	++	+	+	++	++
Ventrolateral preoptic area		+++	++	+	+	+++	++	+++	+++
Ventromedial nucleus		++	+	+	+	++	++	+++	+++
Ventromedial nucleus, anterior		+	+	+	+	++	+	+++	+++
Zona incerta, caudal		++	+	+	+	+	+	-	-
Zona incerta, rostral		++	+	+	+	++	++	+	+
<b>Thalamus</b>									
Anterodorsal nucleus		+	+	++	++	+	+	+	+
Anteromedial nucleus		-	-	-	-	-	-	-	-
Anteroventral nucleus		+	+	+	-	-	-	-	-
Central medial nucleus		++	++	+	+	+	+	++	+
Centrolateral nucleus		+	+	+	+	+	+	+++	+++
Dorsolateral geniculate nucleus		-	-	-	-	-	-	-	-
Interanterodorsal nucleus		+	+	+	+	++	+	-	-
Interanteromedial nucleus		++	+	+	+	+	+	-	-
Intergeniculate leaflet		++	++	++	++	++	++	++	++
Intermediodorsal nucleus		++	++	+++	+++	++	++	+	+
Lateral posterior nucleus		-	-	-	-	-	-	-	-
Laterodorsal thalamic nucleus		+	+	-	-	-	-	-	-
Medial geniculate nucleus		-	-	+	+	-	-	-	-
Mediodorsal thalamic nucleus		+	+	+	+	++	+	++	++
Nucleus of the fields of Forel		+	+	-	-	+	+	-	-
Paracentral nucleus		++	++	-	-	+	+	+++	+++
Parafascicular nucleus		+	+	+	+	+	-	-	-

Table 2.3 (continued) Brain region		LE rat		Grass rat		Hamster		Degu	
		A	B	A	B	A	B	A	B
<b>Thalamus (continued)</b>									
Paratenial nucleus		-	-	++	+	+	+	+	+
Paraventricular nucleus		++++	++++	++++	+++	++++	++++	++++	++++
Posterior intralaminar nucleus		++	++	+	+	+	+	+	+
Posterior limitans		++	++	++	+	++	++	++	++
Posterior nuclear complex		-	-	-	-	-	-	-	-
Reticular thalamic nucleus		+	-	-	-	-	-	-	-
Reuniens nucleus		+	+	+	+	+	+	+	+
Rhomboid nucleus		++	++	-	-	++	++	-	-
Submedius nucleus		-	-	+	+	+	-	-	-
Subparafascicular nucleus		+	+	+	+	+	+	+	+
Ventral anterior nucleus		-	-	-	-	-	-	-	-
Ventral posteriolateral nucleus		-	-	-	-	-	-	-	-
Ventral posteromedial nucleus		-	-	-	-	-	-	-	-
Ventrolateral geniculate nucleus		+	+	+	+	+	+	+	+
Ventrolateral thalamic nucleus		-	-	-	-	-	-	-	-
Ventromedial thalamic nucleus		++	+	-	-	-	-	-	-
Xiphoid nucleus		+++	++	+++	++	+++	+++	+	+
<b>Epithalamus</b>									
Lateral habenular nucleus		++	+	-	-	+	+	+	+
Medial habenular nucleus		-	-	++	+	++	-	-	-
Stria medullaris		-	-	-	-	+	-	-	-
<b>Cerebral isocortex</b>									
Layer 1		+	+	+	+	+	+	+	+
Layer 2		+	+	+	+	+	+	+	+
Layer 3		-/+	-/+	-/+	-/+	-/+	-/+	-/+	-/+
Layer 4		-/+	-/+	-/+	-/+	-/+	-/+	-/+	-/+
Layer 5		+	+	+	+	+	+	+	+
Layer 6		+	+	+	+	+	+	+	+

Table 2.3 (continued) Brain region	LE rat		Grass rat		Hamster		Degu	
	A	B	A	B	A	B	A	B
<b>Cerebral isocortex (continued)</b>								
Agranular insular cortex	++	+	+	+	+	+	+	+
Cingulate and retrosplenial agranular cortex	+	+	+	+	+	+	-	-
Frontal cortex	+	+	+	+	+	+	+	+
Granular insular cortex	+	+	+	+	++	++	+	+
Occipital cortex					+	+	+	+
Orbital cortex					+	+	+	+
Parietal cortex	+	+	+	+	+	+	+	+
<b>Amygdala</b>								
Anterior amygdaloid area	+	+	+	+	++	++	++	++
Anterior, posteromedial, and posterolateral cortical amygdaloid nuclei	++	++	++	++	+	+	++	++
Basolateral amygdaloid nucleus	+	+	-	-	+	+	+	+
Basomedial amygdaloid nucleus	+	+	+	+	+	+	++	++
<b>Bed nucleus of the stria terminalis*</b>								
Intraamygdaloid division	+	+	+	+	+	+	+	+
Lateral division	++	++	++	+	N/A	N/A	+	+
Lateral division, dorsal (Rat), anterolateral (Hamster)	++	+	+	+	++	++	+	+
Lateral division, posterior (Rat), posterolateral (Hamster)	++	++	++	+	++	++	+	+
Lateral division, ventral (Rat), anteroventral (Hamster)	+++	+++	++	+	++	++	++	++
Medial division, anterior (Rat), anteromedial (Hamster)	++	++	++	++	++	++	++	++
Medial division, posterointermediate (Rat), posteromedial (Hamster)	+	+	++	+	++	++	++	++
Medial division, posterolateral (Rat), posterointermediate (Hamster)	+	+	++	+	++	++	++	++
Central amygdaloid nucleus	+	+	+	+	+	+	-	-



Table 2.3 (continued) Brain region		LE rat		Grass rat		Hamster		Degu	
		A	B	A	B	A	B	A	B
<b>Amygdala (continued)</b>									
Intercalated amygdaloid nucleus		++	+	+	-	++	++	++	++
Lateral amygdalohippocampal area				+	-	+	+	++	++
Lateral amygdaloid nucleus		+	+	+	+	+	+	+	+
Medial amygdaloid nucleus		++	+	+	+	+++	+++	+	+
Nucleus of the lateral olfactory tract		+	+	+	+	++	++	+	+
Posteromedial amygdalohippocampal area				+	+	+	+	+++	+++
<b>Hippocampus</b>									
CA1		+	+	+	+	-	-	-	-
CA2		-	-	-	-	+	+	-	-
CA3		-	-	-	-	+	+	+	+
Dentate gyrus				-	-	-	-	+	+
Tenia tecta				++	+	++	++	++	++
Entorhinal cortex		+	+	+	-	+	+	+	+
Indusium griseum		++	++	+	+	++	++	-	-
Subiculum				-	-	-	-	+	+
<b>Olfactory</b>									
Anterior olfactory nuclei								+	+
Islands of Calleja		+	+	+	+	++	++	++	++
Olfactory bulb						-	-	-	-
Olfactory tubercle		-	-	-	-	+	+	+	+
Piriform cortex		+	+	+	+	+	+	+	+
<b>Other Forebrain</b>									
Bed nucleus of the anterior commissure		+++	++	++	++	++	++	++	++
Clastrum		++	++	+	+	++	++	+	+
Dorsal endopiriform nucleus		++	+	+	+	+	+	+	+

Table 2.3 (continued)		LE rat		Grass rat		Hamster		Degu	
Brain region		A	B	A	B	A	B	A	B
<b>Septal nuclei</b>									
Lateral septal nucleus, dorsal part		++	++	++	+	++	+	+	+
Lateral septal nucleus, intermediate part		+	+	+	-	+	+	-	-
Lateral septal nucleus, ventral part		+	+	++	+	++	++	+	+
Medial septal nucleus		++	++	+	+	+++	+++	++	++
Nucleus of the horizontal limb of the diagonal band of Broca		+++	++	+	+	++	++	++	++
Nucleus of the vertical limb of the diagonal band of Broca		+++	+	+	+	+++	++	++	++
Septofimbrial nucleus		+	+	+	+	++	++	+	+
Septohippocampal nucleus		++	+	+	+	+++	+++	++	++
Triangular septal nucleus		+	+	-	-	+	+	-	-
<b>Basal ganglia</b>									
Accumbens nucleus, core		-	-	-	-	+	+	-	-
Accumbens nucleus, shell		+	+	++	+	-	-	+	+
Accumbens shell, lateral		+	+	+	+	+	+	-	-
Caudate putamen		-	-	-	-	+	+	-	-
Dorsal peduncular pontine nucleus		++	+	++	++	+	+	+	+
Globus pallidus, lateral		+	+	+	+	-	-	-	-
Globus pallidus, medial		-	-	-	-	-	-	-	-
Pedunclopontine tegmental nucleus		++	++	++	+	++	++	++	++
Peripeduncular nucleus		+	+	+	+	++	++	+	+
Substantia innominata		++	++	+	+	++	++	++	++
Substantia nigra, compact part		+	+	+	+	+	+	+	+
Substantia nigra, lateral part		++	++	+	+	++	++	+	+
Substantia nigra, reticular part		-	-	-	-	-	-	-	-
Subthalamic nucleus		+	+	+	+	++	++	-	-
Ventral pallidum		++	++	+	+	+	+	+	+
Ventral tegmental area		++	+	++	+	++	++	++	++
Ventral tegmental nucleus		++	+	-	-	+	+	+	+

Table 2.3 (continued) Brain region		LE rat		Grass rat		Hamster		Degu	
		A	B	A	B	A	B	A	B
<b>Brainstem reticular nuclei</b>									
B9 serotoin cells		++	++	+	+	++	++	-	-
Cuneiform nucleus		++	++	++	+	++	++	+	+
Deep mesencephalic nucleus		++	++	+	+	++	+	+	+
Dorsal paragigantocellular nucleus		+	+	-	-	+	+	+	+
Gigantocellular reticular nucleus		++	+	+	+	+	+	+	+
Gigantocellular reticular nucleus, ventral part		++		++		++	++	++	++
Gigantocellular reticular nucleus, $\alpha$ part		++	++	++	+	++	++	++	++
Intermediate reticular nucleus		+++	+	-	-	++	+	+	+
Lateral paragigantocellular nucleus		+++	++	+	+	++	++	+++	+++
Lateral reticular nucleus				+	+	+	+	+	+
Medullary reticular nuclei, dorsal part				+	+	+	+	+	+
Medullary reticular nuclei, ventral part				+	+	+	+	+	+
Paramedian reticular nucleus				-		+	+	+	+
Parvocellular reticular nucleus		++	++	+	+	++	+	+	+
Pontine reticular nucleus, caudal part		+	+	+	-	+	+	+	+
Pontine reticular nucleus, oral part		++	+	+	+	+	+	-	-
Pontine reticular nucleus, ventral part		-	-	+	+	++	++	+	+
Reticulotegmental nucleus of the pons		+++	++	++	++	+	+	+	+
Subcoeruleus nucleus, dorsal part		++	++	+	+	++	++	++	++
Subcoeruleus nucleus, ventral part		++	++	+	-	++	++	+	+
Subcoeruleus nucleus, $\alpha$ part		+++	+++	+++	++	+++	+++	+++	+++
<b>Sensory, somatic and motor nuclei</b>									
Abducens nucleus (VI)		-	-	-	-	-	-	-	-
Ambiguus nucleus		++++	+++	+++	++	++	+	++	++
Barrington's nucleus		++++	+++	+++	+++	++++	+++	+++	+++
Dorsal motor nucleus of vagus (X)				+		++	+	+	+
Facial nucleus (VII)		++	+	++	+	+	+	++	++
Gracile nucleus				-		++	+	+	+

Table 2.3 (continued)		LE rat				Grass rat		Hamster		Degu	
Brain region		A	B	A	B	A	B	A	B	A	B
<b>Sensory, somatic and motor nuclei (continued)</b>											
Hypoglossal nucleus (XII)		+		+		+		-		+	+
Kölliker-Fuse nucleus		+++	++	++	++	++	++	+++	+++	+++	+++
Lateral parabrachial nucleus		+++	+++	++	++	++	++	++	++	++	++
Medial parabrachial nucleus		+++	++	+	+	+	+	++	+	++	++
<b>Nucleus of the solitary tract</b>											
Central				+		+		+	+	++	++
Dorsal				++++		++++		++++	++++	+++	+++
Medial		+	+	+++		+++		+++	+++	+++	+++
Ventrolateral				++		++		++	++	++	++
Oculomotor nucleus (III)				-		-		-		-	-
Trigeminal motor nucleus (V)		+	+	+	+	+	+	-	-	+	+
Trigeminal principal sensory nucleus (V)		+	+	+	+	+	+	+	+	+	+
Trigeminal spinal nucleus, caudal part				++		++		+	+	++	++
Trigeminal spinal nucleus, interpolar part		-		+		+		+	+	+	+
Trigeminal spinal nucleus, oral part		-	-	+		+	+	+	+	++	++
Trochlear motor nucleus (IV)		+	+	-	+	-	-	+	+	-	-
<b>Raphé nuclei</b>											
Dorsal raphé nucleus		++++	++++	+++	+++	+++	+++	+++	+++	+++	+++
Linear nucleus of the raphé		+++	+++	++	++	++	++	++	++	++	++
Median raphé nucleus		++++	++	+++	+++	+++	+++	+++	+++	+++	+++
Pontine raphé nucleus		+++	+++	++	++	++	++	+++	+++	+++	+++
Raphé magnus nucleus		+++	++	++	++	++	++	++	++	++	++
Raphé obscurus nucleus		+++	++	++	++	++	++	+++	+++	+++	+++
Raphé pallidus nucleus		+++	++	++	++	++	++	++	++	+	+
Rhabdoid nucleus		+	+	+	+	+	+	+	+	+	+
<b>Periaqueductal gray</b>											
Dorsolateral periaqueductal gray		++	++	+	+	++	++		++	+	+
Dorsomedial periaqueductal gray		+++	+++	++	++	+++	+++		+++	++	++

Table 2.3 (continued) Brain region		LE rat		Grass rat		Hamster		Degu	
		A	B	A	B	A	B	A	B
<b>Periaqueductal gray (continued)</b>									
Lateral periaqueductal gray		+++	+++	++	++	++	++	++	++
Thalamic periaqueductal gray		++	++	+	+	+++	++	++	++
Ventrolateral periaqueductal gray		+++	++	+++	++	+++	++	+++	+++
<b>Other midbrain</b>									
Dorsolateral pontine nucleus		+	+	++	++	-	-	+	+
Inferior colliculus		+	+	-	-	++	+	++	++
Interpeduncular nucleus		+	+	++	+	++	++	-	-
<b>Pretectal nuclei</b>									
Anterior pretectal nucleus		+	+	+	+	-	-	+	+
Medial pretectal nucleus		++	++	++	+	++	++	++	++
Posterior pretectal nucleus		++	+	+	+	-	-	++	++
Red nucleus		-	-	-	-	-	-	+	-
Superior colliculus		+	+	-	-	-	-	+	+
<b>Tegmental nuclei</b>									
Anterior tegmental nucleus		+	+	-	-	+	+	+	+
Dorsal tegmental nucleus		-	-	-	-	-	-	-	-
Laterodorsal tegmental nucleus		++	++	++	++	++	++	+++	+++
<b>Cerebellum</b>									
Cerebellar cortex		-	-	-	-	-	-	-	-
Flocculus		-	-	-	-	-	-	++	+
Interposed, lateral, and medial cerebellar nuclei		+	+	+	+	-	-	++	++
<b>Other hindbrain</b>									
Central tegmental tract		++	++	+	+	++	+	+	+
<b>Cochlear nuclei</b>									
Dorsal cochlear nucleus		+	+	-	-	+	+	+	+
Ventral cochlear nucleus		-	-	-	-	-	-	-	-

Table 2.3 (continued) Brain region	LE rat		Grass rat		Hamster		Degu	
	A	B	A	B	A	B	A	B
<b>Other hindbrain (continued)</b>								
Inferior olive	++		+++	++	-	-	-	-
Lateral lemniscus	+	+	-	-	+	-	-	-
Locus coeruleus	++++	++++	++++	++++	++++	++++	+++	+++
Nucleus of Darkschewitsch	-	-	++	+	-	-	+	+
Parabigeminal nucleus	+	+	+	+	++	++	+++	++
Prepositus nucleus	++	+	-	-	+	+	++	++
<b>Superior olivary nuclei</b>								
Nucleus of the trapezoid body	++	+	+	+	-	-	+	+
Superior olive	-	-	-	-	-	-	-	-
Trapezoid body	-	-	+	+	+	+	-	-
Vestibular nuclei	+	+	+	+	+	-	++	+
<b>Circumventricular and non-neuronal</b>								
Area postrema			++				++	++
Choroid plexus	+	+	+	+	+	+	+	+
Ependyma	+	+	++	+	+	+	+	+
Median eminence	++++	+	++++	+	++	++	++	++
Subcommissural organ	-	-	-	-	-	-	-	-
Subfornical organ	+	+	+	-	-	-	++	+

### Hypothalamus

In all species examined, OXA- and OXB-IR fibers extended from the lateral hypothalamus throughout much of the brain. These fibers were moderately to densely distributed throughout much of the hypothalamus, with the exception of the zona incerta, where fiber density was low, and the suprachiasmatic (Figure 2.9) and medial mammillary nuclei, which exhibited little to no orexin fibers in any species. Several species differences were observed. First, differences in fiber density were seen in the main regions in which we saw substantial differences in the distribution of labeled cells. In the hamster PeF, fiber density was reduced in comparison with the other species, and in the LE rat and grass rat, many OXA fibers were also present in the magnocellular Pa and SO. OXB fibers in all species and OXA fibers in the hamster and degu were moderate to low in the Pa and SO. Second, in the degu, a very dense network of OXA and OXB fibers was present in the VMH (Figure 2.10), but in the other species fiber densities in this region were moderate to low. The OXA and OXB fiber complex in the degu VMH was the single most densely distributed network of orexin fibers in this animal. Third, in the hamster, orexin-IR fibers in the lateral mammillary nucleus (LM) were fairly dense, while in the other three species fibers in the LM were sparse (Figure 2.11).

### Thalamus

In contrast to the dense networks of OXA and OXB fibers in the hypothalamus, orexin fibers were sparse or absent throughout much of the thalamus. The majority of orexin projections to the thalamus targeted midline

## Suprachiasmatic Nucleus

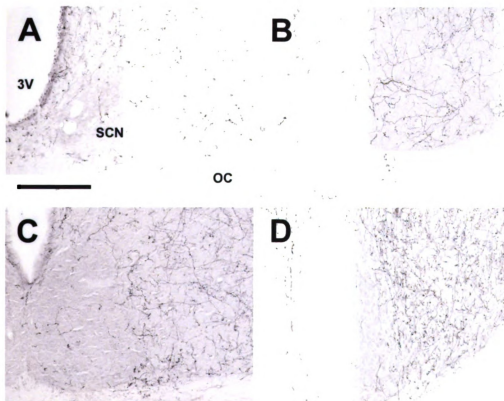


**Figure 2.9.** Photomicrographs of orexin A fibers around the suprachiasmatic nucleus (SCN) of the Long-Evans rat (A), grass rat (B), Syrian hamster (C), and degu (D). 3V: third ventricle; OC: optic chiasm. Scale bar = 200  $\mu$ m.



## Ventromedial Hypothalamic Nucleus

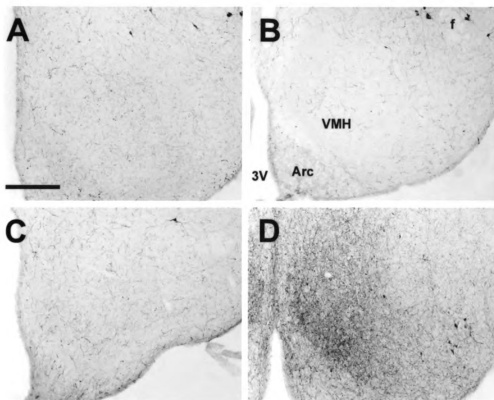


**Figure 2.10.** Photomicrographs of orexin A fibers in the ventromedial hypothalamic nucleus (VMH) of the Long-Evans rat (A), grass rat (B), Syrian hamster (C), and degu (D). Note markedly higher density of orexin fibers in the degu VMH than in the other three species. 3V: third ventricle; Arc: arcuate nucleus. Scale bar = 300  $\mu$ m.

## Lateral Mammillary Nucleus

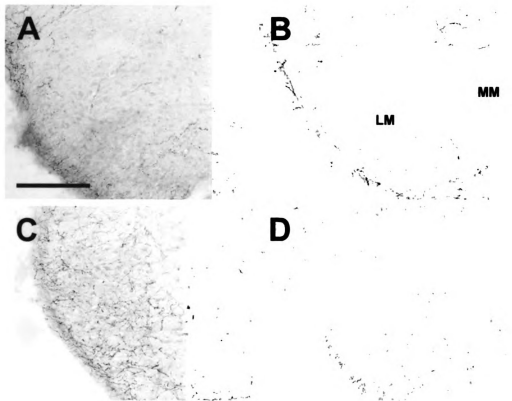


**Figure 2.11.** Photomicrographs of orexin A fibers in the lateral mammillary nucleus (LM) of the Long-Evans rat (A), grass rat (B), Syrian hamster (C), and degu (D). Note higher density of orexin fibers in the hamster LM than in the other three species. MM: medial mammillary nucleus. Scale bar = 200  $\mu$ m.

structures, most notably the paraventricular thalamic nucleus (PV), which received dense or very dense orexin projections in all four species. In all species examined, projections of OXA or OXB fibers to lateral regions of the thalamus were most dense in the intergeniculate leaflet (IGL) (Figure 2.12); other lateral or ventral thalamic nuclei received little to no orexin input. Although the pattern of orexin innervation in the thalamus was fairly consistent, the degu differed from most or all of the other species examined in several regions. First, dense orexin fibers were present in the degu centrolateral (CL) and paracentral nuclei (PC). In the other three species, orexin fibers in these nuclei were mostly sparse or absent, although the LE rat did exhibit moderate innervation in the PC (Figure 2.13). In contrast, the opposite pattern was observed in the xiphoid nucleus (Xi), which contained sparse fibers in the degu and dense orexin innervation in the other three species (Figure 2.14).

### Telencephalon

Outside of the diencephalon, the distribution of orexin-IR fibers was more heterogeneous. Orexin-A and OXB fibers were scattered throughout all areas of the cortex; these fibers were more concentrated in inner and outer cortical layers, and slightly reduced in Layers 3 and 4 in all animals. The olfactory bulbs exhibited no fibers in the degu and hamster (no data were available here for LE rat and grass rat), but sparsely scattered fibers were present in the olfactory cortex and tubercle in all species. Orexin fiber density was uniformly low to moderate in the septal nuclei, claustrum, and amygdala, with the exception of the hamster medial amygdaloid nucleus, where orexin fibers were more dense than

## Intergeniculate Leaflet

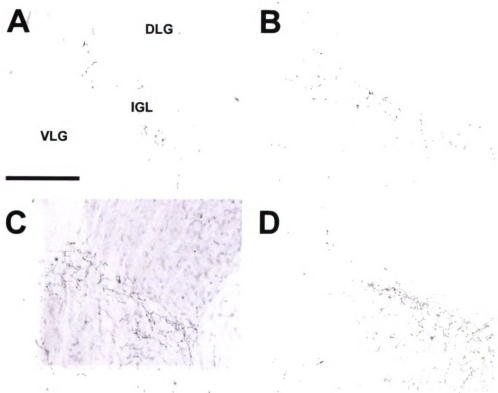


**Figure 2.12.** Photomicrographs of orexin A fibers in the intergeniculate leaflet (IGL) of the Long-Evans rat (**A**), grass rat (**B**), Syrian hamster (**C**), and degu (**D**). DLG: dorsolateral geniculate nucleus; VLG: ventrolateral geniculate nucleus. Scale bar = 200  $\mu$ m.

## Centrolateral Thalamic Nucleus

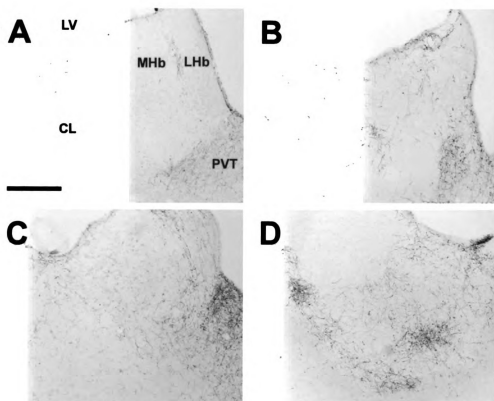


**Figure 2.13.** Photomicrographs of orexin A fibers in the centrolateral nucleus (CL) of the Long-Evans rat (A), grass rat (B), Syrian hamster (C), and degu (D). Note higher density of orexin fibers in the degu CL than in the other three species. LV: lateral ventricle; PVT: paraventricular thalamic nucleus, MHb: medial habenular nucleus; LHb: lateral habenular nucleus. Scale bar = 300  $\mu$ m.

## Xiphoid Nucleus

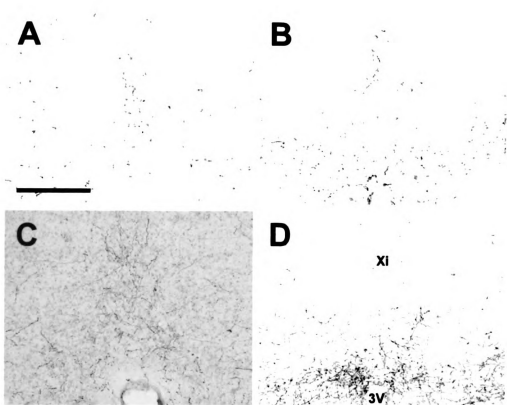


**Figure 2.14.** Photomicrographs of orexin A fibers in the xiphoid nucleus (Xi) of the Long-Evans rat (A), grass rat (B), Syrian hamster (C), and degu (D). Note relative lack of orexin fibers in the degu Xi in comparison with the other three species. 3V: third ventricle. Scale bar = 200  $\mu$ m.

in the grass rat and degu, but not significantly more so than in the LE rat. The density of both OXA and OXB fibers was very low in the hippocampus and basal ganglia in all animals. The bed nucleus of the anterior commissure exhibited moderate to dense orexin fiber innervation in all species.

### Midbrain

In general, OXA and OXB innervation of midbrain structures was moderate to low, with the exception of the dense fiber tracts in the periaqueductal gray and the very dense plexus of OXA and OXB fibers projecting to the raphe nuclei observed in all species (Figure 2.15).

### Hindbrain

In the hindbrain, OXA and OXB-IR fiber densities were moderate to low in the ascending brainstem tracts, motor and precerebellar nuclei, and were sparsely distributed or absent in the cochlear, vestibular, and olivary nuclei in all species. Visceral sensory nuclei, such as the nucleus of the solitary tract (Sol) and the Kölliker-Fuse nucleus, exhibited moderate to dense innervation by OXA and OXB fibers in all species, but the nucleus with the most extensive network of orexin fibers observed in the hindbrain was the LC (Figure 2.16). In the LE rat, grass rat, and hamster, the LC was the most densely innervated structure observed in the brain. In the degu, the network of OXA and OXB fibers present in the LC was quite dense, but was slightly less so than that observed in the VMH.

### Cerebellum

In the cerebellum, very few orexin fibers were observed in the LE rat, grass rat or hamster, but the degu was markedly different. In the degu

## Dorsal Raphé Nucleus

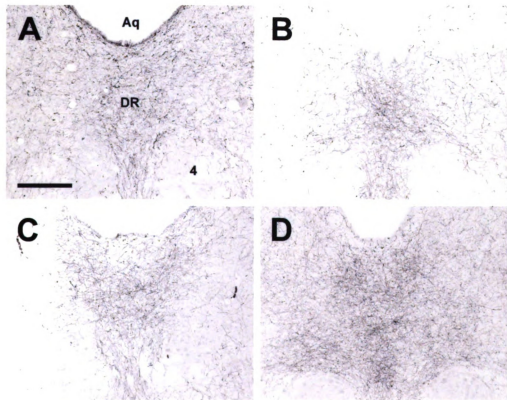


**Figure 2.15.** Photomicrographs of orexin A fibers in the dorsal raphé nucleus (DR) of the Long-Evans rat (A), grass rat (B), Syrian hamster (C), and degu (D). 4: trochlear nucleus; Aq: cerebral aqueduct. Scale bar = 300  $\mu$ m.



## Locus Coeruleus

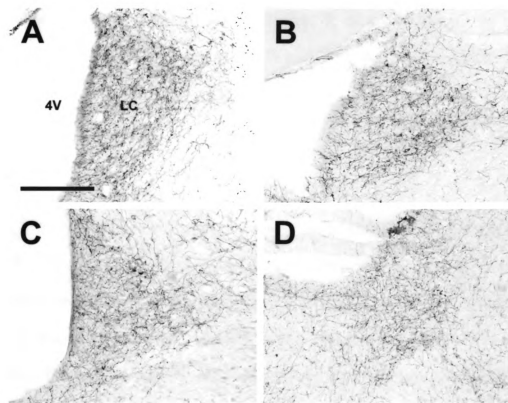


**Figure 2.16.** Photomicrographs of orexin A fibers in the locus coeruleus (LC) of the Long-Evans rat (A), grass rat (B), Syrian hamster (C), and degu (D). 4V: fourth ventricle. Scale bar = 200  $\mu$ m.

cer

cer

to

m

ot

pr

**D**

C

d

a

h

e

M

s

t

c

f

cerebellum, moderate OXA and OXB fiber densities were observed in some deep cerebellar nuclei, as well as the flocculus (Figure 2.17).

#### Circumventricular regions and ependyma

In circumventricular organs, OXA innervation in all animals was moderate to low, and there were even fewer OXB fibers. In the LE rat and grass rat, the median eminence exhibited greater densities of OXA-IR fibers relative to the other two species, although this difference is likely explained by axonal projections from the OXA-IR cells in the Pa and SO in these two species.

## **Discussion**

### **General observations**

We present here a thorough examination of the distribution of OXA- and OXB-IR cell bodies and fibers in four species. Prior to this study, no published data were available describing orexin A or B in the LE rat strain or in the degu, and no data were available for OXA in the grass rat or OXB in the Syrian hamster. The data presented here correspond well with previously published examinations of OXA in the Syrian hamster (McGranaghan and Piggins 2001; Mintz et al. 2001) and of OXB in the grass rat (Novak and Albers 2002).

At the most general level, the three most significant observations in this study were: (1) There is a high degree of correspondence within species between OXA and OXB; (2) The overall pattern of orexin cell and fiber distribution is very similar in these four species and to those described previously for other strains and species of mammal, including Wistar and Sprague-Dawley

## Flocculus

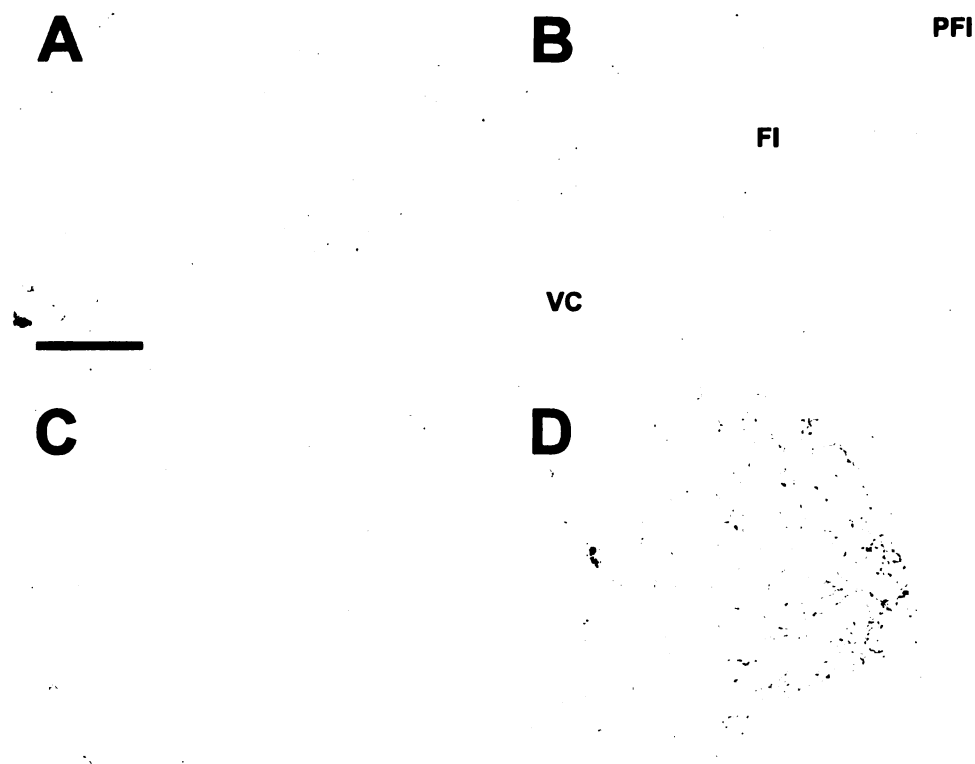


**Figure 2.17.** Photomicrographs of orexin A fibers in the flocculus (FI) of the Long-Evans rat (A), grass rat (B), Syrian hamster (C), and degu (D). Note higher density of orexin fibers in the degu FI than in the other three species. PFI: paraflocculus; VC: ventral cochlear nucleus. Scale bar = 200  $\mu$ m.

rats (Peyron et al. 1998; Chen et al. 1999; Cutler et al. 1999; Date et al. 1999; Nambu et al. 1999), Djungarian hamsters (McGranaghan and Piggins 2001; Khorooshi and Klingenspor 2005) and primates (Horvath et al. 1999a; Arihara et al. 2000; Moore et al. 2001); and (3) Despite the overall similarity between species, there are several striking differences, both with respect to the distribution of orexin-IR cells, as well as in the relative density of orexin-IR fibers in some regions.

The implications of the observation that there are high levels of correspondence between OXA and OXB distribution within species are twofold. First, although at least some OXA-only cell types were identified in the current study (see below), our data support the general assumption that the majority of cells and fibers expressing OXA immunoreactivity also express OXB, consistent with previous reports (Zhang et al. 2002). Second, the overlap between OXA- and OXB-IR fibers in all species studied suggests that the individual actions of OXA and OXB in regulation of physiology and behavior are more likely due to differences in the distribution of the orexin receptor subtypes within the brain than to differential distribution of the two forms of the peptide. The two orexin receptor subtypes do exhibit marked differences in distribution in rats (Lu et al. 2000; Hervieu et al. 2001; Marcus et al. 2001), and both rat and human orexin receptors express differential responsiveness to OXA or OXB (Sakurai et al. 1998; Smart et al. 1999). We did not map the distribution of orexin receptor subtypes in the species examined in the present study and are therefore unable to directly address this issue in the four rodents studied here.

The second major pattern seen in this study, that there are overall similarities in the distribution of orexins between species, suggests that orexin networks are strongly conserved among species. This implies that the functions of orexin are likely to be similar in the LE rat, grass rat, Syrian hamster, and degu, as well as in other species. The orexins are strongly conserved peptides (Sakurai et al. 1999; Shibahara et al. 1999; Ohkubo et al. 2002). The orexin gene arose early in chordate evolution (Alvarez and Sutcliffe 2002), and has been retained in all major vertebrate classes, including fish (Kaslin et al. 2004; Huesa et al. 2005), amphibians (Shibahara et al. 1999; Yamamoto et al. 2004; Singletary et al. 2005), reptiles (Farrell et al. 2003), birds (Ohkubo et al. 2002), and mammals (Sakurai et al. 1999). This pattern is evidence for an essential functional role for the orexins in mediation of behavioral and physiological processes common to all vertebrates, and further implies strong evolutionary constraints against modification of projections from orexin cells.

Lastly, the differences observed between species in such a strongly conserved peptide family may reflect subtle functional differences related to the life history, behavior, or physiological organization of different animals. We focus the rest of our discussion on the species differences in the distribution of orexin-IR cells and fibers.

### **Species differences in OXA and OXB cell distribution**

Though few in number, the three differences observed between species in the overall distribution of orexin-IR cell bodies were striking. First, orexin cells

were conspicuously absent in the hamster PeF. Second, the distribution of the main body of orexin-IR perikarya within the caudal diencephalon in the degu was markedly different from that seen in the other species examined in this study. Third, the presence of OXA-IR cell bodies in the Pa and SO was noted in three of the four species examined.

In the hamster, previous reports stated that orexin-IR neurons were primarily located in LHA and PeF (McGranaghan and Piggins 2001; Mintz et al. 2001). In the present study, orexin-IR cells were largely absent in the PeF, and were primarily found in the LHA dorsal to the perifornical region (Figure 2.7). It is possible that the difference observed between the present data and those described in previous reports reflect differences in delineation of specific hypothalamic areas. The present study relied on a hamster-specific atlas to identify brain regions (Morin and Wood 2001); as noted by the authors of this atlas, the hamster brain is in many respects organized quite differently from that of the rat (Morin and Wood 2001). At least one previous study (McGranaghan and Piggins 2001) used a rat brain atlas (Paxinos and Watson 1998); the second report (Mintz et al. 2001) did not indicate the method used for identification of different regions. In comparison with the rat brain atlas, the region identified as PeF in the hamster atlas is much smaller and situated closer to the fornix (Paxinos and Watson 1998; Morin and Wood 2001). However, even if an expanded rat-like definition of the PeF is applied to the hamster, it is clear that the number of orexin neurons observed near the fornix is lower in the hamster than in the other three species examined in this study (see Figures 2.5 – 2.8).

In the degu, two main differences were noted in the distribution of orexin-IR perikarya within the caudal diencephalon in comparison with the other three species. First, the degu exhibited orexin neurons through a much larger extent of the rostral-caudal axis of the hypothalamus, with cells expressing OXA or OXB extending from the RCh to the SuM (Figure 2.8). Second, the overall organization of the main body of orexin neurons differed in the degu relative to the other species in that two distinct clusters of orexin-IR cells were present, one dorsomedial to the fornix, and a second group ventrolateral to the fornix. In the caudal portion of their distributions, these groups merged into a single scattered group of orexin-IR cells near the midline, below the third ventricle. The differences in the overall distribution of orexin neurons in the degu relative to the other three species raise the possibility that orexin cells in the ventrolateral LHA, TC, and SuM of the degu receive different inputs or project to different targets than orexin cells in the dorsal LHA and PeF of the rat, grass rat, or hamster. Projections from these neurons might contribute to the overall differences in orexin fiber distribution in the degu relative to the other three species (see below).

Although the main body of orexin neurons in the LE rat, grass rat and hamster LHA were fairly consistent with those described previously, the presence of OXA-IR perikarya in the magnocellular nuclei of the hypothalamus in these three species has not been described previously. The presence of orexin-IR neurons outside of the lateral hypothalamus is not without precedent. Earlier reports suggested the presence of OXA-IR neurons in the median eminence



(Chen et al. 1999), and OXB-IR neurons in limbic structures (Ciriello et al. 2003c). In general, the OXA-IR perikarya in the Pa, SO and SOR were not as darkly stained as were OXA-IR neurons in the LHA and PeF, and the number of OXA-IR cells in these nuclei varied between species (Figure 2.2, Figure 2.3). Orexin A-IR cells in the Pa and SO were fairly dense in the grass rat, with fewer OXA-IR cells visible in the LE rat Pa and SO. In the hamster, immunoreactivity for OXA was generally negligible in cells of the Pa, but a small number of well-defined OXA-IR neurons were visible in the SO.

The magnocellular neurosecretory cells of the Pa and SO are primarily known for the production of arginine vasopressin (AVP) and oxytocin (OT), peptide hormones delivered to the pituitary via projections to the median eminence (reviewed in Armstrong 1995). These cells have been studied extensively, and the normal functions of these nuclei are well-understood. The presence of a previously unreported peptide in these cells is therefore quite surprising. Several lines of evidence suggest that the OXA immunoreactivity in these nuclei reflects the presence of the peptide rather than non-specific immunoreactivity. First, tissue that has been blocked by preabsorption of the OXA antibody with OXA blocking peptide reduces or eliminates the staining of cell bodies in the Pa, SO, and LHA of all species examined (Figure 2.4). Second, as immunohistochemical procedures for both OXA and OXB were identical except for the primary antibody used, nonspecific binding of the secondary antibody is unlikely (see Methods). Third, the OXA immunoreactivity seen in the Pa, SO, and SOR does not appear to be the result of the primary antibody

binding to an orexin-like peptide that is normally found in these magnocellular nuclei, as tissue reacted with the same antibodies does not show any evidence of orexin-IR perikarya in the Pa or SO of the degu (present study), Sprague-Dawley rat (personal observation), or the golden-mantled ground squirrel (*Spermophilus lateralis*) (personal observation). Finally, the OXA-IR neurons in the SO and Pa are not the result of the antibody binding to AVP, as other regions known to produce AVP, such as the SCN, do not exhibit similar immunoreactivity (see Figure 2.9)

The Pa and SO are involved in a number of systems in the brain. These nuclei project to the pituitary via the median eminence, where they release vasopressin and oxytocin, peptides involved in reproduction, regulation of blood pressure, and control of the hypothalamic-pituitary-adrenal (HPA) axis (reviewed in Hatton 1990). The presence of OXA in these magnocellular nuclei in the LE rat, but not in the inbred Wistar rat, might be related to the stress response, which is higher in the LE rat than in the Wistar rat (Tohei et al. 2003). Orexin A actions in the Pa appear to potentiate the stress response, in part by modulating the release of corticotrophin releasing factor (CRF) (Ida et al. 2000b; Jászberényi et al. 2000; Samson et al. 2002). In contrast, OXB appears to have a suppressive rather than a stimulatory effect on CRF release (Malendowicz et al. 1999), raising the possibility that differences in OXA distribution might contribute to differences in stress-related behavior and physiology between different strains of rats.

In addition to a potential role in the stress response, the presence of OXA-IR neurons in the magnocellular hypothalamic nuclei could potentially be involved

in strain and species differences in some reproductive behavior, cardiovascular response, or even feeding. With respect to reproductive functions, OXA has been shown to both induce the release of gonadotropin releasing hormone (GnRH) in the hypothalamus, and paradoxically to directly inhibit GnRH actions in the pituitary (Russell et al. 2001). The influence of OXA on the release of both GnRH and CRF seems to be mediated in part by neuropeptide-Y (NPY) (Ida et al. 2000a; Ida et al. 2000b; Jászberényi et al. 2000; Russell et al. 2001), a peptide known both to interact with orexin in the control of ingestive behavior (Yamanaka et al. 2000) and to stimulate the release of OT and AVP from the Pa and SO (Kapoor and Sladek 2001). Furthermore, the magnocellular Pa and SO receive inputs from brain stem nuclei (such as the Sol) involved in regulation of cardiovascular and visceral responses (Armstrong 1995). Many of these nuclei are also heavily innervated by orexin fibers, suggesting a possibility for not only direct actions of orexins within the Pa and SO, but indirect actions through orexin efferents from the main body of orexin neurons within the LHA.

### **Species differences in OXA and OXB fiber distribution**

There were several specific regions in which one or two species tended to strongly diverge from the rest in terms of orexin-IR fiber density. In two of these regions –the magnocellular neurosecretory nuclei of the hypothalamus in the LE rat and grass rat, and the PeF in the hamster – differences in OXA and OXB fiber density are directly related to the presence OXA cell bodies or the absence of any orexin-IR neurons, respectively. A third area, the median eminence in the LE

rat and grass rat, is also likely different with respect to OXA fiber density than in the hamster and degu because of projections originating from OXA-IR cells in the LE rat and grass rat Pa and SO (although it is worth mentioning that the hamster, which also exhibited OXA neurons in the SO, did not differ from the degu with respect to OXA fiber density in this region). The species differences in relative fiber density in other brain regions raise interesting questions. We will focus the remainder of this discussion on the brain regions within each species that showed the most unique patterns of innervation – specifically, the LM in the hamster, and the VMH, CL, Xi, and cerebellum in the degu.

Orexin fiber density in the lateral mammillary nucleus was much higher in the hamster than in the other three species, in which orexin fibers were sparse or absent in this region (Figure 2.11). The mammillary nuclei in general receive dense input from the hippocampus (reviewed in Simerly 1995), and lesion studies suggest a role for the LM in spatial learning and memory in rats (Vann 2005). However, it is unclear at this time why the hamster LM should exhibit increased orexin fiber input relative to the other species.

The most striking differences in orexin fiber distribution in this study were seen in the degu. In this species, orexin fiber density was lower in the xiphoid nucleus (Figure 2.14) and much higher in the centrolateral nucleus of the thalamus (Figure 2.13) in comparison to the other three species. The degu also exhibited an extremely dense network of orexin-IR fibers in the VMH, predominantly in the ventromedial portion of this nucleus (Figure 2.10). In the other species, orexin fiber density in the VMH was moderate to low, while this

nucleus represented the region of greatest fiber density observed in the degu. With respect to the cerebellum, the degu exhibited moderately dense orexin-IR innervation of the cerebellar nuclei and flocculus, while in the other three species these regions were sparsely innervated at best (Figure 2.17). The grass rat, LE rat, and Syrian hamster are relatively closely related to each other (all are members of the Suborder Sciurognathi, Family Muridae), and the degu (Suborder Hystricognathi, Family Octodontidae) is relatively distantly related to them (Nowak 1999). It is therefore possible that the differences in fiber distribution observed between the degu and the other three species are a reflection of phylogenetic history and constraints associated with it, rather than functional differences among these rodents. However, it is tempting to speculate on the function of orexin projections to these regions in the degu.

Although the implication of the lack of orexin input to the xiphoid nucleus is unclear, the networks of orexin-IR fibers in the degu CL, VMH and cerebellum could all play a role in anti-predator behavior during periods of heightened arousal, such as sentinel activity. When feeding, degus alternate sentinel duties and produce alarm calls to warn conspecifics of danger (reviewed in Lee 2004). Sentinel duty in the degu requires that an animal both detect potential threats, and respond properly to threats once identified. The orexin-IR fibers in the flocculus might aid in the visual detection of threats. Predator avoidance behavior in the degu appears to be based primarily upon visual scans for aerial or ground-level threats (Ebensperger and Hurtado 2005). Pursuit of a visually acquired target requires smooth, coordinated eye movements to maintain visual contact

with a constantly moving stimulus (Lisberger et al. 1987). The flocculus has been shown to be important in maintaining such predictive eye movements during visual tracking (Robinson and Fuchs 2001). The CL and the VMH may be involved in appropriate response to predators. Amygdalar projections from the CL and other intralaminar thalamic nuclei are thought to engage fear responses in rats (reviewed in Price 1995), and the CL specifically appears to be important in cognitive awareness and executive decision making (Van der Werf et al. 2002). The VMH is part of the cerebral-hypothalamic “behavior control column” mediating somatomotor aspects of complex motivated behavior (Swanson 2000). The dorsomedial region of this nucleus is specifically implicated in predator-induced defensive responses (Canteras 2002). As the three brain regions in the degu receiving heavier than average orexin innervation may all be involved in anti-predator behaviors, coordination of predator detection, tracking, and appropriate fear and avoidance responses during periods of heightened arousal may be an important function of orexins in the degu.

### **Summary**

In summary, with respect to the overall distribution of orexin, this study confirms the high degree of similarity among species but also reveals some significant differences. The distribution of orexin-IR cell bodies and fibers is quite similar among the Long-Evans rat, grass rat, hamster and degu, and is largely consistent with previously published reports (Peyron et al. 1998; Chen et al. 1999; Cutler et al. 1999; Date et al. 1999; Nambu et al. 1999; McGranaghan and Piggins 2001; Mintz et al. 2001; Novak and Albers 2002). With respect to orexin

fibers, the high levels of congruence between species suggest a strongly conserved common role for OXA and OXB in the maintenance of arousal state, modulation of somatomotor activity, and control of ingestive behavior. On the other hand, there are some significant species differences in the distribution of orexin cell bodies as well as the density of orexin-IR fibers in some regions. With respect to cell bodies, the present study describes specific species differences in the organization of the main body of OXA- and OXB-IR neurons in the lateral hypothalamus, and also provides evidence for a previously undescribed population of OXA-IR neurons in the magnocellular neurosecretory nuclei of the hypothalamus. These differences in orexin cell distribution raise the possibility that some subpopulations of orexin-IR neurons might differ with respect to afferent inputs, suggesting potential differences in activation of orexin neurons among species. In addition, the sometimes considerable differences in the relative density of orexin-IR fiber input to different regions might reflect differences in the importance or function of acute orexin actions in specific nuclei.

### Chapter 3

Nixon, J. P. and L. Smale (2004). "Individual differences in wheel-running rhythms are related to temporal and spatial patterns of activation of orexin a and b cells in a diurnal rodent (*Arvicanthis niloticus*)."  
Neuroscience **127**(1): 25-34.



## **CHAPTER 3**

# **Individual differences in wheel-running rhythms are related to temporal and spatial patterns of activation of orexin A and B cells in a diurnal rodent (*Arvicanthis niloticus*)**

### **Introduction**

In mammals, circadian rhythms in physiology and behavior are generated by the suprachiasmatic nucleus (SCN) and entrained by the light-dark cycle through the retinohypothalamic tract (reviewed in Weaver 1998). In addition to photic cues, circadian rhythms can also be modified by non-photoc signals, such as exposure to a novel running wheel or gentle interruption of sleep, in a variety of nocturnal and diurnal species (Mrosovsky and Salmon 1987; Amir and Stewart 1996; Hastings et al. 1997; Klerman et al. 1998; Hut et al. 1999; Kas and Edgar 1999; Antle and Mistlberger 2000). The geniculohypothalamic tract (GHT), extending to the SCN from the intergeniculate leaflet (IGL) of the lateral geniculate nucleus (LGN) represents one source of non-photoc input to the SCN (reviewed in Harrington 1997). The subpopulation of IGL cells that contain neuropeptide-Y (NPY) play an especially important role. This conclusion is based on studies in hamsters that have looked at c-Fos expression in NPY cells, or at effects of infusions of NPY or NPY antagonists into the SCN (Albers and Ferris 1984; Huhman and Albers 1994; Janik and Mrosovsky 1994; Wickland and Turek 1994; Biello 1995; Janik et al. 1995).

We recently investigated the relationship between NPY-containing cells in the IGL and patterns of wheel running in the grass rat, *Arvicanthis niloticus* (Smale et al. 2001b). The grass rat is endemic to equatorial Africa and exhibits diurnal patterns of activity both in the laboratory and in the wild (Katona and Smale 1997; Blanchong and Smale 2000). Although grass rats do not exhibit phase shifts when given access to a novel wheel (L. Smale, unpublished observations), some switch to a “nocturnal” pattern of activity when given continuous access to a wheel (Blanchong et al. 1999). Several lines of evidence suggest that this change reflects an unusual form of masking, rather than a switch within the circadian timekeeping system. First, several basic features of the activity patterns are the same in day- and night-active grass rats. Specifically, both exhibit a short burst of activity prior to lights-on and a peak immediately after lights-off (Blanchong et al. 1999). Second, night-active animals appear to partition total sleep time equally between the light and dark periods, but they experience more fragmented sleep bouts during the light period (L. Smale and M. Schwartz, unpublished observations), suggesting that a signal promoting diurnal wakefulness remains. Third, although hourly body temperature averages of night-active grass rats are lower than those of day-active animals during the light period, their lowest body temperatures still occur late in the night, as they do in day-active grass rats (Blanchong et al. 1999). Finally, there are no transients during switches from night- to day-active patterns following removal of a wheel, or on the rare occasions that switches occur spontaneously (see below). If the switch between patterns was driven by changes in the SCN, transients would be

expected (Redlin and Mrosovsky 2004). Thus running at night appears to result in increased nocturnal arousal without a change in the fundamental underlying diurnal circadian system. Using this animal model therefore allows us to examine activity-induced arousal either in conjunction with circadian signals promoting wakefulness (in day-active grass rats), or without them (in night-active grass rats). In this model system, the dissociation between activity and circadian influences emerges from the animal's own behavior, running in a wheel that is continuously available, rather than being triggered by periodic changes in the animal's environment.

As in other mammals, the SCN of the grass rat receives NPY input that comes from the IGL (Smale and Boverhof 1999; Smale et al. 2001b). When provided continuous access to running wheels, Fos immunoreactivity (Fos-IR) within NPY cells is high during the day and low at night for day-active grass rats, and low during the day but high at night in night-active ones. Grass rats housed with running wheels show higher percentages of NPY cells expressing Fos than do animals without running wheels (Smale et al. 2001b). The reversed rhythm within NPY cells of night- and day-active grass rats is therefore caused, at least in part, by the differences in when these animals run.

Although projections to the IGL have been well-defined (Morin 1994; Vrang et al. 2003), little is known about the specific route through which information regarding arousal state reaches the NPY cells in the IGL. One possibility involves the orexins (hypocretins), a recently described family of peptides present in cells of the lateral hypothalamus (LH) (Sakurai et al. 1998; de

Lecea and Sutcliffe 1999). The orexins consist of two peptides, orexin A (OXA) and B (OXB), derived from the same precursor protein (Sakurai et al. 1998; de Lecea and Sutcliffe 1999). Orexins are thought to be involved in the regulation of arousal, general activity and feeding (Lubkin and Stricker-Krongrad 1998; Edwards et al. 1999; Hagan et al. 1999; Kunii et al. 1999; Piper et al. 2000; Estabrooke et al. 2001; Hungs et al. 2001; Yoshimichi et al. 2001; Kotz et al. 2002). OXA appears to play a more important role in many of the reported actions of the orexins than does OXB (Sakurai et al. 1998; Edwards et al. 1999; Kunii et al. 1999).

Fibers containing orexin project to the IGL in several species, including the hamster (McGranaghan and Piggins 2001; Mintz et al. 2001) and the grass rat (Novak and Albers 2002), raising the possibility that orexin might mediate the influence of arousal on NPY cells. To investigate this possibility, we first examined patterns of OXA and OXB cell activation in relation to activity state (as indicated by wheel running) and time of day in day- and night-active grass rats. We then examined tissue processed for NPY and either OXA or OXB immunoreactivity (IR) to determine whether orexin fibers could contact NPY cells in the IGL.

## **Methods**

### **Animal housing and determination of activity patterns**

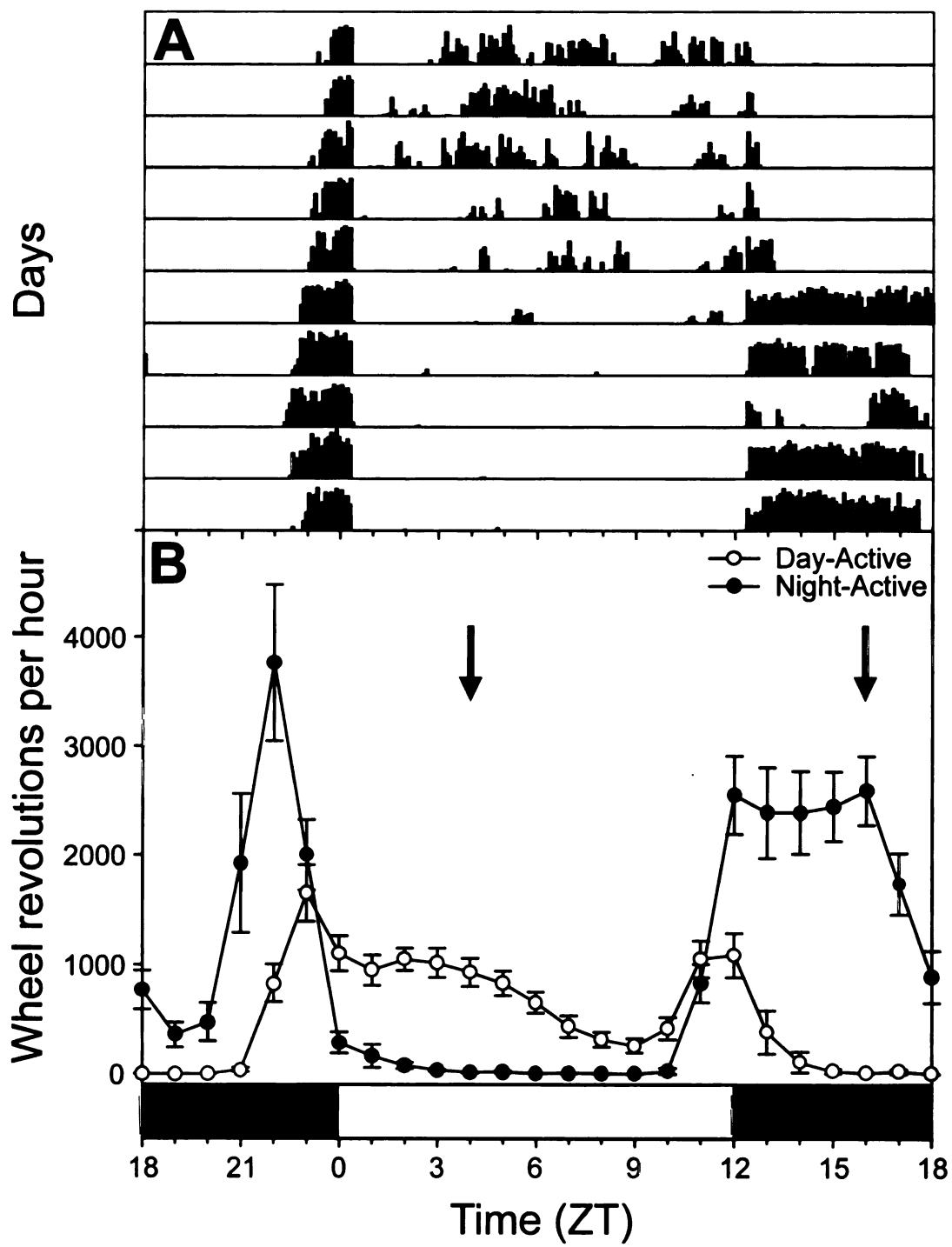
Thirty-nine adult male grass rats bred in a captive colony were used in this study. Animals were kept on a 12:12 light:dark cycle with a red light (< 5 lux) kept

on constantly and were provided food (Harlan Teklad 8640 rodent diet, Harlan Teklad Laboratory, Madison, WI) and water ad libitum. All animal handling procedures followed in this study were approved by the Michigan State University All-University Committee for Animal Use and Care. All animals were individually housed in cages (28 × 34 × 16 cm) that in some cases were equipped with running wheels (26 cm diameter, 8 cm width). Each wheel revolution was recorded when a magnetic bar on the wheel closed a switch mounted on the wheel housing. Wheel running data were collected and quantified using the DSI Dataquest 3 system (MiniMitter, Sunriver, OR). After stable wheel running rhythms had been established for at least one week, animals were classified as day- or night-active. A grass rat was classified as night-active if wheel running continued for more than 4 hours after lights-out, while day-active animals were defined as those that ceased running within 2 hours after lights-out. Animals that exhibited ambiguous activity patterns were excluded from the study. Average hourly numbers of wheel revolutions were calculated from the last 5 days in running wheels, and animals were considered to be inactive during a given hour if the number of wheel revolutions was less than 10% of the daily peak. Average hourly activity levels to illustrate both patterns are presented in Figure 3.1.

### **Tissue processing and analysis**

At the time of sacrifice, all grass rats were deeply anesthetized with sodium pentobarbital (Nembutal; Abbot Laboratories, North Chicago, IN). Animals sacrificed during the dark period were fitted with light-tight hoods to prevent exposure to light during perfusion. Animals were perfused transcardially

**Figure 3.1. (A)** Actogram illustrating wheel running activity of an individual grass rat. Although initially day-active, this individual exhibited a spontaneous switch to a night-active pattern, illustrating both the two basic patterns and the lack of transients during a switch. This spontaneous switch is atypical; most animals in our colony establish stable day- or night-active rhythms shortly after introduction of a wheel. **(B)** Line graph illustrating average hourly wheel revolutions over a 5 day monitoring period of all day-active (n = 18, open circles) and night-active (n = 18, closed circles) grass rats used in this study. Arrows at ZT 4 and ZT 16 indicate sampling times for animals used in this study. Bar at bottom indicates light cycle.



with 0.01 M phosphate-buffered saline (PBS; pH 7.4, 150 – 200 ml/animal) followed by 150 to 200 mL fixative (4% paraformaldehyde with 75 mM lysine and 10 mM sodium periodate, in 0.1 M phosphate buffer, pH 7.2) Brains were post fixed for 8 h, then transferred into 20% sucrose. After 24 h in sucrose, brains were stored at -20°C in cryoprotectant (Watson et al. 1986) until the time of sectioning. All brains were sectioned at 30 µm in three series using a freezing microtome.

For all studies, tissue was processed for immunohistochemical staining using the following general procedure. All sections were incubated in 5% blocking serum in PBS with 0.3% Triton-X 100 (Research Products International, Mount Prospect, IL) for 1 h. Tissue was then incubated in primary antibody for 24 h at 4°C in PBS with 0.3% Triton-X 100 (PBS-TX) and 3% serum. Next, tissue was incubated in biotinylated secondary antibody (1:500; in PBS-TX with 3% serum) for 1 h. Tissue was then placed in avidin-biotin complex (AB complex; 0.9% each avidin and biotin solutions, Vector Laboratories, Burlingame, CA; in PBS-TX) for 1 h. Sections were then rinsed three times for 10 minutes in acetate buffer, then reacted for 7 minutes with diaminobenzidine (DAB; 0.1 mg/ml, Sigma) enhanced with nickel chloride (25 mg/ml; Sigma) in acetate buffer with 3% hydrogen peroxide. Following the nickel-enhanced DAB reaction, tissue was rinsed 5 times for 2 minutes in PBS-TX. Nickel-labeled tissue was then blocked using 5% serum in PBS-TX for 1 h, then allowed to react with primary antibody for 24 h at 4°C (in PBS-TX and 3% serum). This step was followed by incubation in biotinylated secondary antibody for 1 h (1:500; in PBS-TX and 3% serum).



Tissue was then incubated for 1 h in AB complex. Following the AB incubation, tissue was reacted with DAB (0.5 mg/ml, Sigma) in a tris-hydrochloride buffer (Trizma, Sigma; pH 7.2) with hydrogen peroxide (0.35  $\mu$ l 30% hydrogen peroxide/ml buffer). For all reactions, primary antibodies were omitted in control sections. During immunohistochemical processing, all tissue was rinsed three times for 10 minutes in PBS between each step, with the exception of the PBS-TX rinses between AB complex incubation and nickel-DAB reaction.

To evaluate relationships between orexin fibers and NPY cells, tissue was blocked using normal horse serum (NHS; Vector), then reacted with either goat anti-OXA or goat anti-OXB primary (Santa Cruz Biotechnology, Santa Cruz, CA; 1:10,000) and horse anti-goat secondary (Vector). Following PBS-TX rinses after the orexin nickel-DAB reaction, tissue was rinsed for 24 h in PBS at 4°C. For the NPY reaction, tissue was blocked using normal donkey serum (NDS; Jackson Laboratories, West Grove, PA), then incubated in rabbit anti-NPY primary (Peninsula Labs, Belmont, CA; 1:2,000) and donkey anti-rabbit secondary (Jackson). For the orexin-Fos study, tissue was blocked using NDS then nickel-labeled for Fos using a rabbit anti-Fos primary antiserum (Santa Cruz; 1:2000) and donkey anti-sheep secondary (Jackson). Fos-labeled tissue was then reacted for either OXA or OXB antisera using the same serum and antibodies described above. The supplier reports no cross-reactivity between the OXA and OXB antibodies used in this study; preabsorption tests using blocking peptides supplied by Santa Cruz confirm this in our tissue.

After processing for orexin and NPY or for orexin and Fos, all tissue was mounted on gelatin coated slides, dehydrated, and coverslipped. Tissue was examined using a light microscope equipped with a drawing tube (Leitz, Laborlux S; Wetzlar, Germany). High-resolution digital photographs of representative sections were taken using a digital camera (Carl Zeiss, AxioCam MRc; Göttingen, Germany) attached to a Zeiss light microscope (Axioskop 2 plus). Image contrast and color balance were optimized using Zeiss AxioVision software (Carl Zeiss Vision). Graphs were prepared using SigmaPlot (SPSS; SPSS, Chicago, IL). Final figures were assembled using Adobe Illustrator and Adobe Photoshop (Adobe Systems, San Jose, CA).

### **Patterns of Fos Expression in Orexin Cells**

For wheel running studies, tissue from a total of 36 animals (n = 18 day-active, 18 night-active) was collected as follows: Six day-active and six night-active animals were housed with running wheels and sacrificed at Zeitgeber time (ZT) 4. A second group of six day-active and six night-active animals were housed with running wheels and sacrificed at ZT 16. The final twelve day- and night-active grass rats were initially housed with running wheels, but wheels were removed 5 days prior to sacrifice. Day-active animals in this final group were sacrificed at ZT 4, while the night-active animals without running wheels were sacrificed at ZT 16. We did not examine effects of running wheels on day-active animals at ZT 16 or night-active animals at ZT 4, because these animals do not run at these times.

Following immunohistochemical staining for orexin and Fos, three representative sections per animal were chosen for analysis, following the method of Martinez et. al. (2002). Briefly, a box 1200  $\mu\text{m}$  by 700  $\mu\text{m}$  was placed with one side against the third ventricle, and the bottom of the box aligned with the ventral border of the fornix (Figure 3.2). The box was subdivided into three equal regions, referred to here as the medial, central, or lateral regions. Although this box does not include all areas of the grass rat brain containing orexin cells, examination of several animals revealed that the majority of orexin-immunoreactive cell bodies in the lateral hypothalamus and perifornical area fall within the boundaries of the box. The number of orexin, Fos, and double-labeled cells in the box were counted unilaterally in each animal by an observer blind to the experimental group of the animal. The hemisphere chosen for analysis was randomized between subjects. All double-labeled cells were confirmed using a high-power (50x) objective. Camera lucida drawings were prepared for each section examined.

To determine whether differences in wheel running patterns are correlated with differences in orexin cell activity, we compared day- and night-active animals housed with running wheels and sacrificed at either ZT 4 or ZT 16. Percentages of Fos-labeled OXA and OXB cells for each animal were calculated and analyzed using SYSTAT (SPSS). Percentages were arc sine transformed and then analyzed using a two-way analysis of variance (ANOVA), with phenotype (day- vs. night-active) and time of sacrifice (ZT 4 vs. ZT 16) as independent variables. To determine whether heightened Fos-IR in orexin cells was caused by access to

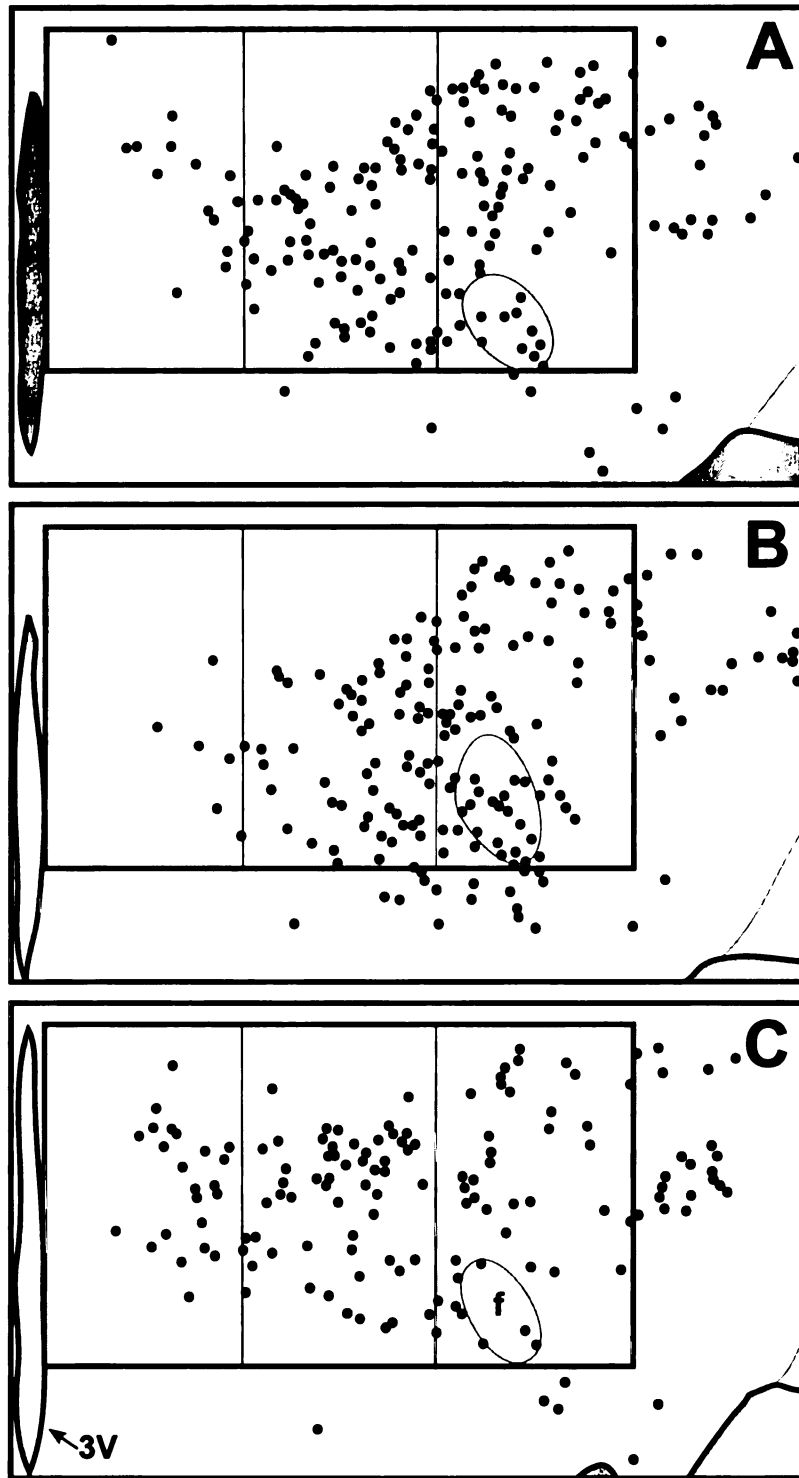


**Figure 3.2.** Drawing of representative sections through (A) rostral, (B) middle and (C) caudal sections of the grass rat LH. Boxes representing sampling area are 1200 x 700  $\mu$ m, divided from left to right into medial, central, and lateral divisions. Dots represent cells stained for OXA. Distribution of OXB cells were similar (not shown). 3V = 3<sup>rd</sup> ventricle; f = fornix.

the running wheel, we compared animals with running wheels to animals that had running wheels removed 5 days prior to sacrifice. Percentages of Fos-labeled OXA and OXB cells were arc sine transformed, and then effects of the wheels were examined with paired t tests for day-active animals at ZT 4 and night-active animals at ZT 16, respectively. Potential differences in distribution of double-labeled cells were analyzed using multivariate repeated measures ANOVA, using presence of wheel as a grouping factor, orexin type (OXA or OXB) as an independent variable, and region of analysis (medial, central, or lateral) as dependent variables. For all statistical analyses, the null hypothesis was accepted when  $P > 0.05$ .

### **IGL Anatomy**

For IGL anatomy studies, tissue from 3 grass rats was collected and alternate series were processed for NPY and either OXA or OXB to determine whether orexin fibers were in proximity to, and appeared to contact, NPY cells in the IGL. Tissue was then examined at high power (100x) and relationships between NPY cells and either OXA or OXB fibers in the IGL were examined and photographed. Total numbers of NPY cells that did or did not appear to be in contact with OXA and OXB fibers were counted for six representative sections through the IGL in each animal.

## Results

### Patterns of Fos Expression in Orexin Cells

Orexin, Fos, and double-labeled cells were clearly visible and distinguishable following immunohistochemical processing of tissue (Figure 3.3). Although absolute numbers of OXA vs. OXB cells did not significantly differ among treatment groups (data not shown), there were significant differences in the percentage of orexin cells expressing Fos. Overall, the percentages of OXA and OXB cells expressing Fos were higher when animals were actively running at the time of sacrifice, and peak Fos expression in orexin cells was reversed among day- and night-active phenotypes (Figure 3.4). Day-active animals showed higher percentages of OXA and OXB cells expressing Fos in at ZT 4, while night-active grass rats had higher percentages at ZT 16. Although OXA cells appeared to be more likely to express Fos than did OXB cells at the time of peak wheel running, the difference was not significant. ANOVA for both OXA and OXB shows a significant interaction between phenotype and time (OXA:  $F = 15.461$ ,  $df = 1$ ,  $p = 0.001$ ; OXB:  $F = 21.559$ ,  $df = 1$ ,  $p < 0.001$ ).

Access to a running wheel significantly affected Fos percentages in OXA and OXB cells in night-active grass rats only (Figure 3.5). No significant differences were observed in OXA or OXB cells in day-active animals. Night-active animals with wheels had significantly higher percentages of OXA cells expressing Fos than animals without wheels (OXA:  $t = -2.861$ ,  $p = 0.032$ ; OXB:  $t = -3.412$ ,  $p = 0.019$ ). Levels of double labeling in day-active grass rats with wheels appeared to be higher than in those without wheels, but the difference

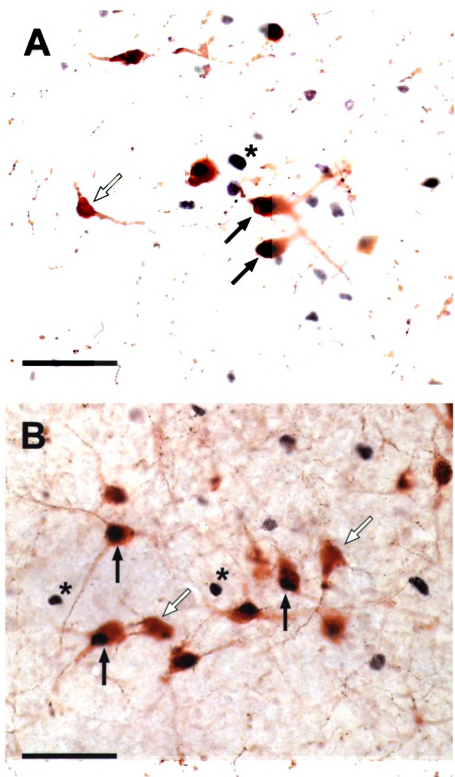


**Figure 3.3.** Photomicrograph (40x) of orexin A and B cells in the grass rat LH. Cells marked \* are expressing Fos-IR only; Open arrows indicate cells expressing only OXA (Panel A) or OXB (Panel B); Solid arrows point to double-labeled cells. Scale bar = 50  $\mu$ m.

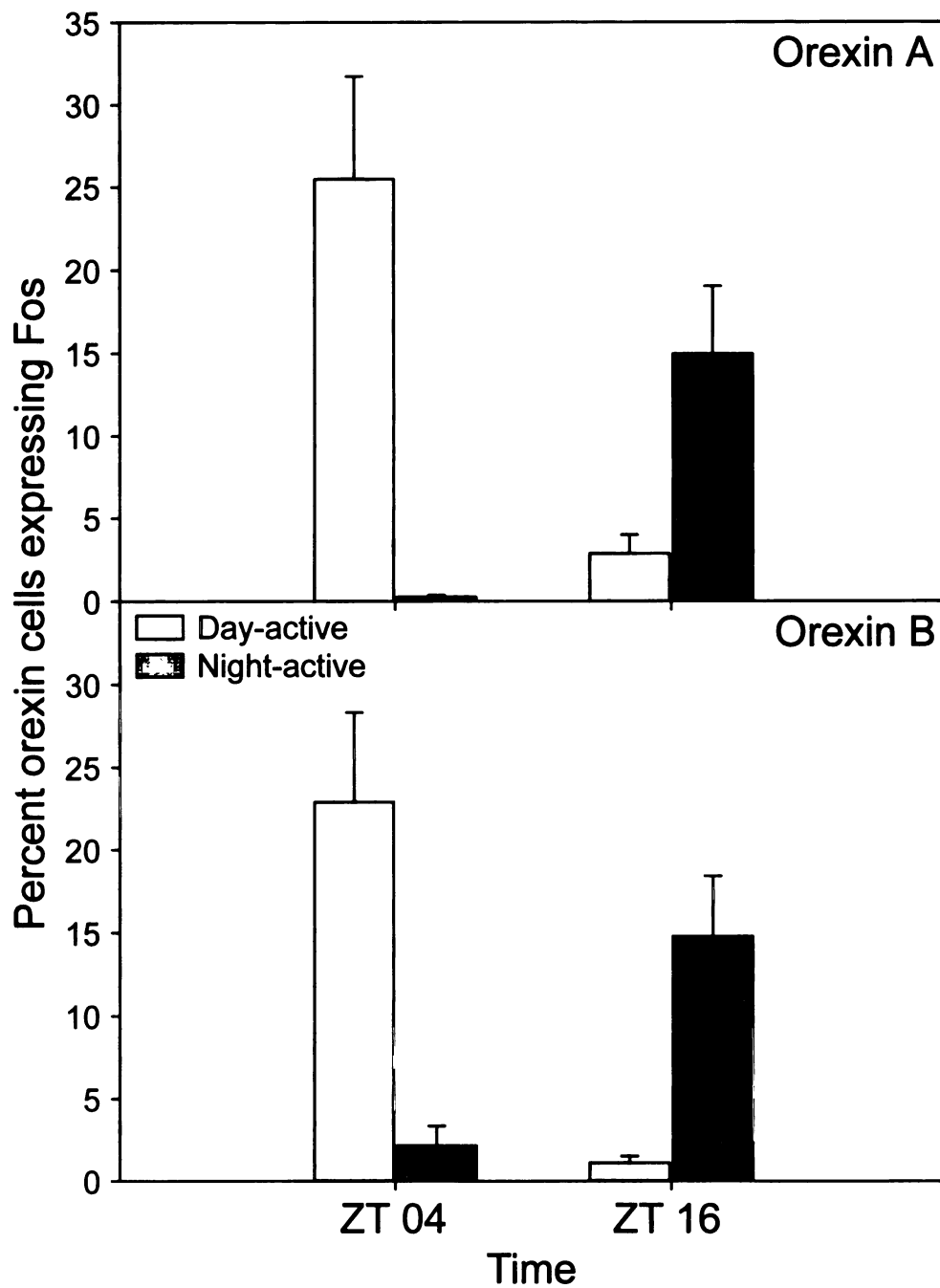


**Figure 3.4.** Temporal patterns of mean ( $\pm$  SEM) levels of Fos expression in OXA (top) and OXB (bottom) cells in day- and night-active animals sacrificed at ZT 4 and ZT 16. Light bars represent day-active animals; dark bars represent night-active grass rats. Significant differences ( $p < 0.05$ ) noted by different letters.



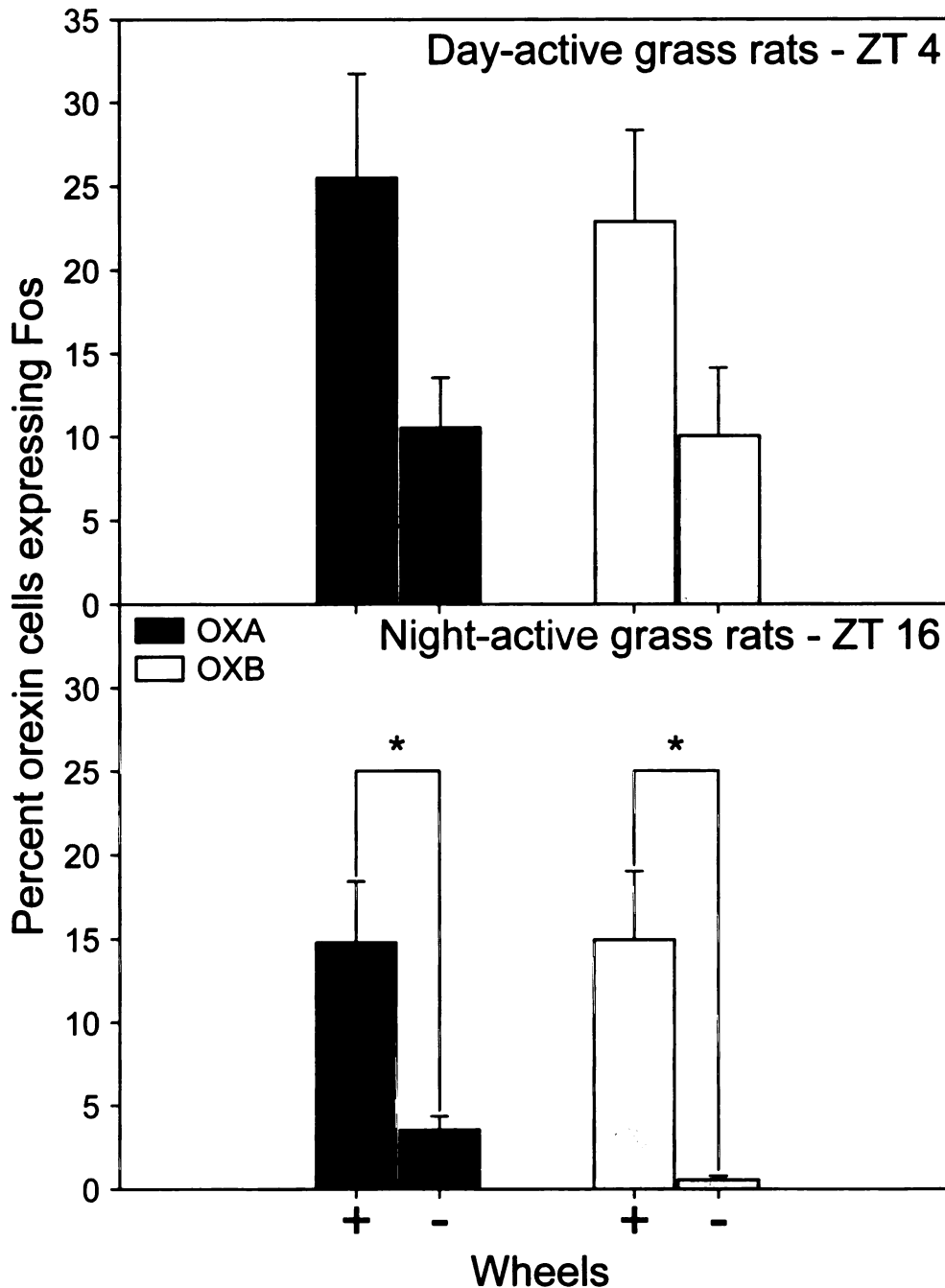


**Figure 3.5.** Fos-IR in orexin cells in grass rats housed with (+) and without (-) running wheels. Day-active grass rats (top) were sacrificed at ZT 4, night-active animals (bottom) at ZT 16. Dark bars = OXA; light bars = OXB. Significant differences ( $p < 0.05$ ) noted by different letters. Removal of running wheel caused significant reductions in Fos-IR only in night-active animals. Effects of wheels were not significant in day-active animals, although trends were similar ( $p = 0.06$  and  $p = 0.08$  for OXA and OXB, respectively).

was not statistically significant (OXA:  $t = -2.230$ ,  $p = 0.060$ ; OXB:  $t = -1.940$ ,  $p = 0.081$ ).

In addition to differences in total percentages of orexin cells expressing Fos-IR, significant differences in distribution of double-labeled cells were observed in night-active grass rats (Figure 3.6). For animals with wheels, ANOVA revealed significant effects of area ( $F = 14.698$ ,  $df = 2$ ,  $p < 0.001$ ), with no interaction with type of orexin (OXA vs. OXB). In animals without wheels, there was an interaction between orexin type and area of analysis ( $F = 5.876$ ,  $df = 2$ ,  $p = 0.010$ ). Night-active grass rats with running wheels showed significantly higher percentages of double-labeled cells in medial regions, and decreased percentages in central and lateral portions of the area of study. Although the overall activation of OXA cells was much lower in night-active animals without wheels (Figure 3.6), the spatial gradient was still apparent. In contrast, OXB cells in this group expressed virtually no Fos (Figure 3.6). In OXA and OXB cells of day-active animals, no significant difference in Fos-IR was observed across medial, central or lateral regions of the LH in any treatment group (day-active with wheels:  $F = 2.401$ ,  $p = 0.116$ ; day-active without wheels:  $F = 1.190$ ,  $p = 0.325$ ).

### **IGL Anatomy**

OXA and OXB fibers were both present in the IGL of all grass rats examined, and clearly distinguished it from surrounding tissue (Figure 3.7). These OXA and OXB fibers appeared to terminate on or follow the borders of NPY cells throughout the rostro-caudal extent of the IGL. In some cases, orexin

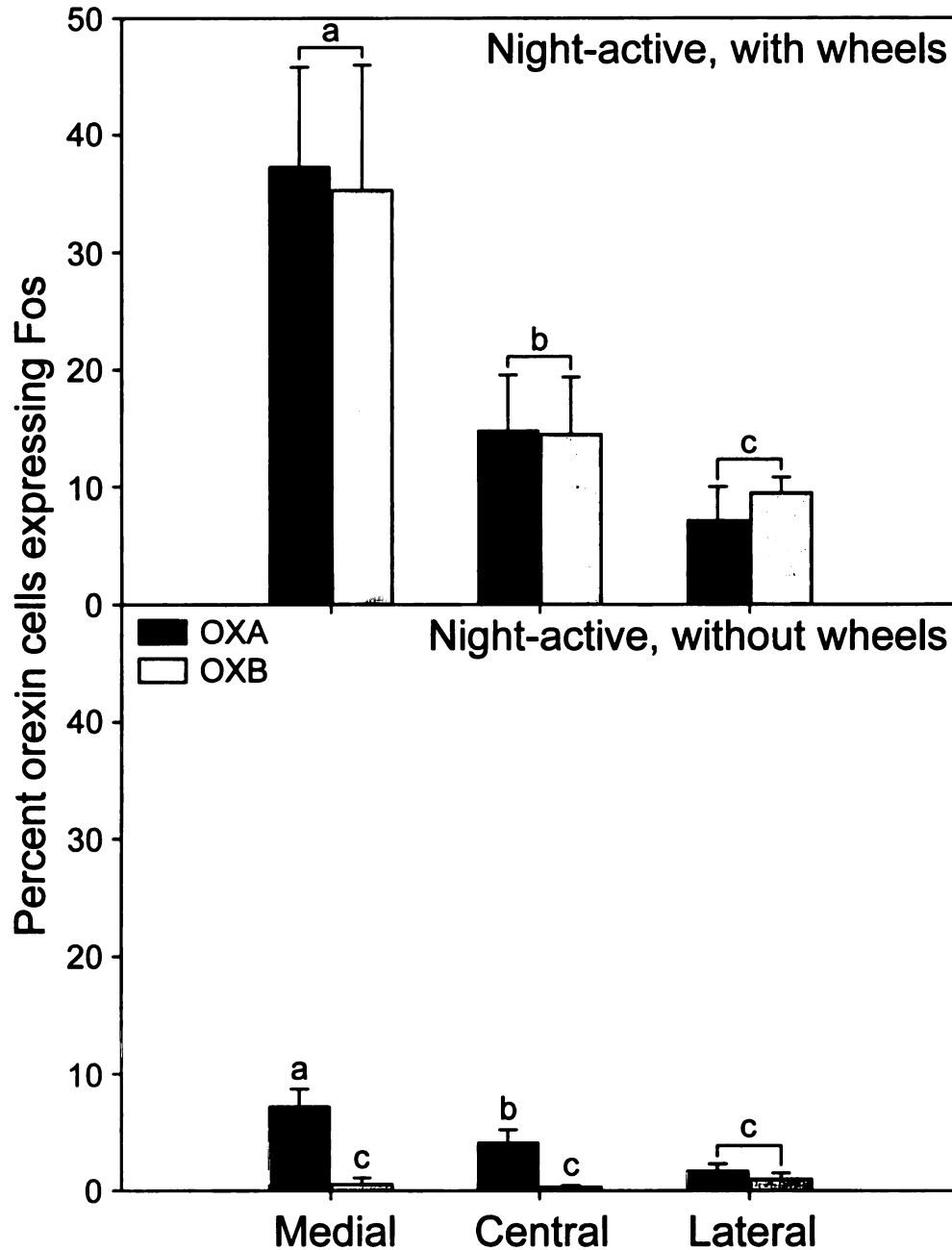


**Figure 3.6.** Regional patterns of orexin Fos-IR in night-active grass rats housed with (top) or without (bottom) running wheels at ZT 16 demonstrating both the medial to lateral gradient in orexin cell activity, and the differences and similarities between OXA- and OXB-labeled cells. Significant differences ( $p < 0.05$ ) noted by different letters. Dark bars = OXA; light bars = OXB.

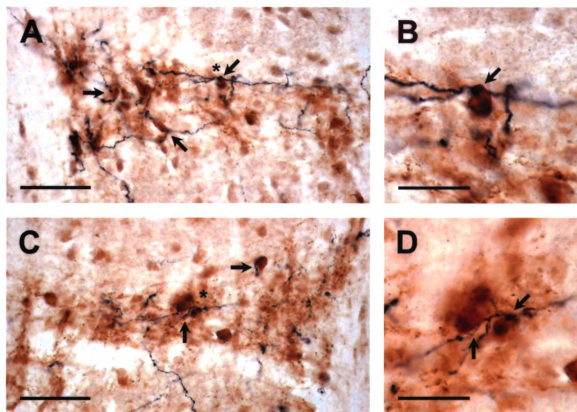


**Figure 3.7.** Photomicrographs of OXA (Panels **A** and **B**) and OXB (Panels **C** and **D**) fibers and NPY cells in the grass rat IGL. Arrows indicate where contacts between NPY cells and orexin fibers appear to be present. Panels (**A**) and (**C**) are 40x; scale bar is 50  $\mu$ m. Panels (**B**) and (**D**) are 100x close-ups of regions marked with \* in panels (**A**) and (**C**), respectively; scale bar is 20  $\mu$ m.

fibers appeared to wrap around the NPY cells. These fibers exhibited numerous varicosities, suggesting the potential for synapses between the orexin fibers and the NPY cells. In all animals, approximately half of the NPY cells appeared to be contacted by OXA or OXB fibers ( $55.90 \pm 6.52\%$  and  $42.58 \pm 6.47\%$ , respectively). Boutons were also present on fibers that were not near NPY cells, suggesting that orexin fibers may form synapses with other cell populations in this region. Although synapses between orexin fibers and NPY cells can not be observed using light microscopy, the nature of the spatial relationship between these cells and fibers clearly suggest the potential for functional contacts between NPY cells of the IGL and orexin fibers originating from the LH in the grass rat.

## **Discussion**

### **IGL Anatomy**

Orexin fibers have been documented in the IGL of several species (McGranaghan and Piggins 2001; Mintz et al. 2001), including the grass rat (Novak and Albers 2002). The data presented here show that both OXA and OXB fibers are not only present in the IGL but that they are closely associated with NPY cells in this structure. While investigation of what appear to be contacts at the light level cannot provide direct information about synapses, it does suggest that the fibers communicate with a particular cell. Light-level investigation of tissue reacted for either OXA or OXB and NPY suggest that orexin fibers in the grass rat IGL may contact about half of the NPY cells visible

in the tissue (Figure 3.7). A greater percentage of NPY cells appeared to be contacted by OXA fibers than by OXB fibers, but the variability was high, and may simply reflect the small sample size or the denser distribution of OXA fibers in the grass rat IGL (J. Nixon, unpublished observations) rather than a functional difference. In many cases, the labeled fibers appeared to be wrapped around or to closely follow the contours of the NPY cells. Numerous varicosities suggestive of synapses were seen on orexin fibers where they appeared to contact NPY cells. Varicosities were also present on orexin fibers that were not near NPY cells, suggesting that they form synapses with other cell populations in the IGL as well. Both the hamster and grass rat IGL contain enkephalin neurons that project to the SCN (Morin and Blanchard 1995; Smale and Boverhof 1999), and neurotensin- and GABA-positive neurons that project to the SCN have recently been identified in the hamster IGL (Morin and Blanchard 2001). The varicosities and boutons that were not near NPY neurons raise the possibility that orexin projections might also be able to influence the circadian system through these populations of neurons. Associations between orexin fibers and NPY cells elsewhere in the brain set a precedent for orexin activation of NPY cells. Orexin fibers form functional synaptic contacts with NPY-containing neurons in the arcuate nucleus (Horvath et al. 1999a), and intraventricular administration of OXA increases Fos expression in this population of NPY cells (Yamanaka et al. 2000). The present double-labeling data suggest that similar interactions between NPY cells and orexinergic inputs could occur in the IGL.

### **Fos expression in orexin cells: general patterns**

Orexin cell function has been correlated with activity state in a variety of contexts, and direct experimental induction of arousal induces Fos in orexin cells (Chemelli et al. 1999; Estabrooke et al. 2001). Here we used day- and night-active grass rats as a model system with which to further examine orexin cell function in relation to time of day and arousal state. Rather than directly arousing the animals, we created conditions that, in some individuals, dramatically alter the temporal patterns of spontaneous rhythms in arousal state by providing them with running wheels (Blanchong et al. 1999). We found that with continuous access to wheels day- and night-active grass rats showed the same general relationship between locomotor activity and Fos expression in orexin cells, but patterns of orexin cell function were reversed with respect to time of day. Specifically, in both groups of animals, Fos-IR percentages in OXA- and OXB-labeled cells were higher when the animals were actively running in wheels, either at ZT 4 in day-active animals or at ZT 16 in night-active individuals (Figure 3.4). This difference between the day- and night- active animals could theoretically reflect differences in direct circadian control over these cells, or they could be consequences of the differences in activity. The latter hypothesis is consistent with the data on how an animals' access to a wheel influenced patterns of Fos expression in orexin neurons. The effects of wheels on day-active animals approached significance ( $p = 0.06$  and  $0.08$  for OXA and OXB, respectively), and they were significant in night-active animals for both OXA and OXB (Figure 3.5). That is, continuous access to a wheel, which maintains arousal at a time when these animals would otherwise sleep, induced orexin cell activity

in these night-active animals. These data provide further evidence that rhythms in orexin cells emerge from mechanisms more directly associated with arousal, rather than being directly driven by the circadian system (Taheri et al. 2000; Estabrooke et al. 2001; Martinez et al. 2002). We also view this hypothesis as more plausible for the same reasons that the effects of the running wheels on circadian rhythms reflect masking, rather than effects on the circadian time-keeping system, in our animals (see above).

#### **Fos expression in orexin cells: heterogeneity of orexin cell function**

Relatively little is known about potential functional differences among orexin cell populations. Here, we found clear regional differences in the distribution of orexin cells that were activated in night-active grass rats, but not in day-active ones (with or without wheels). In night-active animals housed with running wheels there was a medial- to lateral gradient of Fos expression at ZT 16 in both OXA and OXB cells such that these cells were more likely to express Fos in the medial and central regions of the LH (Figure 3.6). This medial to lateral gradient was not seen in any group of day-active animals.

Another surprising finding involved the difference between cells stained for OXA and those stained for OXB in night-active animals without running wheels. In these animals percentages of OXB cells with Fos-IR were extremely low across the entire sampling area. In the same animals a clear medial to lateral gradient was present in OXA cells (Figure 3.6). Thus, in the medial and central regions OXA cells were considerably more likely to express Fos than OXB cells.



This finding was unexpected and may represent the first evidence of a functional difference between cells stained for these two peptides. OXA and OXB originate from the same precursor protein, suggesting that any cell producing OXA should also produce OXB. Although OXA staining has been reported in various studies to be higher than OXB-IR (Cutler et al. 1999; Date et al. 1999; Nambu et al. 1999), the assumption has been that this is because OXB degrades more rapidly than OXA (Sakurai et al. 1998). In the current study it is not the absolute numbers of OXA vs. OXB cells that is at issue, but, rather, the likelihood that these cells express Fos. Percentages of OXA and OXB cells expressing Fos were similar in all groups of animals studied except in night-active grass rats housed without wheels. In these animals, the proportionally high levels of Fos seen in the medial and central groups of OXA compared to OXB cells could reflect either differences in rates of production or degradation of these two proteins. For example, the relative rates of degradation of OXA vs. OXB could be different in these medial and central cells than in orexin cells in the lateral region of the LH. Alternatively, it is possible that some cells may produce OXA but not OXB. Although both peptides come from the same precursor protein, there may be some cellular level of regulation over the final processing such that one peptide is produced in higher quantities than the other. Cells producing other precursor proteins, such as pro-opiomelanocortin, do not always make every peptide that can be derived from the precursor (Raffin-Sanson et al. 2003). Some difference in the function of each orexin peptide is suggested by the reported differences in binding affinity of OXA vs. OXB to each receptor (Sakurai et al.

1998; Smart et al. 1999) coupled with the differential and often non-overlapping distribution of each orexin receptor subtype in many parts of the rodent brain, including the IGL (Trivedi et al. 1998; Marcus et al. 2001). The data presented here therefore raise intriguing questions about the functional impact of heterogeneity among orexin cell populations with respect to possible effects on their target cells.

Interestingly, the conditions under which the OXA, but not OXB cells expressed Fos are the conditions in which behavioral differences between the day- and night-active “wheel-runners” are not apparent (Blanchong et al. 1999). That is, when a wheel is removed from the cage of a night-active grass rat its activity pattern immediately becomes indistinguishable from that of a diurnal grass rat. The tendency to become night-active when presented with a running wheel is heritable (Blanchong et al. 1999), but neural mechanisms underlying the predisposition are unknown. The unexpected finding of Fos expression in some medial OXA neurons of animals pre-disposed to become night-active raises the intriguing possibility that inter-individual differences in the medial OXA cells could actually influence whether animals run at night when a wheel is made available to them.

### **General conclusions**

Orexin cells are uniquely positioned to communicate arousal state information to cell populations elsewhere in the brain because of their widespread fiber distribution and well-established association with sleep-related

nuclei such as the locus coeruleus (Peyron et al. 1998; Cutler et al. 1999; Date et al. 1999; Nambu et al. 1999; McGranaghan and Piggins 2001; Mintz et al. 2001; Novak and Albers 2002). Both the physical contacts we observed between orexin fibers and NPY neurons, and the temporal patterns of orexin cell function, provide some support for the hypothesis that the orexins represent a candidate system for relaying arousal state information to the NPY cells in the IGL. Temporal patterns of change in Fos-IR in orexin cells of grass rats housed with running wheels were very similar to those found previously in NPY cells of animals under the same housing conditions (Smale et al. 2001b), and both populations of cells respond with an increase in Fos to input signals associated with locomotor activity. Although these patterns could reflect similar input signals to these two populations of cells (e.g. from the raphé nucleus), they might reflect a direct functional link through which orexin cells relay activity state information to the NPY cells in IGL.

A second basic theme that emerged from the data involves the functional heterogeneity of the orexin cell population. In night-active grass rats orexin cells located in different regions of the hypothalamus exhibited different patterns of activation, and patterns of Fos activation among OXA cells did not always parallel those of OXB cells. Heterogeneity with respect to patterns of Fos expression in different populations of orexin cells could theoretically reflect differences in the nature of the inputs these cells receive, or in how these cells respond to incoming signals. The heterogeneity of the OX cell population is a subject that warrants further investigation.

The act of running in a wheel has been described as abnormal obsessive behavior, a self-reinforced act that persists in part due to feedback that overrides normal behavioral and physiological signals (reviewed in Sherwin 1998). In night-active grass rats, wheel-running at the beginning of the dark period, perhaps initiated by circadian signals, may feed back on itself in a positive way, overwhelming the influence of physiological systems that would ordinarily lead the animal to sleep. The present results raise the possibility that activation of the orexin system by wheel running could provide a signal that feeds back in some individuals to prolong the period of running well into the night, overwhelming circadian signals that ordinarily promote sleep at this time. Previous studies have linked orexin cell activation to high-arousal states, such as stress (España et al. 2003). It is interesting to note that stress-related arousal has been implicated as a possible cause of insomnia (Bonnet and Arand 2000; Drake et al. 2003). Night-active grass rats, with their obsessive wheel-running, may thus represent an interesting animal model of how arousal systems, such as orexin pathways, might be related to insomnia.

## **Chapter 4**

Nixon, J. P. and L. Smale (2005). "Orexin fibers form appositions with fos expressing neuropeptide-Y cells in the grass rat intergeniculate leaflet." Brain Research **1053**(1-2): 33-37.

## **CHAPTER 4**

### **Orexin fibers form appositions with Fos expressing neuropeptide-Y cells in the grass rat intergeniculate leaflet**

#### **Introduction**

In mammals, circadian rhythms in physiology and behavior are generated by the suprachiasmatic nucleus (SCN) (Ralph et al. 1990) and entrained by the light-dark cycle through the retinohypothalamic tract (Johnson et al. 1988). In several nocturnal and diurnal species, circadian rhythms can also be modified by non-photic signals, such as access to a novel running wheel (Mrosovsky and Salmon 1987; Hastings et al. 1997; Hut et al. 1999; Kas and Edgar 1999; Antle and Mistlberger 2000). One important pathway through which both photic and non-photic information reaches the SCN is the geniculohypothalamic tract (GHT), which originates in the intergeniculate leaflet (IGL) of the lateral geniculate nucleus (Harrington 1997). Although most IGL afferents arise from structures that are part of the visual system (Morin and Blanchard 1998; Vrang et al. 2003; Horowitz et al. 2004), including the retina (Smale et al. 1991; Morin et al. 1992; Moore and Card 1994; Goel et al. 1999; Smale and Boverhof 1999), neural structures and cell groups associated with arousal (such as the raphe nuclei) also project to the IGL (Harrington 1997; Vrang et al. 2003). Lesions of the IGL as well as peptide infusion and blocking studies in several rodent species have shown that the subpopulation of IGL cells that contain neuropeptide-Y (NPY) play an important role in the integration of photic and non-photic effects on circadian

rhythmicity (Albers and Ferris 1984; Johnson et al. 1989; Huhman and Albers 1994; Wickland and Turek 1994; Biello 1995; Marchant et al. 1997).

Although projections to the IGL have been well-defined (Morin 1994; Vrang et al. 2003), little is known about the specific route through which information regarding arousal state reaches the NPY cells in this region. Several lines of evidence suggest that one source of input might be cells in the lateral hypothalamus (LH) that contain orexins (hypocretins), a family of peptides involved in the regulation of arousal, general activity and feeding (Hagan et al. 1999; Estabrooke et al. 2001; Hungs et al. 2001; Kotz et al. 2002). First, fibers containing orexin project to the IGL in several nocturnal and diurnal species (McGranaghan and Piggins 2001; Mintz et al. 2001; Novak and Albers 2002). We have recently shown that in one species these fibers appear to contact NPY cells within the IGL (Nixon and Smale 2004). Second, increases in physical activity associated with sleep deprivation or forced exercise are positively correlated with increased release of orexin into cerebrospinal fluid of several species (Wu et al. 2002; Martins et al. 2004). Finally, orexin release is known to stimulate NPY cells in other brain regions (Yamanaka et al. 2000), raising the possibility that NPY-containing cells might be capable of responding to orexins more generally.

Neuropeptide-Y and orexin have both been associated with non-photic influences on rhythms in the grass rat, *Arvicanthis niloticus*, a murid rodent that exhibits diurnal patterns of general activity both in the laboratory and in the wild (Katona and Smale 1997; Blanchong and Smale 2000). When given continuous access to a novel wheel, some individual grass rats exhibit an unusual form of

masking, switching from a day-active to a night-active pattern of activity (Blanchong et al. 1999). In our colony, this shift from day- to night-active occurs in approximately 30% of animals given free access to a wheel (Mahoney et al. 2001). This switch to a night-active pattern is not associated with transients (Nixon and Smale 2004; Redlin and Mrosovsky 2004), and appears to reflect a masking effect of the wheel rather than a shift in the internal clock (Nixon and Smale 2004).

Recent investigations in our laboratory suggest a relationship between wheel running patterns, orexin cells and NPY-containing cells in the grass rat IGL. Specifically, individual differences in patterns of wheel running in the grass rat are correlated with patterns of Fos expression in both neuropeptide-Y cells in the intergeniculate leaflet (Smale et al. 2001b) and in orexin cells in the lateral hypothalamus (Nixon and Smale 2004). We have also shown that orexin-containing fibers appear to contact NPY cells in the grass rat IGL (Nixon and Smale 2004). Taken together, these data suggest that the orexin fiber-NPY cell appositions may represent a pathway through which signals associated with arousal reach NPY cells in the IGL. To evaluate this hypothesis further, we used day- and night-active grass rats housed with running wheels to determine whether orexin A (OXA) fibers contact NPY cells that express c-Fos, and whether NPY cells with Fos are more likely to receive input from OXA fibers than are NPY cells without Fos.



## **Materials and Methods**

Tissue used in this study was collected during a previous experiment (Smale et al. 2001b). Briefly, adult male grass rats bred in a captive colony were kept on a 12:12 light:dark cycle, with food and water provided ad libitum. All animals were individually housed in cages equipped with running wheels; a magnetic bar on each wheel closed a switch affixed to the cage. Wheel running data were collected and quantified using the DSI Dataquest 3 system (MiniMitter, Sunriver, OR). After establishment of stable wheel running rhythms, animals were classified as day-active (n=3) or night-active (n=4). Tissue was collected at Zeitgeber time (ZT) 4 for day-active animals, and at ZT 16 for night-active grass rats. We did not look at night-active animals during the day or at day-active animals during the night because Fos expression in NPY cells is extremely low in these animals (Smale et al. 2001b). At the time of sacrifice, grass rats were given an overdose of sodium pentobarbital and transcardially perfused using 4% paraformaldehyde in 0.01 M phosphate-buffered saline (PBS). Tissue was sectioned on a freezing microtome at 30 micrometers and stored in cryoprotectant at -20°C. All animal handling procedures in this study followed National Institutes for Health guidelines and were approved by the Michigan State University All-University Committee for Animal Use and Care.

Every third section from each animal was labeled for Fos, OXA, and NPY immunoreactivity using the following procedure: All sections were incubated in 5% normal donkey serum (NDS; Jackson Laboratories, West Grove, PA) in 0.01 M PBS with 0.3% Triton-X 100 (TX; Research Products International, Mount

Prospect, IL) for 1 h. Tissue was then incubated in rabbit anti-Fos antibody (Santa Cruz Biotechnology, Santa Cruz, CA; 1:25,000) for 24 h at 4°C, in PBS with 0.3% TX (PBS-TX), 0.01% sodium azide (Sigma-Aldrich, St. Louis, MO) and 3% NDS. Next, tissue was incubated in biotinylated donkey anti-rabbit antibody (Jackson; 1:500, in PBS-TX with 3% NDS) for 1 h. Tissue was then placed in avidin-biotin complex (AB complex; 0.9% each avidin and biotin solutions, Vector Laboratories, Burlingame, CA; in PBS-TX) for 1 h. Sections were then rinsed in PBS, and reacted for 7 minutes with diaminobenzidine (DAB; 0.1 mg/ml, Sigma) enhanced with cobalt chloride (2 mg/ml; Sigma) in 0.1 M phosphate buffer with hydrogen peroxide (15  $\mu$ l 0.3% H<sub>2</sub>O<sub>2</sub>/ml buffer). Following the cobalt-enhanced DAB reaction, tissue was rinsed in PBS with 0.02% TX. Cobalt-labeled tissue was then blocked using 5% normal horse serum (NHS; Vector) in PBS-TX for 1 h, then incubated in goat anti-orexin A primary antibody for 24 h at 4°C (Santa Cruz; 1:10,000, in PBS-TX, 3% NHS, and 0.01% sodium azide). This step was followed by incubation in biotinylated horse anti-goat antibody for 1 h (Vector; 1:200, in PBS-TX and 3% NHS). Tissue was then incubated for 1 h in AB complex. Following the AB incubation, tissue was rinsed in PBS, then in tris-hydrochloride (Trizma, Sigma; 15.4 g/L, pH 7.2). Tissue was next reacted for 8 minutes with DAB (0.5 mg/ml, Sigma) in tris-hydrochloride with hydrogen peroxide (0.35  $\mu$ l 30% H<sub>2</sub>O<sub>2</sub>/ml buffer). Tissue was then rinsed in tris-hydrochloride, followed by PBS, and then incubated at 4°C with gentle agitation in PBS with 0.01% sodium azide for 24 hours. Tissue was then blocked for 1 h using 5% NHS in PBS-TX, then incubated with rabbit anti-NPY antibody

(Peninsula Laboratories, Belmont, CA; 1:1000, in PBS-TX, 3% NDS, and 0.01% sodium azide) for 24 h at 4°C, followed by incubation in biotinylated donkey anti-rabbit antibody (Jackson, 1:200; in PBS-TX and 3% serum) for 1 h. Tissue was then incubated for 1 h in AB complex, rinsed in PBS with 0.02% TX and then in PBS. Sections were reacted for 45 seconds using the Vector Vectastain VIP kit, following kit directions. Sections were then mounted on gelatin coated slides, dehydrated, and coverslipped. Control sections were obtained by omitting one of the three primary antibodies (anti-Fos, anti-OXA, or anti-NPY) prior to reacting tissue. In these control sections, deletion of the primary antibody produced tissue that was double-labeled for the remaining two antigens (either Fos and OXA, Fos and NPY, or OXA and NPY).

Twelve representative sections from each animal were examined using a light microscope equipped with a drawing tube (Leitz, Laborlux S; Wetzlar, Germany). For each section, bilateral counts of all Fos nuclei in NPY cells that did or did not exhibit appositions with orexin fibers (“NPY+OXA” or “NPY-Only” cells, respectively) within the IGL were performed by an individual blind to the identity of the animal. All Fos nuclei and OXA fiber contacts were verified under high-power (100x) magnification. An NPY cell was counted as Fos-positive only if the nucleus and cell boundary were clearly in the same plane of focus. Each NPY-Fos cell also exhibiting one or more apposition with an OXA fiber was counted as one NPY+OXA cell. In all cases, both Fos-positive nuclei and fiber appositions that were unclear at high-power magnification were not included in the analysis. The percentages of NPY-Only and of NPY+OXA cells that

expressed Fos were determined for each animal. Percentages were arc sine transformed and compared using dependent t-tests. High-resolution digital photographs of representative sections were taken using a digital camera (Carl Zeiss, AxioCam MRc; Göttingen, Germany) attached to a Zeiss light microscope (Axioskop 2 Plus). Image contrast and color balance were optimized using Zeiss AxioVision software (Carl Zeiss Vision). Graphs were prepared using SigmaPlot (SPSS; SPSS, Chicago, IL). Final figures were assembled using Adobe Illustrator and Adobe Photoshop (Adobe Systems, San Jose, CA).

## **Results**

Appositions between NPY-containing cells and OXA fibers were present throughout the rostro-caudal extent of the IGL. Orexin A fibers within the IGL exhibited numerous varicosities visible as distinct thickenings in orexin fibers. Varicosities and boutons were especially apparent when fibers were in close proximity to NPY cells. In many cases OXA fibers closely followed the borders of NPY cell bodies, clearly suggesting that contact between the fibers and NPY cells were not incidental. The NPY cells did not appear to exhibit appositions with more than one OXA fiber, although in many cases individual OXA fibers contacted more than one NPY cell. Orexin A fiber appositions with NPY cells (Figure 4.1) were seen in both day- and night-active animals. In control sections, deletion of each primary antibody eliminated all staining for its antigen (not shown).

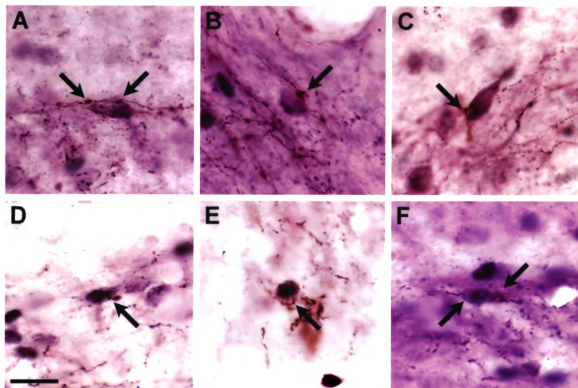


**Figure 4.1.** Photomicrographs (100x) of orexin A (OXA) fiber appositions with neuropeptide-Y (NPY) cells (Panels A, B, C) or NPY cells expressing Fos (Panels D, E, F) in the grass rat IGL. Arrows indicate appositions between OXA fibers and NPY cells; Scale bar is 50  $\mu$ m.

The percentage of all the NPY cells in the IGL that were contacted by OXA fibers appeared to be higher in night-active grass rats than in day-active animals, but the difference was not significant (Night-active mean= $26.84 \pm 3.49\%$ ; Day-active mean= $14.69 \pm 3.77\%$ ;  $t=2.331$ ,  $df=5$ ,  $p=0.067$ ). In day-active animals there was no difference between levels of Fos expression within NPY cells with OXA fiber appositions ("NPY+OXA cells") than in NPY cells that were not contacted by OXA fibers ("NPY-Only cells") ( $t=-1.879$ ,  $df=2$ ,  $p=0.201$ ). In night-active animals, NPY+OXA cells were significantly more likely to express Fos than were NPY-Only cells ( $t=-43.814$ ,  $df=3$ ,  $p<0.001$ ) (Figure 4.2).

## **Discussion**

The NPY cells of the grass rat IGL represent one of a very limited number of cell groups directly involved in the circadian system in which day- and night-active grass rats have been shown to differ. Specifically, Fos expression in NPY cells is highest when animals are actively running in wheels, either during the day (in day-active grass rats) or at night (in night-active grass rats) (Smale et al. 2001b). In contrast, other studies examining day- and night-active grass rats have demonstrated no significant difference with respect to overall expression of c-Fos, or of c-Fos expression rhythms in vasopressin, vasoactive intestinal polypeptide, or calbindin cells within the SCN (Rose et al. 1999; Mahoney et al. 2000; Smale et al. 2001a). Furthermore, grass rats placed in constant conditions continue to show stable day- or night-active activity rhythms, respectively (Mahoney et al. 2001). We have also seen little indication that the switch to a

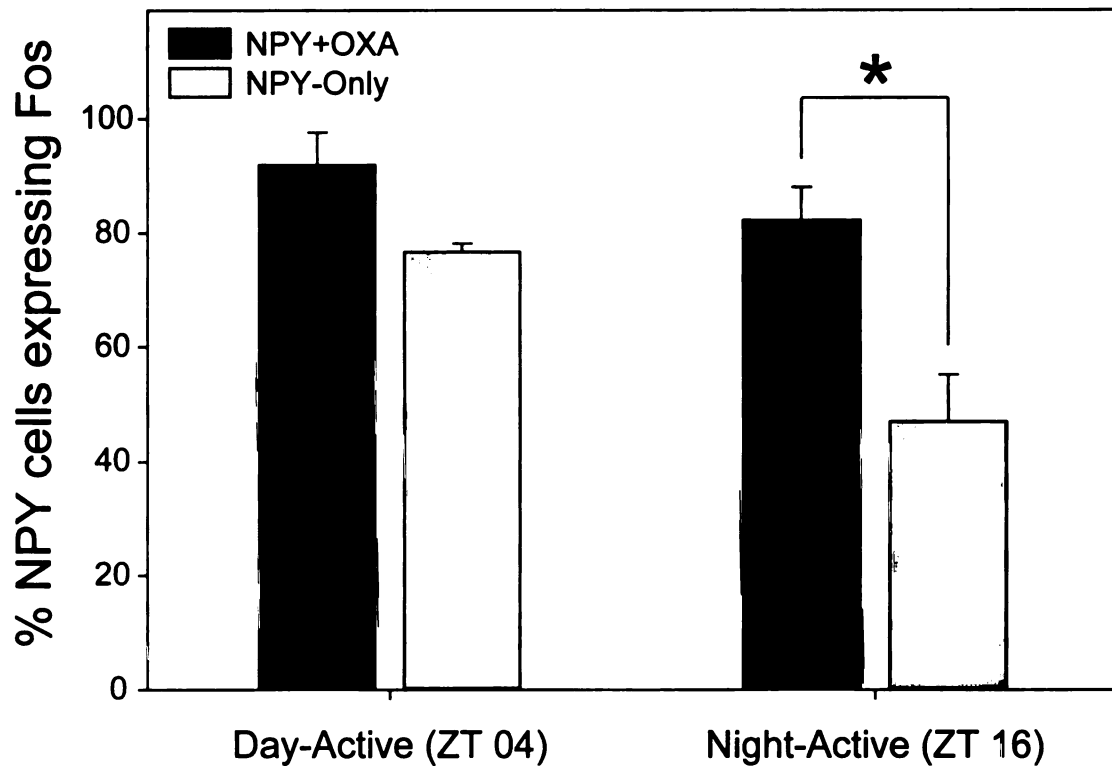


**Figure 4.2.** Percentages ( $\pm$ SEM) of Fos expression in neuropeptide-Y (NPY) cells that do (NPY+OXA) or do not (NPY-Only) exhibit appositions with orexin A (OXA) fibers in the IGL of day- and night-active grass rats. Asterisk indicates significant difference between columns ( $p < 0.0001$ ). Dark bars = NPY+OXA cells; light bars = NPY-Only cells.

night-active running pattern involves a change in responsiveness to light; phase-response curves and light-induced c-Fos within the SCN are quite similar in day- and night-active animals (Mahoney et al. 2001). Taken together, these data suggest that differences in activity rhythms of these grass rats do not simply reflect individual variation in a masking response to light (but see (Redlin and Mrosovsky 2004)). The similarities in SCN characteristics and responsiveness to light suggest that the difference in activation patterns of NPY cells in day- and night-active grass rats is more likely the result of non-photic influences, such as arousal, rather than photic input to the IGL.

The data presented in this study suggest that orexin A fibers could mediate the effects of activity state on NPY cells in the IGL. In the grass rat, patterns of activation of orexin cells in the LH during wheel running parallel patterns of activation of NPY cells in the IGL (Nixon and Smale 2004). Wheel running is a self-motivated behavior involving high levels of physical activity (Sherwin 1998), and previous studies have shown that periods of vigorous activity are associated with increased release of OXA into cerebrospinal fluid (Wu et al. 2002; Martins et al. 2004). Orexin release is capable of inducing Fos in NPY-containing cells in the arcuate nucleus (Yamanaka et al. 2000), raising the possibility that the same might be true in the IGL as well. Taken together, these data provide support for the hypothesis that orexin cells in the LH may transmit information regarding the activity state of an animal directly to NPY cells in the IGL. These NPY cells may then integrate orexin signals with inputs from other brain regions and transmit this information to the SCN.



The relationship between OXA fiber contacts and c-Fos induction in NPY cells was only significant in night-active grass rats. The current data do not allow us to clearly determine whether OXA input to NPY cells is associated with Fos expression in these cells in day-active animals. The differences observed between the day- and night-active animals may reflect differences in the relative importance of other inputs to NPY cells, or differences in the time of day at which they were sampled. The first of these possibilities is supported by the general trend for a greater proportion of NPY cells to be contacted by OXA fibers in the IGL of night-active compared to day-active grass rats. Interestingly, we have recently shown that a medially-located subset of OXA cells is more likely to express Fos in night-active than in day-active grass rats, even in the absence of running wheels (Nixon and Smale 2004). It is possible that individual differences in OXA cell group activation are directly associated with different activity patterns in this animal. That is, feedback from this medial group of OXA cells, perhaps through direct projections to NPY cells in the IGL, might be important in determining whether or not an individual grass rat will establish a nocturnal pattern of wheel running.

This study has two primary findings. First, many NPY cells that express Fos in animals that are running in wheels have appositions with OXA fibers. Second, in night-active grass rats, NPY cells that exhibit OXA fiber appositions are significantly more likely to express Fos during wheel running than NPY cells without such contacts. These data support the hypothesis that orexins may function as an important source of activity state feedback to the circadian system.

It is tempting to speculate that individual differences in this system may contribute to differences in temporal patterns of daily activity, such as those of day- vs. night-active grass rats.

## **CHAPTER 5**

### **Retrograde labeling of orexin neurons projecting to the grass rat intergeniculate leaflet**

#### **Introduction**

The lateral hypothalamus (LH) in mammals is thought to be involved in the mediation of general arousal, ingestive behavior, and modulation of brainstem nuclei in the control of motivated behaviors (reviewed in Simerly 1995). Recent investigations suggest that the orexins (hypocretins), a family of hypothalamic peptides found in neurons primarily restricted to the perifornical region (PeF) of the LH, might be involved in hypothalamic modulation of some or all of the functions ascribed to this region (Sakurai et al. 1998; Date et al. 1999; de Lecea and Sutcliffe 1999). Orexin has been strongly implicated in the regulation of arousal state (Chemelli et al. 1999; Hagan et al. 1999; Lin et al. 1999; Piper et al. 2000), feeding and drinking behaviors (Sakurai et al. 1998; Kunii et al. 1999; Sweet et al. 1999), and the modulation of autonomic functions such as breathing, blood pressure and heart rate (Lin et al. 2002; Shirasaka et al. 2002; Young et al. 2005; Zhang et al. 2005b; Zheng et al. 2005). Although a relatively small number of neurons contain orexin, these cells extend projections to a wide number of brain regions in rats and hamsters (Sakurai et al. 1998; Date et al. 1999; de Lecea and Sutcliffe 1999). Understanding the afferent and efferent connections of these neurons could thus prove to be important in our understanding of LH control of an important suite of physiological and behavioral actions as a whole.

Orexin neurons do not form compact clusters; instead, they are diffusely scattered throughout the PeF (Sakurai et al. 1998; Date et al. 1999; de Lecea and Sutcliffe 1999). Currently, very little is known about the topographical organization of this loose grouping of cells. The orexin neurons could represent a homogenous population of cells, or they might be organized into distinct subgroups with specific functions, either with respect to afferent connections, efferent projections, or both. In other phenotypically distinct populations of neurons that are diffusely distributed, such as those containing gonadotropin hormone releasing hormone, there is evidence for spatial organization that maps onto differences in their inputs, outputs and functions (King et al. 1998). Although there is some evidence from experiments utilizing retrograde tract tracers for spatial partitioning of orexin cells with respect to their efferent connections for some brain regions, such as the locus coeruleus (LC) (España et al. 2005), orexin neurons extending projections to other brainstem nuclei do not display similar spatial partitioning (Ciriello et al. 2003b; Zheng et al. 2005).

While it is clear that orexin efferents do not always originate from topographically isolated groups of neurons, identification of brain regions that do receive input from small groups of orexin cells could be important in understanding the behavioral effects of orexins on specific brain regions. Widescale lesions of the LH (Hetherington and Ranson 1940; Anand and Brobeck 1951) affect more neuron phenotypes than just those containing orexin, while selective destruction of all orexin-containing neurons (Chemelli et al. 1999) affects all brain regions receiving orexin input at once. Orexin infusion studies

have been useful (Mullett et al. 2000; Sato-Suzuki et al. 2002; Kiwaki et al. 2004), but interpretation of results is potentially complicated by the diffusion of orexin into adjacent regions. Finally, although targeting of individual orexin neurons is possible (Mileykovskiy et al. 2005), the technical problems associated with doing so on a large scale are daunting. With the identification of at least some functionally isolated subgroups of orexin neurons, examination of the behavioral effects of orexins might be easier. For example, a targeted lesion could potentially interrupt orexin projections to the LC while leaving input to other nuclei largely intact.

One potential link between orexin and behavior involves arousal state feedback to the intergeniculate leaflet (IGL). The IGL is a subdivision of the lateral geniculate complex of the thalamus. The IGL is best known for its role in the integration of photic and non-photic input to the mammalian circadian system (Morin et al. 1992; Moore and Card 1994; Morin and Blanchard 1995). Neurons containing neuropeptide-Y (NPY) within the IGL are important in the modulation of behavioral responses to arousal (Albers and Ferris 1984; Harrington et al. 1985; Johnson et al. 1989; Huhman and Albers 1994; Wickland and Turek 1994; Biello 1995; Marchant et al. 1997). The IGL receives input from orexin neurons in several species, including rats (Sakurai et al. 1998; de Lecea and Sutcliffe 1999), hamsters (Mintz et al. 2001; Khorrooshi and Klingenspor 2005), and the diurnal grass rat (*Arvicanthis niloticus*) (Novak and Albers 2002). In the grass rat, orexin input is potentially involved in relaying arousal state feedback to the IGL. Specifically, both NPY cells and orexin neurons exhibit similar patterns of Fos

expression in response to running wheel-induced arousal (Nixon and Smale 2004). The orexin neurons that project to the grass rat IGL form close appositions with NPY cells, including those that express Fos in response to arousal (Nixon and Smale 2005). Additionally, in some grass rats orexin cells in medial portions of the LH were more likely to express Fos than those located farther from the midline (Nixon and Smale 2004). In this study, we sought to determine whether orexin cells projecting to the IGL represent a spatially segregated subgroup of orexin cells, or are randomly distributed within the orexin cell population. To do this, we injected a retrograde tract-tracer (cholera toxin subunit B; CTB) into the grass rat IGL, then examined sections labeled for both orexin and CTB.

## **Methods**

### **Animal handling**

Seventeen adult male grass rats bred in a captive colony were used in this study. Animals were kept on a 12:12 light:dark cycle with a red light (< 5 lux) that was kept on constantly, and were provided food (Harlan Teklad 8640 rodent diet, Harlan Teklad Laboratory, Madison, WI) and water *ad libitum*. Animals were individually housed in clear plastic cages (28 × 34 × 16 cm) with wire lids. All animal handling and surgical procedures used in this study follow National Institutes of Health guidelines and were approved by the Michigan State University All-University Committee for Animal Use and Care.

## **Surgical procedures**

All animals received unilateral stereotaxic injections of a retrograde tract tracer directed at the IGL. At the time of surgery, animals were anesthetized with sodium pentobarbital (Nembutal; Abbot Laboratories, North Chicago, IN; 0.1 cc/100 g body weight, i.p.). The top of the head was shaved and covered with iodine (NovaPlus Povidone-Iodine, 10%; Novation Inc, Irving, TX). Artificial tears (Butler Company, Columbus, OH) were applied to protect the eyes. Each animal was then given a 30  $\mu$ l injection of local anesthetic (Lidocaine; Elkins-Sin Inc, Cherry Hill, NJ) and mounted in a Stoelting stereotaxic frame. Injections were made using a Hamilton 701N microliter syringe filled with 0.04  $\mu$ l of either a 1% solution of CTB (Sigma-Aldrich, St. Louis, MO) dissolved in phosphate buffered saline (PBS; 0.01 M, pH 7.4) or of CTB conjugated with AlexaFluor 488 (CTB-FITC; Molecular Probes, Eugene, OR). Injection of tracer was performed using a Starrett 262M manual microstepper over a period of two minutes, with the injection needle left in place for an additional 5 minutes to avoid spread of CTB upon its removal from the brain. Seven animals received injections of CTB, and ten animals were given injections of the CTB-FITC conjugate. For all injections into the IGL, the incisor bar was set at 0.0 mm, and injection coordinates were in the range of 0.3 – 0.5 mm anterior to the bregma, 2.9 – 3.0 mm lateral to the midline and 4.5 mm below the dura. Post-surgically, the wound was closed using autoclips and coated with either Nolvasan antiseptic ointment (Fort Dodge Animal Health, Fort Dodge, IA; 1% chlorhexidine acetate in 10% sterile alcohol base) or iodine. All animals then received 1 cc of sterile saline (s.c.) to prevent

dehydration and 0.06 cc of Bupranex (buprenorphine hydrochloride; Reckitt and Colman, Hull, England, i.m.) to alleviate pain.

### **Tissue collection and processing**

Two days after surgery, animals were given a lethal dose of sodium pentobarbital and perfused transcardially with PBS (150 – 200 ml/animal) followed by 150 to 200 mL fixative (4% paraformaldehyde with 75 mM lysine and 10 mM sodium periodate, in 0.1 M phosphate buffer, pH 7.2) Brains were post fixed for 4 h, then transferred into 20% sucrose. After 24 h in sucrose, brains were sectioned at 30  $\mu$ m in three series using a freezing microtome.

For animals receiving CTB injections, one series of tissue was processed for visualization of CTB. All sections were incubated in 5% normal horse serum (NHS; Vector Laboratories, Burlingame, CA) in PBS with 0.3% Triton-X 100 (PBS-TX; Research Products International, Mount Prospect, IL) for 1 h. Tissue was then incubated in goat anti-cholera toxin B subunit antibody (List Biologicals, Campbell, CA; 1:5000, in PBS-TX and 3% NHS) for 24 h at 4°C. Next, tissue was incubated in biotinylated horse anti-goat secondary antibody (Vector; 1:200; in PBS-TX with 3% NHS) for 1 h. Tissue was then placed in avidin-biotin complex (AB complex; 0.9% each avidin and biotin solutions, Vector; in PBS-TX) for 1 h and then reacted with DAB (0.5 mg/ml, Sigma) in a tris-hydrochloride buffer (Trizma, Sigma; pH 7.2) with hydrogen peroxide (0.35  $\mu$ l 30% hydrogen peroxide/ml buffer). Tissue was then mounted on gelatin-coated slides, dehydrated, and coverslipped.



For animals receiving CTB-FITC injections, tissue was processed for orexin using the same general procedure as described above, with the following changes: Blocking steps were performed using normal donkey serum (NDS, Jackson Laboratories, West Grove, PA), and tissue was incubated in goat anti-orexin A antibody (Santa Cruz; 1:10,000, in PBS-TX, with 3% NDS) followed by Texas Red sulfonyl chloride-conjugated donkey anti-goat secondary (AbCam Inc, Cambridge, MA; 1:200, in PBS-TX with 3% NDS). Following incubation with the secondary antibody, tissue was mounted on gelatin-coated slides and coverslipped using an anti-fading reagent for fluorescent labeling (ProLong Gold; Molecular Probes).

#### **Cell counts and analysis**

Tissue was examined using either a light microscope (Leitz, Laborlux S; Wetzlar, Germany) for CTB staining, or a fluorescent microscope (Zeiss Axioskop 2 plus; Carl Zeiss, Göttingen, Germany) equipped with a high-resolution digital camera (AxioCam MRc) for CTB-FITC / orexin colocalization. To evaluate the distribution of double-labeled cells, three representative sections ipsilateral to the site of injection were examined. Images were taken under 20x magnification at several planes of focus through the lateral hypothalamus using green channel filters for visualization of CTB-FITC, and red channel filters for visualization of Texas Red-labeled orexin neurons. Additional images were taken at 40x for confirmation of labeling in individual neurons. Composite images were obtained by combining red and green color channels using Adobe Photoshop

(Adobe Systems, San Jose, CA). Individual composite images were overlaid in Photoshop to create a multi-layer mosaic for use in performing cell counts.

For all tissue labeled with CTB-FITC, the average number and distribution of cells labeled for both CTB-FITC and orexin were counted. The area sampled was within a 700  $\mu\text{m}$  by 1600  $\mu\text{m}$  rectangle aligned to the edge of the third ventricle and ventral border of the fornix. The sampling area was divided into four equal 400  $\mu\text{m}$  wide divisions, referred to as “medial”, “central”, “lateral 1”, and “lateral 2” (Figure 5.1). The regions labeled “medial”, “central” and “lateral 1” in this study corresponds to regions labeled “medial”, “central”, and “lateral” used in Martinez et al. (2002). In all areas sampled, numbers of cells clearly labeled with orexin alone or with both CTB-FITC and orexin were counted using the composite image mosaic described above. Cells labeled with orexin were only counted as double-labeled if they expressed CTB-FITC labeling and the two labels were clearly in the same plane of focus. Total percentages of neurons expressing both orexin and CTB-FITC labeling were compiled, arcsine transformed, and analyzed using a two-way ANOVA to test for effects of area (medial, central, lateral 1, and lateral 2) and section examined (rostral, middle, or caudal). Analyses were calculated using Statistica, (StatSoft, Tulsa, OK). Graphs were prepared using SigmaPlot (SPSS, SPSS, Chicago, IL). Final figures were prepared using Adobe Photoshop and Adobe Illustrator (Adobe Systems).

## **Results**

In six grass rats, the tracer was successfully deposited in or near the IGL, with variable spread to adjacent regions of the hippocampus and geniculate

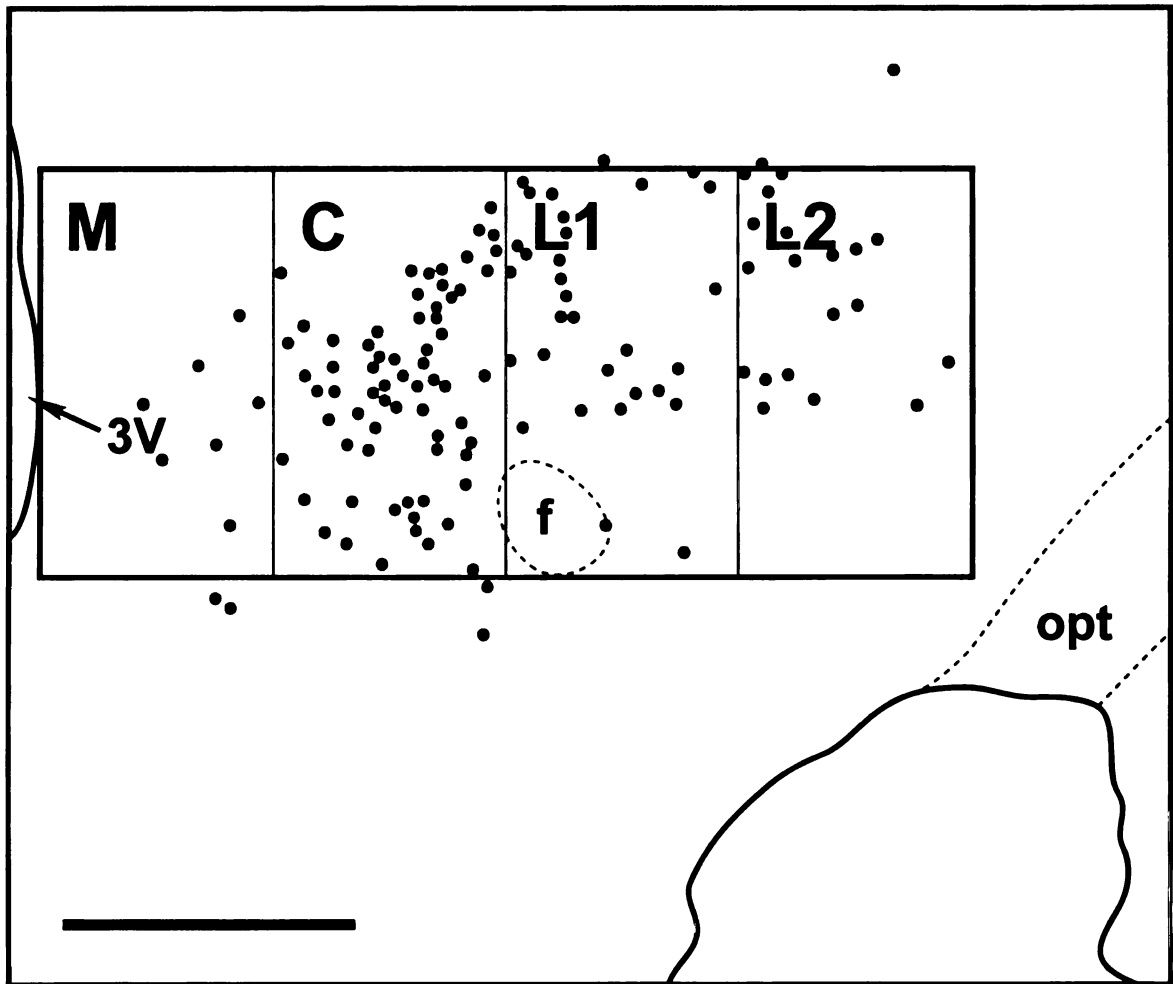


**Figure 5.1.** Line drawing of the lateral hypothalamic area at low magnification (5x) depicting the 1600  $\mu\text{m}$  x 700  $\mu\text{m}$  sampling area used in this study. The sampling box is aligned to the third ventricle and ventral border of the fornix, and divided from left to right into 40  $\mu\text{m}$  divisions labeled Medial (M), Central (C), Lateral 1 (L1), and Lateral 2 (L2), respectively. Circles represent cells containing orexin A. Scale bar = 500  $\mu\text{m}$ ; f = fornix, mt = mammalothalamic tract, 3V = third ventricle.

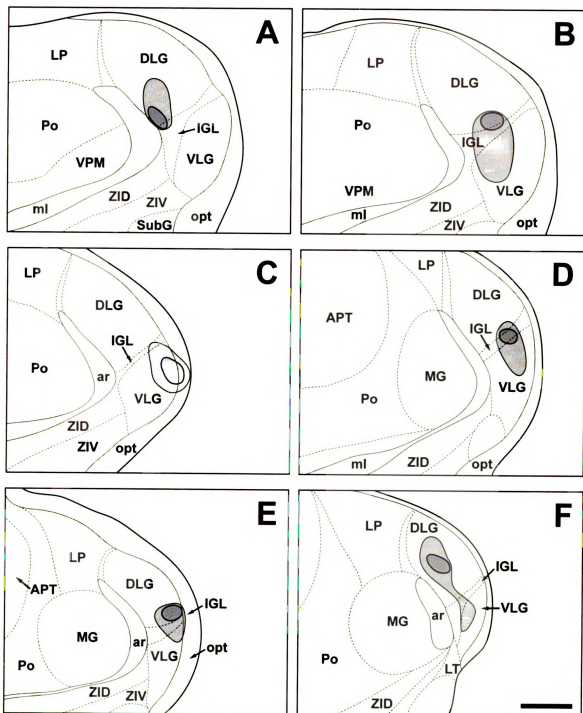
complex (CTB, n = 1; CTB-FITC, n = 5; Figure 5.2). For CTB injections that were centered on these regions rather than on the IGL, the majority of backfilled cells in the hypothalamus were located in the ventromedial hypothalamus and arcuate nucleus rather than in the perifornical region (not shown). In the animal with a CTB injection centered on the IGL, neurons backfilled with CTB were visible in the perifornical region of the LH. Very few CTB-positive neurons were observed in the perifornical region contralateral to the injection site in this animal.

Ipsilateral to the injection site of CTB-FITC injections, individual neurons expressing both CTB-FITC and orexin were visible throughout the LH (Figure 5.3). On average, approximately 20 percent (range = 17.29 to 27.23%; mean =  $18.54 \pm 1.77\%$ , n = 5) of all orexin neurons in the area of analysis also expressed CTB-FITC (Mean by area: medial =  $30.80 \pm 8.15\%$ ; central =  $19.06 \pm 2.05\%$ ; lateral 1 =  $16.93 \pm 2.14\%$ ; lateral 2 =  $17.35 \pm 3.99\%$ ). The percentage of orexin neurons that were double-labeled did not vary significantly across regions (Two-way ANOVA; df=9, F= 1.469, p = 0.199).

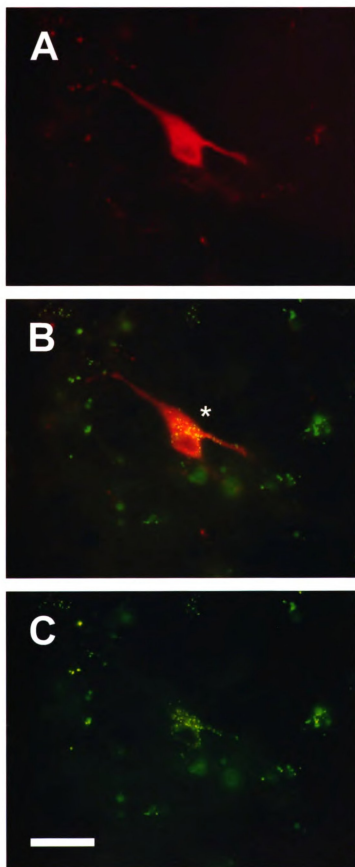
## **Discussion**

We have shown here that the orexin cells that project to the grass rat IGL represent a diffusely distributed subpopulation of orexin neurons, rather than a topographically distinct subset of cells. Although the CTB injections were not restricted to the IGL, we are confident that cells double-labeled for CTB and OXA accurately reflect the neurons that project to the IGL, as the hippocampus and other regions of the geniculate complex receive little or no input from orexin

**Figure 5.2.** Line drawings depicting injection sites for animals described in this study. Darkly shaded area indicates placement of needle tip; lighter shaded area indicates spread of cholera toxin tracer from injection site. All drawings were traced under low magnification (10x). Drawings are arranged rostrally to caudally through the intergeniculate leaflet. Scale bar = 300  $\mu$ m. APT: anterior pretectal nucleus; ar: acoustic radiation; DLG: dorsolateral geniculate nucleus; IGL: intergeniculate leaflet; LP: lateral posterior thalamic nucleus; ml: medial lemniscus; opt: optic tract; Po: posterior thalamic nuclear group; SubG: subgeniculate nucleus; VLG: ventrolateral geniculate nucleus; VPM: ventral posteromedial thalamic nucleus; ZID: zona inserta, dorsal; ZIV: zona incerta, ventral.



**Figure 5.3.** Photomicrographs depicting cells in the lateral hypothalamus after staining with Texas Red labeled orexin (red fluorescence, panels **A**, **D**, and **G**) and injection of FITC-conjugated cholera toxin B (green fluorescence, panels **C**, **F**, and **I**). Panels **B**, **E**, and **H** are composite images showing both labels. Neurons exhibiting immunoreactivity for both orexin and cholera toxin B are marked with an asterisk (\*). Arrows indicate cells labeled with cholera toxin B only. Scale bar = 25  $\mu\text{m}$ .





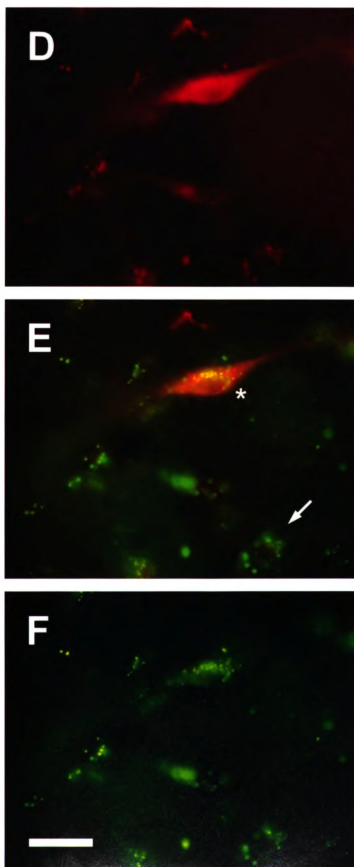


**Figure 5.3**  
(continued)

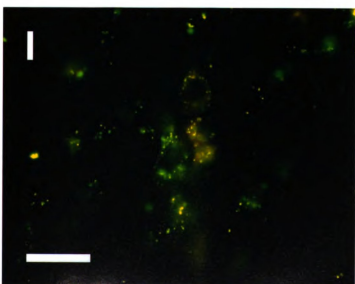
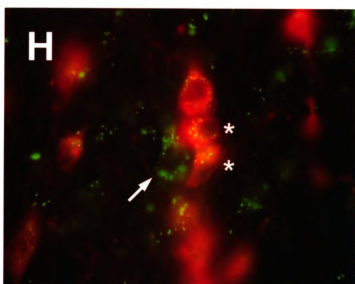
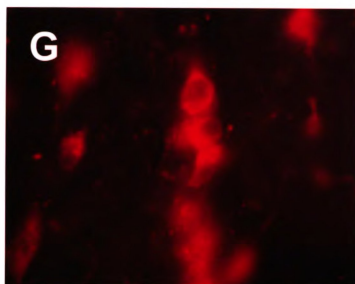


**Figure 5.3**  
(continued)

neurons in the grass rat (see Chapter 2). In animals with injections centered on the medial geniculate nuclei or hippocampus, CTB-labeled cells were more prevalent in the arcuate nucleus and ventral hypothalamus; few or no neurons were backfilled in the perifornical region in these animals (not shown).

Because the IGL extends the entire rostral-caudal length of the lateral geniculate complex, no single injection in this experiment covered the IGL as a whole. The 20% of orexin neurons labeled with CTB in this study therefore represents a minimum estimate. In other investigations utilizing retrograde tract-tracing in rats, a similar percentage of orexin cells has been shown to project to the dorsal vagal complex (20%; Zheng et al. 2005) and nucleus ambiguus (16%; Ciriello et al. 2003b), while 8 to 12% of orexin neurons exhibit projections to locus coeruleus and basal forebrain structures (España et al. 2005). Experiments examining colocalization of multiple retrograde tracers have shown that single orexin neurons in rats often project to more than one structure (Ciriello et al. 2003b; España et al. 2005). Given the large number of brain regions innervated by orexin fibers and the relatively small number of orexin neurons in the grass rat brain, it is likely that axonal projections from orexin neurons in the grass rat bifurcate to innervate multiple structures as well. Although the orexin cells projecting to the IGL do not form a topographically isolated cluster, they may still differ from the other orexin neurons with respect to their afferent projections as a whole. That is, the orexin neurons examined in this study may project to the IGL as well as to other arousal-related areas, while other orexin neurons may preferentially project to regions important in the regulation of ingestive behavior.

There is some evidence for such a segregation of orexin neurons by efferent pathways; dual tract-tracing experiments have identified individual orexin neurons that project to two different feeding- or arousal-related brain regions (Ciriello et al. 2003b; España et al. 2005).

Overall, it appears that parcellation of orexin neurons into groups projecting to specific brain regions is unlikely to be an easy task. In this study we did not find evidence that neurons projecting to the IGL represent a spatially distinct subset of the orexin cell population, similar to findings in some other studies examining retrogradely labeled orexin neurons. A similar conclusion was reached for populations of orexin neurons that project to basal forebrain structures, the dorsal vagal complex, and the nucleus of the solitary tract are randomly distributed within the larger orexin cell population (Ciriello et al. 2003b; España et al. 2005; Zheng et al. 2005). However, orexin neurons projecting to locus coeruleus are predominantly located in the dorsal half of the orexin cell population (España et al. 2005), while those projecting to the nucleus ambiguus are clustered lateral to the fornix (Ciriello et al. 2003b). It is interesting to note that although examination of single injections did not consistently identify specific isolated groups of orexin neurons, in at least one study in rats utilizing multiple retrograde tracers, orexin cells that expressed both retrograde labels did form two distinct clusters (Ciriello et al. 2003b). These clusters of cells represent only a small proportion of the orexin neurons projecting to one specific region, but the clusters of neurons identified may be different with respect to their afferent inputs. (that statement above was a little unclear) For example, although many

orexin neurons project to the IGL, not all of these neurons may be activated under the same conditions; those located closer to the third ventricle may be more responsive to arousal-induced activity, while those farther from the midline may receive input from other areas. It is thus possible that future identification of functional subgroups of orexin cells could be revealed by injection of retrograde tract-tracers into multiple rather than single brain regions.

Orexins have been implicated in the control or modulation of a wide variety of physiological or behavioral actions, including arousal (Hagan et al. 1999; Hara et al. 2001; Yoshimichi et al. 2001; Sato-Suzuki et al. 2002; Yamanaka et al. 2003), sexual behavior (Iqbal et al. 2001; Russell et al. 2001; Gulia et al. 2003), feeding (Sweet et al. 1999; Kotz et al. 2002; Thorpe and Kotz 2005), and autonomic functions (Shirasaka et al. 2002; Voisin et al. 2003; Young et al. 2005; Zheng et al. 2005). Currently, our understanding of orexin actions in the brain has largely been based upon experiments involving the infusion of orexins into discrete brain regions (Sweet et al. 1999; Bourgin et al. 2000; Methippara et al. 2000; Sato-Suzuki et al. 2002; Kiwaki et al. 2004). However, these experiments are not likely to reflect the physiological effects of orexins under normal circumstances. Because orexin neurons can project to multiple brain regions orexin would ordinarily be released at a number of target sites at the same time. The extensive projections of orexin neurons to structures involved a wide range of functions (Peyron et al. 1998; Cutler et al. 1999; Date et al. 1999) are thus likely to provide signals synchronously to multiple functional systems to aid in the coordination of behavioral state with state-dependent processes.

Identification of specific regions receiving concurrent input from subgroups of orexin neurons may prove important in understanding the function of orexin in the integration of these behaviors.

## References

- Abrahamson, E. E., R. K. Leak, et al. (2001). "The suprachiasmatic nucleus projects to posterior hypothalamic arousal systems." Neuroreport **12**(2): 435-440.
- Albers, H. E. and C. F. Ferris (1984). "Neuropeptide y: Role in light-dark cycle entrainment of hamster circadian rhythms." Neuroscience Letters **50**(1-3): 163-168.
- Alheid, G. F., J. S. de Olmos, et al. (1995). Amygdala and extended amygdala. The rat nervous system. G. Paxinos. San Diego, Academic Press: 495-578.
- Alvarez, C. E. and J. G. Sutcliffe (2002). "Hypocretin is an early member of the incretin gene family." Neuroscience Letters **324**(3): 169-172.
- Amir, S. and J. Stewart (1996). "Resetting of the circadian clock by a conditioned stimulus." Nature **379**(6565): 542-545.
- Anand, B. K. and J. R. Brobeck (1951). "Hypothalamic control of food intake in rats and cats." Yale Journal of Biology and Medicine **24**: 123-140.
- Antle, M. C. and R. E. Mistlberger (2000). "Circadian clock resetting by sleep deprivation without exercise in the syrian hamster." The Journal of Neuroscience **20**(24): 9326-9332.
- Archer, Z. A., P. A. Findlay, et al. (2002). "Orexin gene expression and regulation by photoperiod in the sheep hypothalamus." Regulatory Peptides **104**(1-3): 41-45.
- Arihara, Z., K. Takahashi, et al. (2000). "Orexin-a in the human brain and tumor tissues of ganglioneuroblastoma and neuroblastoma." Peptides **21**(4): 565-570.
- Armstrong, W. E. (1995). Hypothalamic supraoptic and paraventricular nuclei. The rat nervous system. G. Paxinos. San Diego, Academic Press: 377-390.
- Bayer, L., E. Eggemann, et al. (2002). "Selective action of orexin (hypocretin) on nonspecific thalamocortical projection neurons." The Journal of Neuroscience **22**(18): 7835-7839.
- Berthoud, H. R., L. M. Patterson, et al. (2005). "Orexin inputs to caudal raphe neurons involved in thermal, cardiovascular, and gastrointestinal regulation." Histochem Cell Biol **123**(2): 147-156.

- Biello, S. M. (1995). "Enhanced photic phase shifting after treatment with antiserum to neuropeptide y." Brain Research **673**(1): 25-29.
- Blanchong, J. A., T. L. McElhinny, et al. (1999). "Nocturnal and diurnal rhythms in the unstriped nile rat, *arvicanthis niloticus*." The Journal of Biological Rhythms **14**(5): 364-377.
- Blanchong, J. A. and L. Smale (2000). "Temporal patterns of activity of the unstriped nile grass rat, *arvicanthis niloticus*." Journal of Mammalogy **81**(2): 595-599.
- Blanco, M., M. Lopez, et al. (2001). "Cellular localization of orexin receptors in human pituitary." J Clin Endocrinol Metab **86**(4): 1616-1619.
- Bonnet, M. H. and D. L. Arand (2000). "Activity, arousal, and the mslt in patients with insomnia." Sleep **23**(2): 205-212.
- Bourgin, P., S. Huitron-Resendiz, et al. (2000). "Hypocretin-1 modulates rapid eye movement sleep through activation of locus coeruleus neurons." The Journal of Neuroscience **20**(20): 7760-7765.
- Broberger, C., L. De Lecea, et al. (1998). "Hypocretin/orexin- and melanin-concentrating hormone-expressing cells form distinct populations in the rodent lateral hypothalamus: Relationship to the neuropeptide y and agouti gene-related protein systems." J Comp Neurol **402**(4): 460-474.
- Brown, R. E., O. A. Sergeeva, et al. (2002). "Convergent excitation of dorsal raphe serotonin neurons by multiple arousal systems (orexin/hypocretin, histamine and noradrenaline)." The Journal of Neuroscience **22**(20): 8850-8859.
- Cai, X. J., M. L. Evans, et al. (2001). "Hypoglycemia activates orexin neurons and selectively increases hypothalamic orexin-b levels: Responses inhibited by feeding and possibly mediated by the nucleus of the solitary tract." Diabetes **50**(1): 105-112.
- Campbell, R. E., K. L. Grove, et al. (2003). "Gonadotropin-releasing hormone neurons coexpress orexin 1 receptor immunoreactivity and receive direct contacts by orexin fibers." Endocrinology **144**(4): 1542-1548.
- Canteras, N. S. (2002). "The medial hypothalamic defensive system: Hodological organization and functional implications." Pharmacol Biochem Behav **71**(3): 481-491.



- Challet, E., B. Pitrosky, et al. (2002). "Circadian organization in a diurnal rodent, *arvicantis ansorgei thomas* 1910: Chronotypes, responses to constant lighting conditions, and photoperiodic changes." The Journal of Biological Rhythms **17**(1): 52-64.
- Chemelli, R. M., J. T. Willie, et al. (1999). "Narcolepsy in orexin knockout mice: Molecular genetics of sleep regulation." Cell **98**(4): 437-451.
- Chen, C. T., S. L. Dun, et al. (1999). "Orexin a-like immunoreactivity in the rat brain." Neuroscience Letters **260**(3): 161-164.
- Ciriello, J., Z. Li, et al. (2003a). "Cardioacceleratory responses to hypocretin-1 injections into rostral ventromedial medulla." Brain Research **991**(1-2): 84-95.
- Ciriello, J., J. C. McMurray, et al. (2003b). "Collateral axonal projections from hypothalamic hypocretin neurons to cardiovascular sites in nucleus ambiguus and nucleus tractus solitarius." Brain Research **991**(1-2): 133-141.
- Ciriello, J., M. P. Rosas-Arellano, et al. (2003c). "Identification of neurons containing orexin-b (hypocretin-2) immunoreactivity in limbic structures." Brain Research **967**(1-2): 123-131.
- Cutler, D. J., R. Morris, et al. (1999). "Differential distribution of orexin-a and orexin-b immunoreactivity in the rat brain and spinal cord." Peptides **20**(12): 1455-1470.
- Date, Y., Y. Ueta, et al. (1999). "Orexins, orexigenic hypothalamic peptides, interact with autonomic, neuroendocrine and neuroregulatory systems." Proceedings of the National Academy of Sciences of the United States of America **96**(2): 748-753.
- de Lecea, L., T. S. Kilduff, et al. (1998). "The hypocretins: Hypothalamus-specific peptides with neuroexcitatory activity." Proceedings of the National Academy of Sciences of the United States of America **95**(1): 322-327.
- de Lecea, L. and J. G. Sutcliffe (1999). "The hypocretins/orexins: Novel hypothalamic neuropeptides involved in different physiological systems." Cellular and Molecular Life Sciences **56**(5-6): 473-480.
- de Oliveira, C. V. and J. Ciriello (2003). "Cardiovascular responses to hypocretin-1 in nucleus ambiguus of the ovariectomized female rat." Brain Research **986**(1-2): 148-156.

- Deurveilher, S. and K. Semba (2005). "Indirect projections from the suprachiasmatic nucleus to major arousal-promoting cell groups in rat: Implications for the circadian control of behavioural state." Neuroscience **130**(1): 165-183.
- Diano, S., B. Horvath, et al. (2003). "Fasting activates the nonhuman primate hypocretin (orexin) system and its postsynaptic targets." Endocrinology **144**(9): 3774-3778.
- Drake, C. L., T. Roehrs, et al. (2003). "Insomnia causes, consequences, and therapeutics: An overview." Depress Anxiety **18**(4): 163-176.
- Duxon, M. S., J. Stretton, et al. (2001). "Evidence that orexin-a-evoked grooming in the rat is mediated by orexin- 1 (ox1) receptors, with downstream 5-HT<sub>2C</sub> receptor involvement." Psychopharmacology (Berl) **153**(2): 203-209.
- Ebensperger, L. A. and M. J. Hurtado (2005). "On the relationship between herbaceous cover and vigilance activity of degus (octodon degus)." Ethology **111**(6): 593-608.
- Edwards, C. M., S. Abusnana, et al. (1999). "The effect of the orexins on food intake: Comparison with neuropeptide Y, melanin-concentrating hormone and galanin." J Endocrinol **160**(3): R7-12.
- Ehrstrom, M., T. Gustafsson, et al. (2005). "Inhibitory effect of exogenous orexin A on gastric emptying, plasma leptin and the distribution of orexin and orexin receptors in the gut and pancreas in man." J Clin Endocrinol Metab **90**(4): 2370-2377.
- España, R. A., K. M. Reis, et al. (2005). "Organization of hypocretin/orexin efferents to locus coeruleus and basal forebrain arousal-related structures." J Comp Neurol **481**(2): 160-178.
- España, R. A., R. J. Valentino, et al. (2003). "Fos immunoreactivity in hypocretin-synthesizing and hypocretin-1 receptor-expressing neurons: Effects of diurnal and nocturnal spontaneous waking, stress and hypocretin-1 administration." Neuroscience **121**(1): 201-217.
- Estabrooke, I. V., M. T. McCarthy, et al. (2001). "Fos expression in orexin neurons varies with behavioral state." The Journal of Neuroscience **21**(5): 1656-1662.
- Farrell, W. J., Y. Delville, et al. (2003). "Immunocytochemical localization of orexin in the brain of the green anole lizard (anolis carolinensis)." Abstracts - Society for Neuroscience **33**: 828.824.

- Gautvik, K. M., L. de Lecea, et al. (1996). "Overview of the most prevalent hypothalamus-specific mRNAs, as identified by directional tag PCR subtraction." Proceedings of the National Academy of Sciences of the United States of America **93**(16): 8733-8738.
- Goel, N., T. M. Lee, et al. (1999). "Suprachiasmatic nucleus and intergeniculate leaflet in the diurnal rodent octodon degus: Retinal projections and immunocytochemical characterization." Neuroscience **92**(4): 1491-1509.
- Governale, M. and T. Lee (2001). "Olfactory cues accelerate reentrainment following phase shifts and entrain free-running rhythms in female octodon degus (rodentia)." Journal of Biological Rhythms **16**(5): 489-501.
- Gulia, K. K., H. N. Mallick, et al. (2003). "Orexin a (hypocretin-1) application at the medial preoptic area potentiates male sexual behavior in rats." Neuroscience **116**(4): 921-923.
- Hagan, J. J., R. A. Leslie, et al. (1999). "Orexin a activates locus coeruleus cell firing and increases arousal in the rat." Proceedings of the National Academy of Sciences of the United States of America **96**(19): 10911-10916.
- Hara, J., C. T. Beuckmann, et al. (2001). "Genetic ablation of orexin neurons in mice results in narcolepsy, hypophagia, and obesity." Neuron **30**(2): 345-354.
- Harrington, M. E. (1997). "The ventral lateral geniculate nucleus and the intergeniculate leaflet: Interrelated structures in the visual and circadian systems." Neurosci Biobehav Rev **21**(5): 705-727.
- Harrington, M. E., D. M. Nance, et al. (1985). "Neuropeptide y immunoreactivity in the hamster geniculo-suprachiasmatic tract." Brain Research Bulletin **15**(5): 465-472.
- Hastings, M. H., G. E. Duffield, et al. (1997). "Non-phototic signalling in the suprachiasmatic nucleus." Biol Cell **89**(8): 495-503.
- Hatton, G. I. (1990). "Emerging concepts of structure-function dynamics in adult brain: The hypothalamo-neurohypophyseal system." Prog Neurobiol **34**(6): 437-504.
- Hervieu, G. J., J. E. Cluderay, et al. (2001). "Gene expression and protein distribution of the orexin-1 receptor in the rat brain and spinal cord." Neuroscience **103**(3): 777-797.

- Hetherington, A. W. and S. W. Ranson (1940). "Hypothalamic lesions and adiposity in the rat." Anatomical Record **78**: 149-172.
- Honda, Y., Y. Doi, et al. (1986). "Increased frequency of non-insulin-dependent diabetes mellitus among narcoleptic patients." Sleep **9**(1(Pt 2)): 254-259.
- Horowitz, S. S., J. H. Blanchard, et al. (2004). "Intergeniculate leaflet and ventral lateral geniculate nucleus afferent connections: An anatomical substrate for functional input from the vestibulo-visuomotor system." J Comp Neurol **474**(2): 227-245.
- Horvath, T. L., S. Diano, et al. (1999a). "Synaptic interaction between hypocretin (orexin) and neuropeptide y cells in the rodent and primate hypothalamus: A novel circuit implicated in metabolic and endocrine regulations." The Journal of Neuroscience **19**(3): 1072-1087.
- Horvath, T. L., C. Peyron, et al. (1999b). "Hypocretin (orexin) activation and synaptic innervation of the locus coeruleus noradrenergic system." J Comp Neurol **415**(2): 145-159.
- Huesa, G., A. N. van den Pol, et al. (2005). "Differential distribution of hypocretin (orexin) and melanin-concentrating hormone in the goldfish brain." J Comp Neurol **488**(4): 476-491.
- Huhman, K. L. and H. E. Albers (1994). "Neuropeptide y microinjected into the suprachiasmatic region phase shifts circadian rhythms in constant darkness." Peptides **15**(8): 1475-1478.
- Hungs, M., J. Fan, et al. (2001). "Identification and functional analysis of mutations in the hypocretin (orexin) genes of narcoleptic canines." Genome Res **11**(4): 531-539.
- Hungs, M. and E. Mignot (2001). "Hypocretin/orexin, sleep and narcolepsy." Bioessays **23**(5): 397-408.
- Hut, R. A., N. Mrosovsky, et al. (1999). "Nonphotic entrainment in a diurnal mammal, the european ground squirrel (*spermophilus citellus*)." The Journal of Biological Rhythms **14**(5): 409-419.
- Ida, T., K. Nakahara, et al. (1999). "Effect of lateral cerebroventricular injection of the appetite- stimulating neuropeptide, orexin and neuropeptide y, on the various behavioral activities of rats." Brain Research **821**(2): 526-529.
- Ida, T., K. Nakahara, et al. (2000a). "Both corticotropin releasing factor and neuropeptide y are involved in the effect of orexin (hypocretin) on the food intake in rats." Neuroscience Letters **293**(2): 119-122.

- Ida, T., K. Nakahara, et al. (2000b). "Possible involvement of orexin in the stress reaction in rats." Biochemical and Biophysical Research Communications **270**(1): 318-323.
- Iqbal, J., S. Pompolo, et al. (2001). "Evidence that orexin-containing neurones provide direct input to gonadotropin-releasing hormone neurones in the ovine hypothalamus." J Neuroendocrinol **13**(12): 1033-1041.
- Janik, D., J. D. Mikkelsen, et al. (1995). "Cellular colocalization of fos and neuropeptide y in the intergeniculate leaflet after nonphotic phase-shifting events." Brain Research **698**(1-2): 137-145.
- Janik, D. and N. Mrosovsky (1994). "Intergeniculate leaflet lesions and behaviorally-induced shifts of circadian rhythms." Brain Research **651**(1-2): 174-182.
- Jászberényi, M., E. Bujdosó, et al. (2000). "Effects of orexins on the hypothalamic-pituitary-adrenal system." J Neuroendocrinol **12**(12): 1174-1178.
- Jechura, T. and T. Lee (2004). "Ovarian hormones influence olfactory cue effects on reentrainment in the diurnal rodent, octodon degus." Hormones and Behavior **46**(3): 349-355.
- Jechura, T. J., J. M. Walsh, et al. (2000). "Testicular hormones modulate circadian rhythms of the diurnal rodent, octodon degus." Horm Behav **38**(4): 243-249.
- Jiao, Y., T. Lee, et al. (1999). "Photic responses of suprachiasmatic area neurons in diurnal degus (octodon degus) and nocturnal rats (rattus norvegicus)." Brain Research **817**(1-2): 93-103.
- Johnson, R. F., R. Y. Moore, et al. (1989). "Lateral geniculate lesions alter circadian activity rhythms in the hamster." Brain Research Bulletin **22**(2): 411-422.
- Johnson, R. F., L. P. Morin, et al. (1988). "Retinohypothalamic projections in the hamster and rat demonstrated using cholera toxin." Brain Research **462**(2): 301-312.
- Johren, O., S. J. Neidert, et al. (2001). "Prepro-orexin and orexin receptor mRNAs are differentially expressed in peripheral tissues of male and female rats." Endocrinology **142**(8): 3324-3331.

- Jones, D. N., J. Gartlon, et al. (2001). "Effects of centrally administered orexin-b and orexin-a: A role for orexin-1 receptors in orexin-b-induced hyperactivity." Psychopharmacology (Berl) **153**(2): 210-218.
- Kapoor, J. R. and C. D. Sladek (2001). "Substance p and npy differentially potentiate atp and adrenergic stimulated vasopressin and oxytocin release." Am J Physiol Regul Integr Comp Physiol **280**(1): R69-78.
- Kas, M. J. H. and D. M. Edgar (1999). "A nonphotic stimulus inverts the diurnal-nocturnal phase preference in octodon degus." Journal of Neuroscience **19**(1): 328-333.
- Kaslin, J., J. M. Nystedt, et al. (2004). "The orexin/hypocretin system in zebrafish is connected to the aminergic and cholinergic systems." The Journal of Neuroscience **24**(11): 2678-2689.
- Katona, C., S. Rose, et al. (1998). "The expression of fos within the suprachiasmatic nucleus of the diurnal rodent arvicantis niloticus." Brain Research **791**(1-2): 27-34.
- Katona, C. and L. Smale (1997). "Wheel-running rhythms in arvicantis niloticus." Physiology and Behavior **61**(3): 365-372.
- Khorooshi, R. M. and M. Klingenspor (2005). "Neuronal distribution of melanin-concentrating hormone, cocaine- and amphetamine-regulated transcript and orexin b in the brain of the djungarian hamster (phodopus sungorus)." Journal of Chemical Neuroanatomy **29**(2): 137-148.
- Kilduff, T. S. and L. de Lecea (2001). "Mapping of the mrnas for the hypocretin/orexin and melanin- concentrating hormone receptors: Networks of overlapping peptide systems." J Comp Neurol **435**(1): 1-5.
- King, J. C., E. Liu, et al. (1998). "Expression of fos within luteinizing hormone-releasing hormone neurons, in relation to the steroid-induced luteinizing hormone surge in guinea pigs." Biol Reprod **58**(2): 316-322.
- Kirchgessner, A. L. and M. Liu (1999). "Orexin synthesis and response in the gut." Neuron **24**(4): 941-951.
- Kiwaki, K., C. M. Kotz, et al. (2004). "Orexin a (hypocretin 1) injected into hypothalamic paraventricular nucleus and spontaneous physical activity in rats." Am J Physiol Endocrinol Metab **286**(4): E551-559.
- Klerman, E. B., D. W. Rimmer, et al. (1998). "Nonphotic entrainment of the human circadian pacemaker." Am J Physiol Regul Integr Comp Physiol **274**(4): R991-996.

- Kodama, T., S. Usui, et al. (2005). "High fos expression during the active phase in orexin neurons of a diurnal rodent, tamias sibiricus barberi." Peptides **26**(4): 631-638.
- Kotz, C. M., J. A. Teske, et al. (2002). "Feeding and activity induced by orexin a in the lateral hypothalamus in rats." Regulatory Peptides **104**(1-3): 27-32.
- Krajnak, K., L. Dickenson, et al. (1997). "The induction of fos-like proteins in the suprachiasmatic nuclei and intergeniculate leaflet by light pulses in degus (octodon degus) and rats." Journal of Biological Rhythms **12**(5): 401-412.
- Kummer, M., S. J. Neidert, et al. (2001). "Orexin (hypocretin) gene expression in rat ependymal cells." Neuroreport **12**(10): 2117-2120.
- Kunii, K., A. Yamanaka, et al. (1999). "Orexins/hypocretins regulate drinking behaviour." Brain Research **842**(1): 256-261.
- Lee, T. M. (2004). "Octodon degus: A diurnal, social, and long-lived rodent." Ilar J **45**(1): 14-24.
- Lin, L., J. Faraco, et al. (1999). "The sleep disorder canine narcolepsy is caused by a mutation in the hypocretin (orexin) receptor 2 gene." Cell **98**(3): 365-376.
- Lin, Y., K. Matsumura, et al. (2002). "Chronic central infusion of orexin-a increases arterial pressure in rats." Brain Research Bulletin **57**(5): 619-622.
- Lisberger, S. G., E. J. Morris, et al. (1987). "Visual motion processing and sensory-motor integration for smooth pursuit eye movements." Annu Rev Neurosci **10**: 97-129.
- Lu, X. Y., D. Bagnol, et al. (2000). "Differential distribution and regulation of ox1 and ox2 orexin/hypocretin receptor messenger rna in the brain upon fasting." Horm Behav **37**(4): 335-344.
- Lubkin, M. and A. Stricker-Krongrad (1998). "Independent feeding and metabolic actions of orexins in mice." Biochemical and Biophysical Research Communications **253**(2): 241-245.
- Mahoney, M., A. Bult, et al. (2001). "Phase response curve and light-induced fos expression in the suprachiasmatic nucleus and adjacent hypothalamus of arvicantis niloticus." The Journal of Biological Rhythms **16**(2): 149-162.

- Mahoney, M. M., A. A. Nunez, et al. (2000). "Calbindin and fos within the suprachiasmatic nucleus and the adjacent hypothalamus of arvicantis niloticus and rattus norvegicus." Neuroscience **99**(3): 565-575.
- Mahoney, M. M., C. Sisk, et al. (2004). "Circadian regulation of gonadotropin-releasing hormone neurons and the preovulatory surge in luteinizing hormone in the diurnal rodent, arvicantis niloticus, and in a nocturnal rodent, rattus norvegicus." Biol Reprod **70**(4): 1049-1054.
- Mahoney, M. M. and L. Smale (2005a). "Arginine vasopressin and vasoactive intestinal polypeptide fibers make appositions with gonadotropin-releasing hormone and estrogen receptor cells in the diurnal rodent arvicantis niloticus." Brain Research **In press**.
- Mahoney, M. M. and L. Smale (2005b). "A daily rhythm in mating behavior in a diurnal murid rodent arvicantis niloticus." Horm Behav **47**(1): 8-13.
- Malendowicz, L. K., C. Tortorella, et al. (1999). "Acute effects of orexins a and b on the rat pituitary-adrenocortical axis." Biomedical Research **20**(5): 301-304.
- Marchant, E. G., N. V. Watson, et al. (1997). "Both neuropeptide y and serotonin are necessary for entrainment of circadian rhythms in mice by daily treadmill running schedules." The Journal of Neuroscience **17**(20): 7974-7987.
- Marcus, J. N., C. J. Aschkenasi, et al. (2001). "Differential expression of orexin receptors 1 and 2 in the rat brain." J Comp Neurol **435**(1): 6-25.
- Martinez, G. S., L. Smale, et al. (2002). "Diurnal and nocturnal rodents show rhythms in orexinergic neurons." Brain Research **955**(1-2): 1-7.
- Martins, P. J., V. D'Almeida, et al. (2004). "Increased hypocretin-1 (orexin-a) levels in cerebrospinal fluid of rats after short-term forced activity." Regulatory Peptides **117**(3): 155-158.
- McElhinny, T. L. (1996). Reproductive biology and biological rhythms in arvicantis niloticus. Department of Zoology. East Lansing, Michigan State University: xi, 126 leaves.
- McElhinny, T. L., L. Smale, et al. (1997). "Patterns of body temperature, activity, and reproductive behavior in a tropical murid rodent, arvicantis niloticus." Physiology and Behavior **62**(1): 91-96.
- McGranaghan, P. A. and H. D. Piggins (2001). "Orexin a-like immunoreactivity in the hypothalamus and thalamus of the syrian hamster (mesocricetus



- auratus) and siberian hamster (phodopus sungorus), with special reference to circadian structures." Brain Research **904**(2): 234-244.
- Methippara, M. M., M. N. Alam, et al. (2000). "Effects of lateral preoptic area application of orexin-a on sleep- wakefulness." Neuroreport **11**(16): 3423-3426.
- Mileyskiy, B. Y., L. I. Kiyashchenko, et al. (2005). "Behavioral correlates of activity in identified hypocretin/orexin neurons." Neuron **46**(5): 787-798.
- Mintz, E. M., A. N. van den Pol, et al. (2001). "Distribution of hypocretin-(orexin) immunoreactivity in the central nervous system of syrian hamsters (mesocricetus auratus)." Journal of Chemical Neuroanatomy **21**(3): 225-238.
- Mohawk, J. A., K. Cashen, et al. (2005). "Inhibiting cortisol response accelerates recovery from a photic phase shift." Am J Physiol Regul Integr Comp Physiol **288**(1): R221-228.
- Mohawk, J. A. and T. M. Lee (2005). "Restraint stress delays reentrainment in male and female diurnal and nocturnal rodents." The Journal of Biological Rhythms **20**(3): 245-256.
- Mondal, M. S., M. Nakazato, et al. (1999a). "Characterization of orexin-a and orexin-b in the microdissected rat brain nuclei and their contents in two obese rat models." Neuroscience Letters **273**(1): 45-48.
- Mondal, M. S., M. Nakazato, et al. (1999b). "Widespread distribution of orexin in rat brain and its regulation upon fasting." Biochemical and Biophysical Research Communications **256**(3): 495-499.
- Moore, R. Y., E. A. Abrahamson, et al. (2001). "The hypocretin neuron system: An arousal system in the human brain." Arch Ital Biol **139**(3): 195-205.
- Moore, R. Y. and J. P. Card (1994). "Intergeniculate leaflet: An anatomically and functionally distinct subdivision of the lateral geniculate complex." J Comp Neurol **344**(3): 403-430.
- Moore, R. Y., J. C. Speh, et al. (1998). "Hypocretin localization in the human hypothalamus." Society for Neuroscience Abstracts **24**: 1918.
- Moriguchi, T., T. Sakurai, et al. (1999). "Neurons containing orexin in the lateral hypothalamic area of the adult rat brain are activated by insulin-induced acute hypoglycemia." Neuroscience Letters **264**(1-3): 101-104.

- Morin, L. P. (1994). "The circadian visual system." Brain Res Brain Res Rev **19**(1): 102-127.
- Morin, L. P. and J. Blanchard (1995). "Organization of the hamster intergeniculate leaflet: Npy and enk projections to the suprachiasmatic nucleus, intergeniculate leaflet and posterior limitans nucleus." Visual Neuroscience **12**(1): 57-67.
- Morin, L. P., J. Blanchard, et al. (1992). "Intergeniculate leaflet and suprachiasmatic nucleus organization and connections in the golden hamster." Visual Neuroscience **8**(3): 219-230.
- Morin, L. P. and J. H. Blanchard (1998). "Interconnections among nuclei of the subcortical visual shell: The intergeniculate leaflet is a major constituent of the hamster subcortical visual system." J Comp Neurol **396**(3): 288-309.
- Morin, L. P. and J. H. Blanchard (2001). "Neuromodulator content of hamster intergeniculate leaflet neurons and their projection to the suprachiasmatic nucleus or visual midbrain." J Comp Neurol **437**(1): 79-90.
- Morin, L. P. and R. I. Wood (2001). A stereotaxic atlas of the golden hamster brain, Academic Press.
- Mrosovsky, N. and P. A. Salmon (1987). "A behavioural method for accelerating re-entrainment of rhythms to new light-dark cycles." Nature **330**(6146): 372-373.
- Mullett, M. A., C. J. Billington, et al. (2000). "Hypocretin i in the lateral hypothalamus activates key feeding-regulatory brain sites." Neuroreport **11**(1): 103-108.
- Nakamura, T., K. Uramura, et al. (2000). "Orexin-induced hyperlocomotion and stereotypy are mediated by the dopaminergic system." Brain Research **873**(1): 181-187.
- Nambu, T., T. Sakurai, et al. (1999). "Distribution of orexin neurons in the adult rat brain." Brain Research **827**(1-2): 243-260.
- Nevsimalova, S., J. Vankova, et al. (2005). "Hypocretin deficiency in prader-willi syndrome." Eur J Neurol **12**(1): 70-72.
- Niimi, M., M. Sato, et al. (2001). "Neuropeptide y in central control of feeding and interactions with orexin and leptin." Endocrine **14**(2): 269-273.
- Nishino, S., B. Ripley, et al. (2000). "Hypocretin (orexin) deficiency in human narcolepsy." Lancet **355**(9197): 39-40.

- Nishino, S., B. Ripley, et al. (2001). "Low cerebrospinal fluid hypocretin (orexin) and altered energy homeostasis in human narcolepsy." Ann Neurol **50**(3): 381-388.
- Nixon, J. P. and L. Smale (2004). "Individual differences in wheel-running rhythms are related to temporal and spatial patterns of activation of orexin a and b cells in a diurnal rodent (arvicanthis niloticus)." Neuroscience **127**(1): 25-34.
- Nixon, J. P. and L. Smale (2005). "Orexin fibers form appositions with fos expressing neuropeptide-y cells in the grass rat intergeniculate leaflet." Brain Research **1053**(1-2): 33-37.
- Novak, C. M. and H. E. Albers (2002). "Localization of hypocretin-like immunoreactivity in the brain of the diurnal rodent, arvicanthis niloticus." Journal of Chemical Neuroanatomy **23**(1): 49-58.
- Novak, C. M., J. A. Harris, et al. (2000a). "Suprachiasmatic nucleus projections to the paraventricular thalamic nucleus in nocturnal rats (rattus norvegicus) and diurnal Nile grass rats (arvicanthis niloticus)." Brain Research **874**(2): 147-157.
- Novak, C. M., L. Smale, et al. (1999). "Fos expression in the sleep-active cell group of the ventrolateral preoptic area in the diurnal murid rodent, arvicanthis niloticus." Brain Research **818**(2): 375-382.
- Novak, C. M., L. Smale, et al. (2000b). "Rhythms in fos expression in brain areas related to the sleep-wake cycle in the diurnal arvicanthis niloticus." Am J Physiol Regul Integr Comp Physiol **278**(5): R1267-1274.
- Nowak, R. M., Ed. (1999). Walker's mammals of the world. Baltimore, Johns Hopkins University Press.
- Núñez, A. A., A. Bult, et al. (1999). "Daily rhythms of fos expression in hypothalamic targets of the suprachiasmatic nucleus in diurnal and nocturnal rodents." The Journal of Biological Rhythms **14**(4): 300-306.
- Ohkubo, T., T. Boswell, et al. (2002). "Molecular cloning of chicken prepro-orexin cDNA and preferential expression in the chicken hypothalamus." Biochim Biophys Acta **1577**(3): 476-480.
- Paxinos, G., Ed. (1995). The rat nervous system. San Diego, Academic Press.
- Paxinos, G. and C. Watson (1998). The rat brain in stereotaxic coordinates. San Diego, Academic Press.

- Petersén, Å., J. Gil, et al. (2005). "Orexin loss in huntington's disease." Hum Mol Genet **14**(1): 39-47.
- Peyron, C., D. K. Tighe, et al. (1998). "Neurons containing hypocretin (orexin) project to multiple neuronal systems." The Journal of Neuroscience **18**(23): 9996-10015.
- Piper, D. C., N. Upton, et al. (2000). "The novel brain neuropeptide, orexin-a, modulates the sleep-wake cycle of rats." Eur J Neurosci **12**(2): 726-730.
- Price, J. L. (1995). Thalamus. The rat nervous system. G. Paxinos. San Diego, Academic Press: 629-648.
- Qu, D., D. S. Ludwig, et al. (1996). "A role for melanin-concentrating hormone in the central regulation of feeding behaviour." Nature **380**(6571): 243-247.
- Raffin-Sanson, M. L., Y. de Keyser, et al. (2003). "Proopiomelanocortin, a polypeptide precursor with multiple functions: From physiology to pathological conditions." Eur J Endocrinol **149**(2): 79-90.
- Ralph, M. R., R. G. Foster, et al. (1990). "Transplanted suprachiasmatic nucleus determines circadian period." Science **247**(4945): 975-978.
- Rauch, M., T. Riediger, et al. (2000). "Orexin a activates leptin-responsive neurons in the arcuate nucleus." Pflugers Arch **440**(5): 699-703.
- Redlin, U. and N. Mrosovsky (2004). "Nocturnal activity in a diurnal rodent (*arvicanthis niloticus*): The importance of masking." The Journal of Biological Rhythms **19**(1): 58-67.
- Robinson, F. R. and A. F. Fuchs (2001). "The role of the cerebellum in voluntary eye movements." Annu Rev Neurosci **24**: 981-1004.
- Rodgers, R. J., J. C. Halford, et al. (2000). "Dose-response effects of orexin-a on food intake and the behavioural satiety sequence in rats." Regulatory Peptides **96**(1-2): 71-84.
- Rose, S., C. M. Novak, et al. (1999). "Fos expression within vasopressin-containing neurons in the suprachiasmatic nucleus of diurnal rodents compared to nocturnal rodents." The Journal of Biological Rhythms **14**(1): 37-46.
- Russell, S. H., C. J. Small, et al. (2001). "Orexin a interactions in the hypothalamo-pituitary gonadal axis." Endocrinology **142**(12): 5294-5302.

- Sakurai, T. (2003). "Orexin: A link between energy homeostasis and adaptive behaviour." Curr Opin Clin Nutr Metab Care **6**(4): 353-360.
- Sakurai, T., A. Amemiya, et al. (1998). "Orexins and orexin receptors: A family of hypothalamic neuropeptides and g protein-coupled receptors that regulate feeding behavior." Cell **92**(4): 573-585.
- Sakurai, T., T. Moriguchi, et al. (1999). "Structure and function of human prepro-orexin gene." J Biol Chem **274**(25): 17771-17776.
- Samson, W. K., M. M. Taylor, et al. (2002). "Orexin actions in hypothalamic paraventricular nucleus: Physiological consequences and cellular correlates." Regulatory Peptides **104**(1-3): 97-103.
- Sato-Suzuki, I., I. Kita, et al. (2002). "Cortical arousal induced by microinjection of orexins into the paraventricular nucleus of the rat." Behav Brain Res **128**(2): 169-177.
- Schwartz, M. D., A. A. Nunez, et al. (2004). "Differences in the suprachiasmatic nucleus and lower subparaventricular zone of diurnal and nocturnal rodents." Neuroscience **127**(1): 13-23.
- Schwartz, M. W., S. C. Woods, et al. (2000). "Central nervous system control of food intake." Nature **404**(6778): 661-671.
- Sherwin, C. M. (1998). "Voluntary wheel running: A review and novel interpretation." Animal Behaviour **56**(1): 11-27.
- Shibahara, M., T. Sakurai, et al. (1999). "Structure, tissue distribution, and pharmacological characterization of xenopus orexins." Peptides **20**(10): 1169-1176.
- Shirasaka, T., T. Kunitake, et al. (2002). "Neuronal effects of orexins: Relevant to sympathetic and cardiovascular functions." Regulatory Peptides **104**(1-3): 91-95.
- Simerly, R. B. (1995). Anatomical substrates of hypothalamic integration. The rat nervous system. G. Paxinos. San Diego, Academic Press: 353-376.
- Singletary, K. G., Y. Delville, et al. (2005). "Distribution of orexin/hypocretin immunoreactivity in the nervous system of the green treefrog, hyla cinerea." Brain Research **1041**(2): 231-236.
- Smale, L., J. Blanchard, et al. (1991). "Immunocytochemical characterization of the suprachiasmatic nucleus and the intergeniculate leaflet in the diurnal ground squirrel, spermophilus lateralis." Brain Research **563**(1-2): 77-86.

- Smale, L. and J. Boverhof (1999). "The suprachiasmatic nucleus and intergeniculate leaflet of *arvicanthis niloticus*, a diurnal murid rodent from east africa." J Comp Neurol **403**(2): 190-208.
- Smale, L., C. Castleberry, et al. (2001a). "Fos rhythms in the hypothalamus of *rattus* and *arvicanthis* that exhibit nocturnal and diurnal patterns of rhythmicity." Brain Research **899**(1-2): 101-105.
- Smale, L., T. McElhinny, et al. (2001b). "Patterns of wheel running are related to fos expression in neuropeptide-  $\gamma$ -containing neurons in the intergeniculate leaflet of *arvicanthis niloticus*." Journal of Biological Rhythms **16**(2): 163-172.
- Smart, D., J. C. Jerman, et al. (1999). "Characterization of recombinant human orexin receptor pharmacology in a chinese hamster ovary cell-line using flipr." Br J Pharmacol **128**(1): 1-3.
- Sutcliffe, J. G. and L. de Lecea (2000). "The hypocretins: Excitatory neuromodulatory peptides for multiple homeostatic systems, including sleep and feeding." Journal of Neuroscience Research **62**(2): 161-168.
- Swanson, L. W. (2000). "Cerebral hemisphere regulation of motivated behavior." Brain Research **886**(1-2): 113-164.
- Sweet, D. C., A. S. Levine, et al. (1999). "Feeding response to central orexins." Brain Research **821**(2): 535-538.
- Taheri, S., D. Sunter, et al. (2000). "Diurnal variation in orexin a immunoreactivity and prepro-orexin mrna in the rat central nervous system." Neuroscience Letters **279**(2): 109-112.
- Takenoya, F., M. Hirayama, et al. (2005). "Neuronal interactions between galanin-like-peptide- and orexin- or melanin-concentrating hormone-containing neurons." Regulatory Peptides **126**(1-2): 79-83.
- Thannickal, T. C., R. Y. Moore, et al. (2000). "Reduced number of hypocretin neurons in human narcolepsy." Neuron **27**(3): 469-474.
- Thorpe, A. J. and C. M. Kotz (2005). "Orexin a in the nucleus accumbens stimulates feeding and locomotor activity." Brain Research **1050**(1-2): 156-162.
- Tohei, A., Y. Mogi, et al. (2003). "Strain difference in pituitary-adrenal axis between wistar-imamichi and long evans adult male rats." Exp Anim **52**(5): 437-439.

- Tritos, N. A., J. W. Mastaitis, et al. (2001). "Characterization of melanin concentrating hormone and preproorexin expression in the murine hypothalamus." Brain Research **895**(1-2): 160-166.
- Trivedi, P., H. Yu, et al. (1998). "Distribution of orexin receptor mrna in the rat brain." FEBS Lett **438**(1-2): 71-75.
- van den Pol, A. N. (1999). "Hypothalamic hypocretin (orexin): Robust innervation of the spinal cord." The Journal of Neuroscience **19**(8): 3171-3182.
- van den Pol, A. N., X. B. Gao, et al. (1998). "Presynaptic and postsynaptic actions and modulation of neuroendocrine neurons by a new hypothalamic peptide, hypocretin/orexin." The Journal of Neuroscience **18**(19): 7962-7971.
- Van der Werf, Y. D., M. P. Witter, et al. (2002). "The intralaminar and midline nuclei of the thalamus. Anatomical and functional evidence for participation in processes of arousal and awareness." Brain Res Brain Res Rev **39**(2-3): 107-140.
- Vann, S. D. (2005). "Transient spatial deficit associated with bilateral lesions of the lateral mammillary nuclei." Eur J Neurosci **21**(3): 820-824.
- Voisin, T., P. Rouet-Benzineb, et al. (2003). "Orexins and their receptors: Structural aspects and role in peripheral tissues." Cellular and Molecular Life Sciences **60**(1): 72-87.
- Vrang, N., N. Mrosovsky, et al. (2003). "Afferent projections to the hamster intergeniculate leaflet demonstrated by retrograde and anterograde tracing." Brain Research Bulletin **59**(4): 267-288.
- Wang, J. B., T. Murata, et al. (2003). "Variation in the expression of orexin and orexin receptors in the rat hypothalamus during the estrous cycle, pregnancy, parturition, and lactation." Endocrine **22**(2): 127-134.
- Watson, R. E., Jr., S. J. Wiegand, et al. (1986). "Use of cryoprotectant to maintain long-term peptide immunoreactivity and tissue morphology." Peptides **7**(1): 155-159.
- Weaver, D. R. (1998). "The suprachiasmatic nucleus: A 25-year retrospective." The Journal of Biological Rhythms **13**(2): 100-112.
- Wickland, C. and F. W. Turek (1994). "Lesions of the thalamic intergeniculate leaflet block activity-induced phase shifts in the circadian activity rhythm of the golden hamster." Brain Research **660**(2): 293-300.

- Wu, M. F., J. John, et al. (2002). "Hypocretin release in normal and narcoleptic dogs after food and sleep deprivation, eating, and movement." Am J Physiol Regul Integr Comp Physiol **283**(5): R1079-1086.
- Yamamoto, T., H. Suzuki, et al. (2004). "Localization of orexin-a-like immunoreactivity in prolactin cells in the bullfrog (*Rana catesbeiana*) pituitary." Gen Comp Endocrinol **135**(2): 186-192.
- Yamanaka, A., C. T. Beuckmann, et al. (2003). "Hypothalamic orexin neurons regulate arousal according to energy balance in mice." Neuron **38**(5): 701-713.
- Yamanaka, A., K. Kunii, et al. (2000). "Orexin-induced food intake involves neuropeptide Y pathway." Brain Research **859**(2): 404-409.
- Yoshimichi, G., H. Yoshimatsu, et al. (2001). "Orexin-a regulates body temperature in coordination with arousal status." Exp Biol Med (Maywood) **226**(5): 468-476.
- Young, J. K., M. Wu, et al. (2005). "Orexin stimulates breathing via medullary and spinal pathways." J Appl Physiol **98**(4): 1387-1395.
- Zhang, J. H., S. Sampogna, et al. (2002). "Co-localization of hypocretin-1 and hypocretin-2 in the cat hypothalamus and brainstem." Peptides **23**(8): 1479-1483.
- Zhang, J. H., S. Sampogna, et al. (2004). "Distribution of hypocretin (orexin) immunoreactivity in the feline pons and medulla." Brain Research **995**(2): 205-217.
- Zhang, S., D. Blache, et al. (2005a). "Expression of orexin receptors in the brain and peripheral tissues of the male sheep." Regulatory Peptides **124**(1-3): 81-87.
- Zhang, W., Y. Fukuda, et al. (2005b). "Respiratory and cardiovascular actions of orexin-a in mice." Neuroscience Letters **385**(2): 131-136.
- Zheng, H., L. M. Patterson, et al. (2005). "Orexin-a projections to the caudal medulla and orexin-induced c-fos expression, food intake, and autonomic function." J Comp Neurol **485**(2): 127-142.



MICHIGAN STATE UNIVERSITY LIBRARIES



3 1293 02736 4185